


Search for a heavy charged boson in events with a charged lepton and missing transverse momentum from pp collisions at $\sqrt{s} = 13$ TeV with the ATLAS detector

G. Aad *et al.**
(ATLAS Collaboration)

 (Received 14 June 2019; published 23 September 2019)

A search for a heavy charged-boson resonance decaying into a charged lepton (electron or muon) and a neutrino is reported. A data sample of 139 fb^{-1} of proton-proton collisions at $\sqrt{s} = 13$ TeV collected with the ATLAS detector at the LHC during 2015–2018 is used in the search. The observed transverse mass distribution computed from the lepton and missing transverse momenta is consistent with the distribution expected from the Standard Model, and upper limits on the cross section for $pp \rightarrow W' \rightarrow \ell\nu$ are extracted ($\ell = e$ or μ). These vary between 1.3 pb and 0.05 fb depending on the resonance mass in the range between 0.15 and 7.0 TeV at 95% confidence level for the electron and muon channels combined. Gauge bosons with a mass below 6.0 and 5.1 TeV are excluded in the electron and muon channels, respectively, in a model with a resonance that has couplings to fermions identical to those of the Standard Model W boson. Cross-section limits are also provided for resonances with several fixed Γ/m values in the range between 1% and 15%. Model-independent limits are derived in single-bin signal regions defined by a varying minimum transverse mass threshold. The resulting visible cross-section upper limits range between 4.6 (15) pb and 22 (22) ab as the threshold increases from 130 (110) GeV to 5.1 (5.1) TeV in the electron (muon) channel.

DOI: [10.1103/PhysRevD.100.052013](https://doi.org/10.1103/PhysRevD.100.052013)

I. INTRODUCTION

One of the main goals of the Large Hadron Collider (LHC) remains the search for physics beyond the Standard Model (SM). Much progress has been made in this search thanks to a broad program that encompasses many different final states. Leptonic final states provide a low-background and efficient experimental signature that brings excellent sensitivity to new phenomena at the LHC. In this article, the results of a search for resonances decaying into a charged lepton and a neutrino are presented, based on 139 fb^{-1} of proton-proton (pp) collisions at a center-of-mass energy of 13 TeV. The data were collected with the ATLAS detector during the 2015–2018 running period of the LHC, referred to as Run 2.

The search results are interpreted in terms of the production of a heavy spin-1 W' boson with subsequent decay into the $\ell\nu$ final state ($\ell = e$ or μ). Such production is predicted in many models of physics beyond the SM as in grand unified theory models, left-right symmetry models [1,2], little Higgs models [3], or models with extra

dimensions [4,5], most of which aim to solve the hierarchy problem. The interpretation in this article uses a simplified model referred to as the sequential Standard Model (SSM) [6], in which the W' boson couples to fermions with the same strength as the W boson in the SM but with suppressed coupling to SM bosons. Alternative interpretations in terms of generic resonances with different fixed widths (Γ/m between 1% and 15%) are also provided for possible reinterpretation in the context of other models. Finally, results are also presented in terms of model-independent upper limits on the number of signal events and on the visible cross section.

Previous searches for W' bosons have been carried out at the LHC in leptonic, semileptonic, and hadronic final states by the ATLAS and CMS Collaborations. The most sensitive searches for W' bosons are those in the $e\nu$ and $\mu\nu$ channels [7,8], with the most stringent limits to date being set by ATLAS and CMS in the analysis of about 36 fb^{-1} of pp collisions at $\sqrt{s} = 13$ TeV. A lower limit of 5.2 TeV is set on the W' boson mass in the electron channel [7] and 4.9 TeV in the muon channel [8], at the 95% confidence level (C.L.) in the SSM.

The search relies on events collected using single-electron or single-muon triggers with high transverse momentum thresholds. The dominant background source originates from Drell-Yan (DY) production of W bosons. Discrimination between signal and background events relies on the transverse mass (m_T) computed from the

*Full author list given at the end of the article.

Published by the American Physical Society under the terms of the [Creative Commons Attribution 4.0 International license](https://creativecommons.org/licenses/by/4.0/). Further distribution of this work must maintain attribution to the author(s) and the published article's title, journal citation, and DOI. Funded by SCOAP³.

charged-lepton transverse momentum (p_T) and the missing transverse momentum (whose magnitude is denoted E_T^{miss}) in the event:

$$m_T = \sqrt{2p_T E_T^{\text{miss}}(1 - \cos \phi_{\ell\nu})},$$

where $\phi_{\ell\nu}$ is the angle between the charged lepton and missing transverse momentum directions in the transverse plane.¹ Final interpreted results are based on a statistical analysis in which the shape of the signal and both the shape and normalization of the background expectations are derived from Monte Carlo (MC) simulation, except for the background contribution arising from jets misidentified as leptons or from hadron decays. The results presented in this article compared with those from Ref. [7] benefit from an increase in the integrated luminosity by a factor of 4; several upgrades in reconstruction software, including a new algorithm for electron reconstruction [9] and an improved treatment of the relative alignment between the inner tracker and the muon spectrometer; and several interpretations with reduced or no model dependence.

II. ATLAS DETECTOR

The ATLAS experiment [10] at the LHC is a multipurpose particle detector with a forward-backward symmetric cylindrical geometry and a near 4π coverage in solid angle. It consists of an inner detector for tracking surrounded by a thin superconducting solenoid providing a 2T axial magnetic field, electromagnetic (EM) and hadronic calorimeters, and a muon spectrometer. The inner detector covers the pseudorapidity range $|\eta| < 2.5$. It consists of silicon pixel, silicon microstrip, and transition radiation tracking detectors. An additional innermost pixel layer [11,12] inserted at a radius of 3.3 cm has been used since 2015. Liquid-argon (LAr) sampling calorimeters provide EM energy measurements with high granularity. A hadronic scintillator-tile calorimeter covers the central pseudorapidity range ($|\eta| < 1.7$). The end cap and forward regions are instrumented with LAr calorimeters for both the EM and hadronic energy measurements up to $|\eta| = 4.9$. The muon spectrometer surrounds the calorimeters and features three large air-core toroidal superconducting magnet systems with eight coils each. The field integral of the toroids ranges between 2.0 and 6.0 Tm across most of the detector. The muon spectrometer includes a system of precision tracking chambers and fast detectors for

¹ATLAS uses a right-handed coordinate system with its origin at the nominal interaction point (IP) in the center of the detector and the z axis along the beam pipe. The x axis points from the IP to the center of the LHC ring, and the y axis points upwards. Cylindrical coordinates (r, ϕ) are used in the transverse plane, ϕ being the azimuthal angle around the z axis. The pseudorapidity is defined in terms of the polar angle θ as $\eta = -\ln \tan(\theta/2)$. Angular distance is measured in units of $\Delta R \equiv \sqrt{(\Delta\eta)^2 + (\Delta\phi)^2}$.

triggering. A two-level trigger system [13] is used to select events. The first-level trigger is implemented in hardware and uses a subset of the detector information to reduce the accepted rate to at most 100 kHz. This is followed by a software-based trigger level that reduces the accepted event rate to 1 kHz on average.

III. DATA AND MONTE CARLO SIMULATION SAMPLES

The data for the analysis were collected during Run 2 at the LHC at $\sqrt{s} = 13$ TeV and correspond to an integrated luminosity of 139 fb^{-1} after the requirement that beams were stable, all detector systems were functional, and the data satisfied a set of quality criteria. Single-electron triggers required that electron candidates satisfy either medium identification criteria [9] and have a transverse energy $E_T > 60$ GeV or loose identification criteria and have $E_T > 140$ GeV. For the 3.2 fb^{-1} collected in 2015, the E_T thresholds were 24 and 120 GeV, respectively. Single-muon triggers required the presence of at least one muon reconstructed in both the inner detector and the muon spectrometer with $p_T > 50$ GeV. The trigger efficiency for DY W boson events (relative to the full event selection described in Sec. IV) is estimated to be 99% in the electron channel and 85% in the muon channel, with little dependence on the m_T value.

Signal MC events with $W' \rightarrow e\nu$ and $W' \rightarrow \mu\nu$ decays in the SSM were produced at leading order (LO) with the PYTHIA v8.183 event generator [14] and the NNPDF23LO parton distribution function (PDF) set [15]. The A14 set of tuned parameters (i.e., the A14 tune) [16] was used for the parton showering and hadronization process. In the SSM, the couplings of the W' boson to SM fermions are chosen to be identical to those of the SM W boson, whereas the couplings to SM bosons are set to zero. The corresponding branching fraction for W' boson decays into leptons of one generation is 10.8% for $m(W') = 150$ GeV and decreases above the tb threshold to a nearly constant value of 8.2% for $m(W')$ above 1 TeV. Similarly, the ratio of the W' boson width to its mass varies from 2.7% for $m(W') = 150$ GeV to 3.5% above the tb threshold. Decays into the $\tau\nu$ final state with subsequent leptonic decay of the τ lepton are not included as they were found to add negligible signal acceptance in previous studies [17]. Interference between W' and W boson production is not included in this analysis.

The dominant background due to DY production of W bosons decaying into $e\nu$, $\mu\nu$, and $\tau\nu$ final states was simulated at next-to-leading order (NLO) with the POWHEG-BOX v2 event generator [18–21] using the CT10 PDF set [22]. Background events from DY production of Z/γ^* bosons decaying into ee , $\mu\mu$, and $\tau\tau$ final states were also simulated with the same event generator and PDF set. In both cases, PYTHIA v8.186 was used for the parton showering and hadronization process with the AZNLO tune [23]. The DY processes were generated separately in

different $\ell\nu$ or $\ell\ell$ mass ranges to guarantee that sufficiently large numbers of events remain after event selection in the full mass range relevant to the analysis. Cross sections calculated by POWHEG-BOX for both DY processes were corrected via mass-dependent K factors to account for QCD effects at next-to-next-to-leading order (NNLO) and electroweak (EW) effects at NLO. The QCD corrections were computed with VRAP v0.9 [24] and the CT14 NNLO PDF set [25]. These corrections increased the cross section by about 5% for $m_{\ell\nu} = 1$ TeV and 15% for $m_{\ell\nu} = 6$ TeV. The EW corrections were computed with MCSANC [26] in the case of QED effects due to initial-state radiation, interference between initial- and final-state radiation, and Sudakov logarithm single-loop corrections. These corrections were added to the NNLO QCD cross-section prediction in the so-called additive approach (see Sec. VI) because of a lack of calculations of mixed QCD and EW terms. As a result, the cross section decreased by about 10% for $m_{\ell\nu} = 1$ TeV and 20% for $m_{\ell\nu} = 6$ TeV. The effects due to QED final-state radiation were already included in the event generation using PHOTOS++ [27]. The QCD corrections based on VRAP and the CT14 NNLO PDF set were also applied to the signal samples. No electroweak corrections, beyond those already accounted for with PHOTOS++, were applied to the signal samples as those are model dependent.

Additional background sources from diboson (WW , WZ , and ZZ) production were simulated with the SHERPA v2.2.1 event generator [28] and the NNPDF30 NNLO PDF set [29]. These processes were computed at NLO for up to one additional parton and at LO for up to three partons. The production of top-quark pairs and single top quarks (in the s and Wt channels) was performed at NLO with POWHEG-BOX [30–32] and the NNPDF30 NLO PDF set interfaced with PYTHIA v8.183 and the A14 tune. Single top-quark production in the t channel was performed in the same way except for the use of the NNPDF3.04f NLO PDF set. The cross sections used to normalize the diboson MC samples are computed with SHERPA, and the top-quark pair cross section is taken to be 832_{-52}^{+46} pb for a top-quark mass of 172.5 GeV. This value is calculated at NNLO in QCD, including the summation of next-to-next-to-leading logarithmic soft gluon terms, with Top++2.0 [33–39]. A correction depending on the top-quark p_T value is applied to account for shape effects due to NNLO QCD and NLO EW corrections according to Ref. [40]. The cross sections for single top-quark production are computed at approximate NNLO accuracy [41–43].

For all MC samples, except those produced with SHERPA, b -hadron and c -hadron decays were handled by EVTGEN v1.2.0 [44]. Inelastic pp events generated using PYTHIA v8.186 with the A3 tune [45] and the NNPDF23LO PDF set were added to the hard-scattering interaction in such a way as to reproduce the effects of additional pp interactions in each bunch crossing during data collection

(pileup). The detector response was simulated with GEANT 4 [46,47], and the events were processed with the same reconstruction software as for the data. Energy/momentum scale and efficiency corrections are applied to the results of the simulation to account for small differences between the simulation and the performance measured directly from the data [9,48].

IV. EVENT RECONSTRUCTION AND SELECTION

The analysis relies on the reconstruction and identification of electrons and muons, as well as the missing transverse momentum in each event. Collision vertices are reconstructed with inner detector tracks that satisfy $p_T > 0.5$ GeV, and the primary vertex is chosen as the vertex with the largest Σp_T^2 for the tracks associated with the vertex.

Electron candidates are reconstructed by matching inner detector tracks to clusters of energy deposited in the EM calorimeter. Electrons must lie within $|\eta| < 2.47$, excluding the barrel–end cap transition region defined by $1.37 < |\eta| < 1.52$, and satisfy calorimeter energy cluster quality criteria. The cluster must have $E_T > 65$ GeV, and the associated track must have a transverse impact parameter significance relative to the beam axis $|d_0|/\sigma_{d_0} < 5$. Successful candidates are identified with a likelihood method and need to satisfy the tight identification criteria [9]. The likelihood relies on the shape of the EM shower measured in the calorimeter, the quality of the track reconstruction, and the quality of the match between the track and the cluster. To suppress electron candidates originating from photon conversions, hadron decays, or jets misidentified as electrons (hereafter referred to as fake electrons), electron candidates are required to satisfy the gradient isolation criteria [9] based on both tracking and calorimeter measurements. The reconstruction and identification efficiency rises from approximately 80% at $p_T = 60$ GeV to 90% above 500 GeV, and the isolation efficiency is slightly higher than 99% for p_T values above 200 GeV. The electron energy resolution for $E_T > 1$ TeV can be characterized by $\sigma(E)/E = c_e$, with c_e varying between 0.007 and 0.012 [9] in the range $|\eta| < 1.2$ which dominates the high-mass part of the search. The corresponding m_T resolution ranges from approximately 1.3% at m_T values near 2 TeV to 1.0% near 6 TeV.

Muon candidates are reconstructed by matching inner detector tracks with muon spectrometer tracks and by reconstructing a final track combining the measurements from both detector systems while taking the energy loss in the calorimeter into account. The candidates must satisfy quality selection criteria optimized for high- p_T performance [48] by requiring the candidate tracks to have associated measurements in the three different chamber layers of the muon spectrometer. The tracks must also have consistent charge-to-momentum ratio measurements in the inner detector and muon spectrometer, have sufficiently

small relative uncertainty in the charge-to-momentum ratios for the combined tracks, and be located in detector regions with high-quality chamber alignment. Candidates must have $|\eta| < 2.5$, $p_T > 55$ GeV, $|d_0|/\sigma_{d_0} < 3$, and $|z_0| \sin \theta < 0.5$ mm, where z_0 is the longitudinal impact parameter relative to the primary vertex. The reconstruction and identification efficiency is 69% for $p_T = 1$ TeV and decreases to 57% for $p_T = 2.5$ TeV. Muon candidates from hadron decays are suppressed by imposing a track-based isolation [48] that achieves an efficiency higher than 99% for the full p_T range of interest. The muon p_T resolution at $p_T > 1$ TeV can be described as $\sigma(p_T)/p_T = c_\mu p_T$, with c_μ varying between 0.08 and 0.20 TeV^{-1} depending on the detector region [48]. This resolution dominates the m_T resolution in the muon channel.

Jets are reconstructed from topological clusters of energy deposits in calorimeter cells [49] with the anti- k_r clustering algorithm [50] implemented in FASTJET [51]. A radius parameter R equal to 0.4 is used, and the clusters are calibrated at the EM scale [52]. Jets are required to have $p_T > 20$ (30) GeV for $|\eta|$ smaller (greater) than 2.4. To remove jets originating from pileup, jet-vertex tagging is applied [53].

The event's missing transverse momentum is computed as the vectorial sum of the transverse momenta of leptons, photons, and jets. The overlap between these is resolved according to Ref. [54]. Electrons and muons must pass the selection requirements described above. In addition to the above particles and jets, the E_T^{miss} calculation includes a *soft term* [54] accounting for the contribution from tracks associated with the primary vertex but not associated with leptons, converted photons, or jets already included in the E_T^{miss} calculation.

Events are required to have a primary vertex. They are rejected if any of the jets fail to pass a cleaning procedure designed to suppress noncollision background and calorimeter noise [55].

In the electron channel, events must have exactly one electron passing the selection described above. Events are vetoed if they contain any additional electron candidate satisfying the medium selection criteria and having $p_T > 20$ GeV. Events are also vetoed if they contain any muon candidate satisfying the medium selection criteria and having $p_T > 20$ GeV. The missing transverse momentum must satisfy $E_T^{\text{miss}} > 65$ GeV, and the transverse mass must satisfy $m_T > 130$ GeV. In the muon channel, events must have exactly one selected muon as detailed above, and the same veto on additional electron and muon candidates is applied, except that electron candidates close to the muon ($\Delta R < 0.1$) are assumed to arise from photon radiation from the muon and are thus not considered as additional electron candidates. Events are required to satisfy $E_T^{\text{miss}} > 55$ GeV and $m_T > 110$ GeV in the muon channel. The event selection described above defines the signal regions in the electron and muon

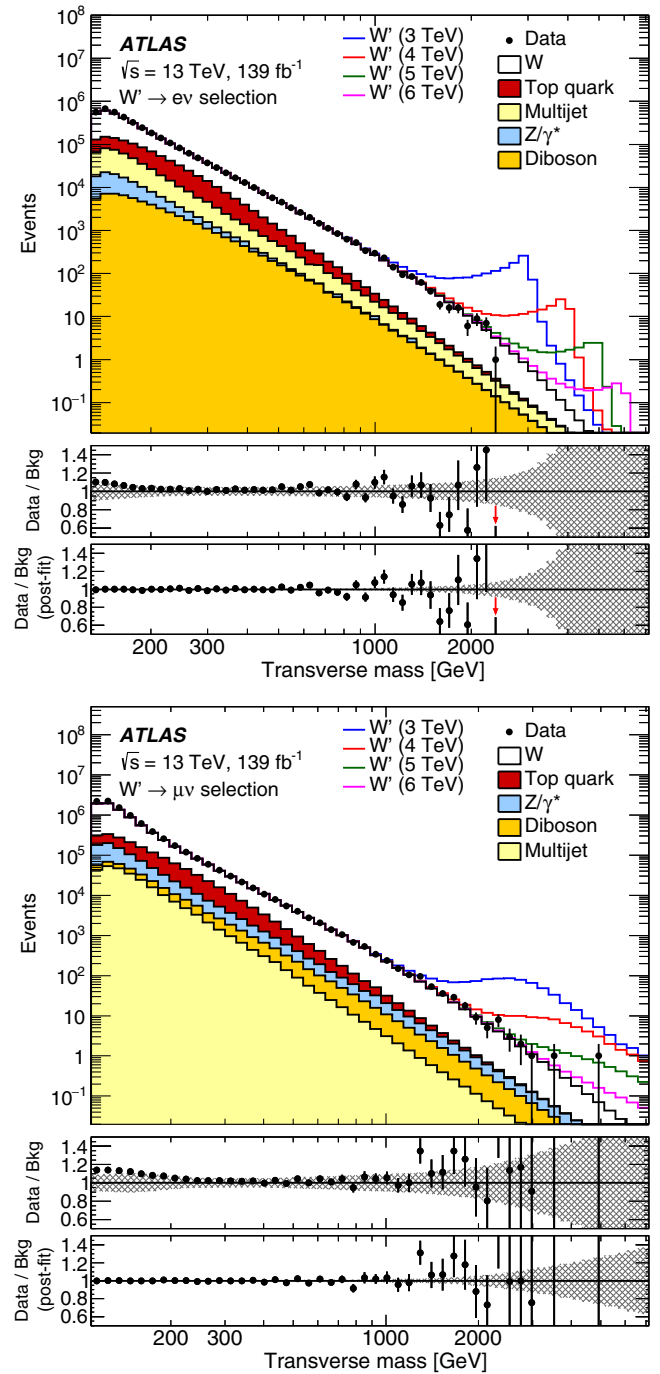


FIG. 1. Distributions of the transverse mass for data and predicted background events in the electron (top) and muon (bottom) channels. Expected signal distributions for several SSM W' boson masses are shown stacked on top of the total expected background. The middle panels show ratios of the number of events observed in the data to the expected total background count, while the lower panels show the same ratio when taking into account the pulls on the nuisance parameters observed in the statistical analysis (Sec. VII). The hatched bands represent the total uncertainty in the background estimate (Sec. VI). Arrows in the middle and lower panels for the electron channel indicate data points that lie outside the vertical axis range.

channels. In these regions, the acceptance times efficiency for W' signal events decreases from 79% (52%) to 64% (44%) as the W' boson mass increases from 2 to 7 TeV in the electron (muon) channel. The decrease at high $m(W')$ is generally due to the combined effect of a growing low-mass tail at larger $m(W')$ and the kinematic selection thresholds. In the case of the muon channel, it also originates from a decrease in the identification efficiency at higher p_T values due to the requirements on the charge-to-momentum measurement.

V. BACKGROUND ESTIMATION AND EVENT YIELDS

The background from DY production of W and Z/γ^* bosons as well as from top-quark pair, single top quark, and diboson production is modeled with the MC samples described in Sec. III. To compensate for the limited number of events at high m_T , the smoothly falling m_T distributions for top-quark (corresponding to both pair and single production) and diboson samples are fitted and extrapolated to high m_T with the following functions commonly used in dijet searches (e.g., Refs. [56,57]):

$$f^{\text{bkg1}}(m_T) = e^{-a} m_T^b m_T^{c \log(m_T)} \quad \text{and} \quad (1)$$

$$f^{\text{bkg2}}(m_T) = \frac{a}{(m_T + b)^c}.$$

Function f^{bkg1} is the nominal extrapolation function for the top-quark background in both the electron and muon

channels as well as for the diboson background in the electron channel. Function f^{bkg2} is the nominal function for the diboson background in the muon channel. In all cases, checks are performed to guarantee that the function reproduces the event yields at lower m_T values and that its cumulative distribution (starting from the highest m_T values) is consistent with the small integrated event yields available in the MC samples.

The background contribution from events with fake electrons or muons mostly originates from multijet production and is extracted from the data using the same matrix method as used in previous analyses and described in Ref. [58]. This method relies on data samples in which the electron or muon selection is loosened (referred to as the *loose* selection). The efficiency for those lepton candidates to pass the nominal lepton selection (*tight*) is measured to derive an estimate of the background from fake leptons. The *loose* selection is close to that applied by the trigger requirements. The fraction f of fake leptons passing the *loose* selection that also pass the nominal lepton selection is estimated from the data in background-enriched control regions that are orthogonal to the signal regions. These control regions are built by requiring that there are no $Z \rightarrow \ell\ell$ candidates formed by combining the selected lepton with a loose lepton in the event and that the E_T^{miss} value is less than 60 (55) GeV in the electron (muon) channel. Additional requirements are placed on the minimum impact parameter, the presence of at least one jet, and the proximity of the missing transverse momentum vector to the lepton in the muon channel to reduce the contribution

TABLE I. Number of events in the data and the total expected background passing the full event selection in different m_T ranges. Expected numbers of W' signal events are provided for several different masses. The uncertainties include both statistical and systematic sources of uncertainty.

| Electron channel | | | | | | |
|------------------|----------------------------|--------------------|-----------------|-----------------|-----------------|-----------------|
| m_T [GeV] | 130–400 | 400–600 | 600–1000 | 1000–2000 | 2000–3000 | 3000–10 000 |
| Data | 3 538 403 | 35 568 | 7358 | 818 | 17 | 0 |
| Background | $3\,320\,000 \pm 250\,000$ | $34\,800 \pm 1500$ | 7200 ± 400 | 830 ± 80 | 20.2 ± 3.1 | 1.3 ± 0.5 |
| W' (2 TeV) | 574 ± 22 | 720 ± 40 | 2190 ± 120 | 12200 ± 600 | 1130 ± 290 | 3.20 ± 0.25 |
| W' (3 TeV) | 68.4 ± 1.9 | 58.6 ± 2.6 | 127 ± 7 | 448 ± 22 | 860 ± 40 | 87 ± 23 |
| W' (4 TeV) | 19.6 ± 0.5 | 13.2 ± 0.5 | 22.1 ± 1.1 | 44.3 ± 2.2 | 49.2 ± 2.3 | 86 ± 4 |
| W' (5 TeV) | 7.85 ± 0.19 | 4.99 ± 0.18 | 7.26 ± 0.35 | 9.9 ± 0.5 | 5.82 ± 0.28 | 13.6 ± 0.7 |
| W' (6 TeV) | 3.76 ± 0.09 | 2.35 ± 0.08 | 3.28 ± 0.16 | 3.82 ± 0.18 | 1.41 ± 0.07 | 2.01 ± 0.10 |
| Muon channel | | | | | | |
| m_T [GeV] | 110–400 | 400–600 | 600–1000 | 1000–2000 | 2000–3000 | 3000–10 000 |
| Data | 8 751 095 | 26 225 | 5393 | 622 | 22 | 2 |
| Background | $7\,800\,000 \pm 700\,000$ | $25\,800 \pm 1400$ | 5300 ± 400 | 570 ± 50 | 18 ± 4 | 2.3 ± 0.9 |
| W' (2 TeV) | 490 ± 14 | 594 ± 26 | 1680 ± 90 | 6700 ± 500 | 1520 ± 210 | 70 ± 50 |
| W' (3 TeV) | 58.1 ± 1.4 | 45.5 ± 1.9 | 102 ± 6 | 322 ± 31 | 380 ± 50 | 160 ± 40 |
| W' (4 TeV) | 16.3 ± 0.4 | 9.64 ± 0.34 | 15.9 ± 0.8 | 32.2 ± 3.4 | 34 ± 5 | 44 ± 13 |
| W' (5 TeV) | 6.50 ± 0.15 | 3.55 ± 0.12 | 4.98 ± 0.22 | 6.7 ± 0.6 | 3.9 ± 0.6 | 7.2 ± 2.3 |
| W' (6 TeV) | 3.11 ± 0.07 | 1.67 ± 0.06 | 2.22 ± 0.10 | 2.45 ± 0.17 | 0.88 ± 0.12 | 1.09 ± 0.35 |

from prompt muons. The remaining contributions from prompt electrons and muons in these control regions are subtracted using MC simulation. The number of jets misidentified as leptons (N_T^{multijet}) in the signal regions is computed as

$$N_T^{\text{multijet}} = fN_F = \frac{f}{r-f} [r(N_L + N_T) - N_T],$$

where N_F is the number of fake leptons that pass the *loose* lepton selection, N_L is the number of lepton candidates that pass the *loose* lepton selection but fail the nominal lepton selection, and N_T is the number of lepton candidates that pass the nominal lepton selection. The numbers N_L and N_T are extracted from the signal regions. In addition, the quantity r , corresponding to the fraction of real leptons satisfying the nominal selection in the sample of *loose* candidates, is computed from the DY W boson MC samples. Like for the top-quark and diboson background sources, the m_T distribution is extrapolated to high values by using a function with the same form as in Eq. (1) in the electron channel and the function $f^{\text{multijet}}(m_T) = am_T^{-b}$ in the muon channel. The same set of checks concerning the quality of the extrapolation are performed as for the top-quark and diboson backgrounds.

The m_T distributions in data and simulation are shown in Fig. 1, and the numbers of events in several m_T ranges are presented in Table I. No event is observed beyond m_T values of 10 TeV in either channel. The features observed in these distributions are discussed in Sec. VII. The DY W boson contribution dominates the total background with a fraction varying between approximately 69% (72%) and 95% (88%) in the electron (muon) channel. Other background contributions arise mostly from DY Z/γ^* boson, top-quark, and diboson production. The contribution from multijet events in the electron channel decreases from approximately 10% at the lowest m_T values to less than 5% at high m_T , and in the muon channel it is less than 3.2% (1.7%) for m_T values below (above) 600 GeV.

VI. SYSTEMATIC UNCERTAINTIES

Systematic uncertainties arise from experimental sources affecting the lepton reconstruction and identification as well as the missing transverse momentum, from the data-driven multijet background estimate, from theoretical sources affecting the shape and normalization of background processes, and from the extrapolation of background estimates to high m_T values.

Experimental uncertainties in the electron trigger, reconstruction, identification, and isolation efficiencies are extracted individually from studies of $Z \rightarrow ee$ and $J/\psi \rightarrow ee$ decays in the data using a tag-and-probe method [9]. These studies also yield uncertainties in the electron energy scale and resolution [9]. Uncertainties in the muon trigger, reconstruction, identification, and isolation

efficiencies are derived from studies of $Z \rightarrow \mu\mu$ and $J/\psi \rightarrow \mu\mu$ decays in the data [48]. The muon momentum scale and resolution uncertainties are extracted from those studies as well as from special chamber-alignment datasets with the toroidal magnetic field turned off [48]. Extrapolation uncertainties toward higher p_T are based on the above studies as well as on the simulation. The impact of those uncertainties is generally small due to the limited p_T dependence of the efficiencies, except for the high- p_T muon reconstruction and identification efficiency. The latter is estimated from differences between data and simulation in the fraction of muons passing the requirement on the maximum allowed relative error in the charge-to-momentum ratio measurement. This uncertainty grows with the muon p_T up to 35% (55%) for $|\eta| < 1.05$ (> 1.05) at the highest m_T values probed in this analysis; it becomes a dominant source of uncertainty at the highest m_T values. Uncertainties in the reconstruction and calibration of jets are taken into account since those are input to the E_T^{miss} calculation. Finally, all uncertainties affecting electrons, muons, jets, and the soft term are propagated to the E_T^{miss} calculation. The jet energy resolution and soft term contributions have the largest impact at low m_T , and their uncertainties are treated as fully correlated between the electron and muon channels. Uncertainties in the simulation of pileup contributions have little impact on the m_T distribution and are thus neglected.

The uncertainty in the multijet background estimate includes the effect of varying the criteria used in the background-enriched sample selection, and changes in the fractions f are propagated. As this background estimate is extrapolated with a functional fit at high m_T values, the uncertainty includes the additional impact of variations in the fit range. In the electron channel, the uncertainty also includes a contribution from the variation of the functional form due to the larger multijet contribution at high m_T in this channel. This extrapolation uncertainty dominates the overall background uncertainty at m_T values above 3 TeV in the electron channel.

No theory uncertainty is applied to the signal. Uncertainties in the theory inputs used for the background estimation are evaluated as follows. One of the largest uncertainties affecting the dominant DY background comes from the use of 90% C.L. eigenvector variations for the CT14 NNLO PDF set. This uncertainty range encompasses the predictions based on the ABM12 [59], CT10 [22], MMHT14 [60], and JR14 [61] PDF sets. It also allows for a sufficiently robust range of predictions in the very high mass region (i.e., at high Bjorken x). In addition, a reduced set of CT14 NNLO PDF eigenvectors that preserves the potential mass-dependent shape changes is used in the limit-setting procedure. The PDF uncertainty is enlarged in specific $\ell\nu$ mass regions to encompass the DY prediction based on the alternative NNPDF30 PDF set if this prediction lies outside the range from the CT14 NNLO

eigenvector variations. A smaller PDF choice uncertainty is obtained in the muon channel at high m_T values than in the electron channel because the significantly worse muon p_T resolution causes migration of events from low m_T values (where the PDF uncertainty is small) to high m_T values. The uncertainty in the mass-dependent K factors used to correct the mass distributions to predictions at NNLO accuracy in α_s is evaluated by simultaneously varying the renormalization and factorization scales up and down by factors of 2. The largest change (up or down) at each mass value is then applied as a symmetric scale uncertainty. The EW correction uncertainty is taken to be the difference between the predictions obtained with either the multiplicative scheme $[(1 + \delta_{EW}) \times (1 + \delta_{QCD})]$ or the additive scheme $(1 + \delta_{EW} + \delta_{QCD})$ for the combination of higher-order EW (δ_{EW}) and QCD (δ_{QCD}) effects. The DY cross-section prediction accounts for varying the strong coupling constant according to $\alpha_s(m_Z) = 0.118 \pm 0.002$, a variation that corresponds to a 90% C.L. uncertainty range [25] that nevertheless has a small impact on the analysis. Although the $t\bar{t}$ cross-section uncertainty is only about 6% [62] and the corresponding impact on the total background is small, it is accounted for in the statistical analysis due the characteristic m_T distribution shape for this background source. An m_T -dependent uncertainty in the $t\bar{t}$ shape is also included. It corresponds to the remaining level of disagreement between the data and the simulation after the correction described in Sec. III. This uncertainty is evaluated in a control region consisting of events with both an electron and a muon candidate, which is a region dominated by $t\bar{t}$ events.

The diboson cross-section uncertainty is neglected due to its small impact on the analysis. However, the extrapolation uncertainty for the diboson background is included in the statistical analysis as it grows to become significant at higher m_T values. This uncertainty is estimated by varying the range of m_T values over which the fit is performed and by changing the functional form. The extrapolation uncertainty for the top-quark background is neglected due to its small impact.

The uncertainty in the integrated luminosity is 1.7% [63].

Table II summarizes the systematic uncertainties for the total background and signal in the electron and muon channels at m_T values near 2 and 6 TeV. The values in Table II correspond to the uncertainties that are incorporated as input to the statistical analysis described in Sec. VII. Large uncertainties in the background yields near m_T values of 6 TeV are obtained but those have little impact on the statistical analysis due to the small background expectation at such high m_T values (e.g., the number of background events for $m_T > 5.1$ TeV is 0.02 in the electron channel and 0.11 in the muon channel).

VII. RESULTS

The m_T distributions in the electron and muon channels (Fig. 1) provide the input data to the statistical analysis. This analysis proceeds as a multibin counting experiment with a likelihood accounting for the Poisson probability to observe a number of events in data given the expected number of background and signal events in each bin.

TABLE II. Systematic uncertainties in the expected number of events for the total background and for a W' boson with a mass of 2 (6) TeV. The uncertainties are estimated with the binning shown in Fig. 1 at $m_T = 2$ (6) TeV for the background and in a three-bin window around $m_T = 2$ (6) TeV for the signal. Uncertainties that are not applicable are denoted “N/A,” and “negl.” means that the uncertainty is not included in the statistical analysis because its impact on the result is negligible at any m_T value. Small uncertainties that appear in the table (e.g., those listed as $<0.5\%$) are not negligible at m_T values lower than 2 TeV and are thus listed. Sources of uncertainty not included in the table are neglected in the statistical analysis.

| Source | Electron channel | | | | Muon channel | | | |
|--|------------------|---------------|---------------|---------------|---------------|---------------|---------------|---------------|
| | Background | | Signal | | Background | | Signal | |
| | $m_T = 2$ TeV | $m_T = 6$ TeV | $m_T = 2$ TeV | $m_T = 6$ TeV | $m_T = 2$ TeV | $m_T = 6$ TeV | $m_T = 2$ TeV | $m_T = 6$ TeV |
| Trigger | negl. | (negl.) | negl. | (negl.) | 1.1% | (1.0%) | 1.2% | (1.2%) |
| Lepton reconstruction and identification | 4.1% | (1.4%) | 4.3% | (4.3%) | 8.9% | (37%) | 6.6% | (38%) |
| Lepton momentum scale and resolution | 3.9% | (2.7%) | 2.7% | (4.5%) | 12% | (47%) | 13% | (20%) |
| E_T^{miss} resolution and scale | $<0.5\%$ | ($<0.5\%$) | $<0.5\%$ | ($<0.5\%$) | $<0.5\%$ | ($<0.5\%$) | $<0.5\%$ | ($<0.5\%$) |
| Jet energy resolution | $<0.5\%$ | ($<0.5\%$) | $<0.5\%$ | ($<0.5\%$) | $<0.5\%$ | (0.6%) | $<0.5\%$ | ($<0.5\%$) |
| Multijet background | 4.4% | (420%) | N/A | (N/A) | 0.8% | (1.5%) | N/A | (N/A) |
| Top-quark background | 0.8% | (1.9%) | N/A | (N/A) | 0.7% | ($<0.5\%$) | N/A | (N/A) |
| Diboson extrapolation | 1.5% | (47%) | N/A | (N/A) | 1.3% | (9.7%) | N/A | (N/A) |
| PDF choice for DY | 1.0% | (10%) | N/A | (N/A) | $<0.5\%$ | (1.0%) | N/A | (N/A) |
| PDF variation for DY | 8.1% | (13%) | N/A | (N/A) | 7.4% | (14%) | N/A | (N/A) |
| EW corrections for DY | 4.2% | (4.5%) | N/A | (N/A) | 3.7% | (7.0%) | N/A | (N/A) |
| Luminosity | 1.6% | (1.1%) | 1.7% | (1.7%) | 1.7% | (1.7%) | 1.7% | (1.7%) |
| Total | 12% | (430%) | 5.4% | (6.4%) | 17% | (62%) | 15% | (43%) |

The uncertainties are taken into account via nuisance parameters implemented as log-normal constraints on the expected event yields. The parameter of interest is the cross section $\sigma(pp \rightarrow W' \rightarrow \ell\nu)$. The combined fits to the electron and muon channels are performed taking correlations between the two channels into account.

The compatibility of the observed data with the background-only model is tested by computing a frequentist p value based on the profile likelihood ratio as the test statistic [64]. The p value corresponds to the probability for the background to yield an excess equal to or larger than that observed in data. In the electron channel, the lowest p value is obtained for $m(W') = 625$ GeV with a local significance of 2.8 standard deviations, corresponding to a global significance of 1.3 standard deviations when taking the look-elsewhere effect into account. In the muon channel, the lowest p value is obtained for $m(W') = 200$ GeV with local and global significances of 2.1 and 0.4 standard deviations, respectively. For the combination of the two channels, the lowest p value occurs for $m(W') = 625$ GeV with local significance of 1.8 standard deviations, and the corresponding global significance is -0.5 standard deviations (i.e., the fluctuation in the data is smaller than the median of the distribution obtained with background-only pseudoexperiments). In all cases, the interpretation is performed in the context of the SSM.

Given that no significant deviation from the background expectation is observed, upper limits are set on $\sigma(pp \rightarrow W' \rightarrow \ell\nu)$ following a Bayesian approach with a uniform and positive prior for the cross section. This choice of prior is the same as that used in previous searches [7,8]. The marginalization of the posterior probability is performed using Markov chain sampling with the Bayesian Analysis Toolkit [65]. Upper limits set at the 95% C.L. in the context of the SSM are presented in Fig. 2 for the electron and muon channels individually as well as for their combination, assuming universal W' boson couplings to leptons. The combined results are provided in terms of W' boson decays into leptons of a single generation. The corresponding lower limits on the W' boson mass are summarized in Table III. Weaker limits are obtained in the muon channel due to the lower signal acceptance times efficiency and the worse momentum resolution at high p_T .

The lower panels of Fig. 1 show the ratio of the data to the background prediction before (middle panel) and after (lower panel) marginalization of the nuisance parameters, with the latter resulting from the combined fit to the electron and muon channels. A difference in event yields is observed at low m_T values for both the electron and muon channels, although it remains within the range of uncertainty before marginalization. This difference decreases after marginalization, with the largest deviations from nominal values occurring for the jet energy resolution and E_T^{miss} track soft term nuisance parameters. The latter

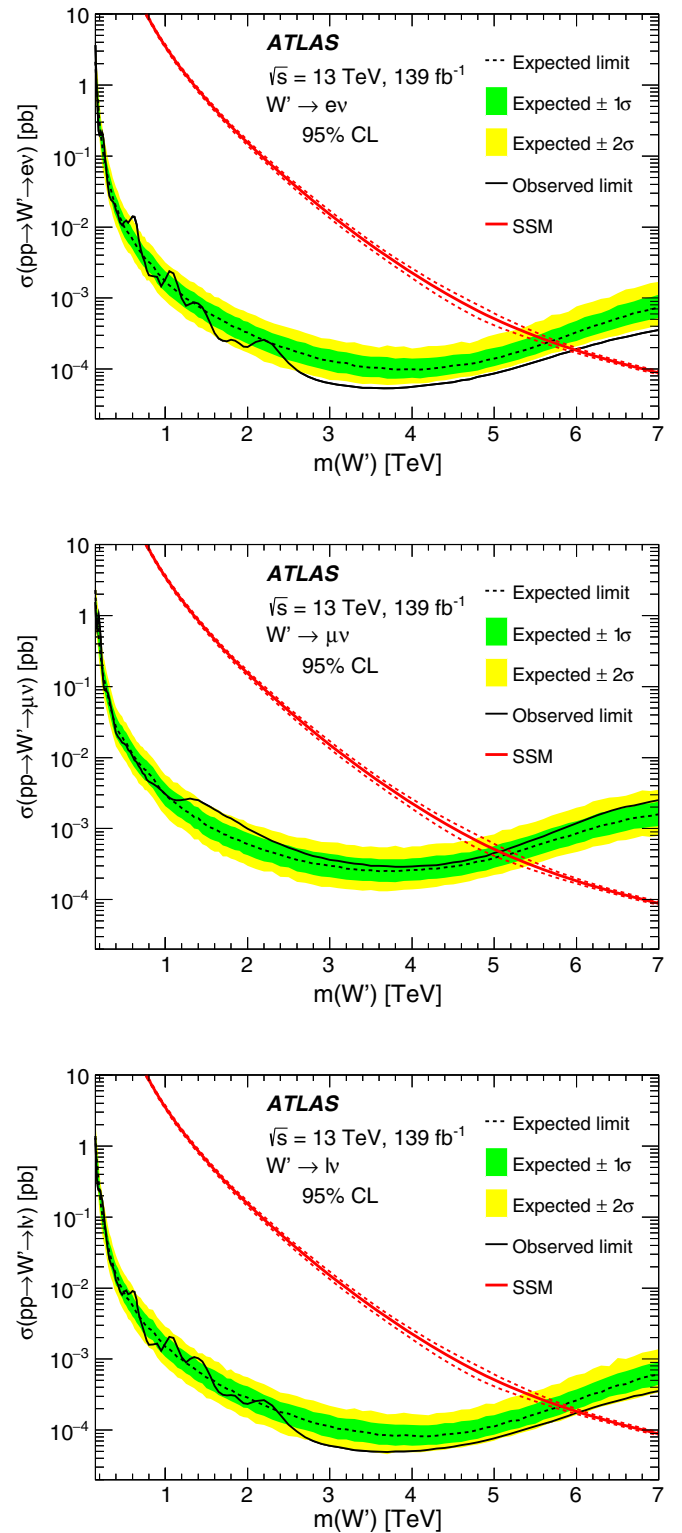


FIG. 2. Observed and expected upper limits at the 95% C.L. on the $pp \rightarrow W' \rightarrow \ell\nu$ cross section in the electron (top), muon (middle), and combined (bottom) channels as a function of W' mass in the sequential Standard Model. The dashed lines surrounding the SSM cross-section curve (solid line) correspond to the combination of PDF, α_s , renormalization, and factorization scale uncertainties (for illustration only).

TABLE III. Observed and expected 95% C.L. lower limits on the W' mass in the electron and muon channels and their combination for the sequential Standard Model.

| Decay | $m(W')$ lower limit [TeV] | |
|--------------------------|---------------------------|----------|
| | Observed | Expected |
| $W' \rightarrow e\nu$ | 6.0 | 5.7 |
| $W' \rightarrow \mu\nu$ | 5.1 | 5.1 |
| $W' \rightarrow \ell\nu$ | 6.0 | 5.8 |

includes a significant model dependence found by comparing the predictions from the POWHEG-BOX, MADGRAPH5_aMC@NLO [66], and SHERPA event generators, with the first two interfaced with PYTHIA 8 for parton showering and hadronization.

The results displayed in Fig. 2 are obtained with the full signal line shape from the SSM with no interference between the W' signal and the SM DY background. If the signal line shape is restricted to the W' peak region by the requirement $m_{\ell\nu} > 0.85 \times m(W')$, the interference effects in the low-mass tail of the distributions are largely suppressed and the observed (expected) mass limits become weaker by 270 (100) GeV in the electron channel and 30 (90) GeV in the muon channel, relative to the mass limits shown in Table III. The $m_{\ell\nu} > 0.85 \times m(W')$ requirement is applied at the event generator level, considering charged leptons before final-state radiation.

Limits are provided for the production of a generic resonance with a fixed Γ/m value. For these results, fiducial cross-section limits are obtained with a requirement that removes the low-mass tail: $m_{\ell\nu} > 0.3 \times m(W')$. The region below $0.3 \times m(W')$ coincides with the lower- m_T region where the background is large and the sensitivity to signal contributions is reduced. The observed 95% C.L. upper limits on the fiducial cross section for $pp \rightarrow W' \rightarrow \ell\nu$ with different choices of Γ/m from 1% to 15% are shown in Fig. 3. Less stringent limits are obtained for larger resonance widths since a larger fraction of the signal occurs in the low- m_T tail where the background is higher. The cross-section upper limits obtained in the fiducial region are lower than the ones obtained in the full phase space, in particular at high $m(W')$ where the total cross section has a large contribution from outside the fiducial region due to the low- m_T tail. The lower values of the cross-section limits do not indicate that the fiducial limits exclude a broader set of models, as corresponding theoretical predictions are also lower in the fiducial than in the total phase space.

To facilitate further interpretations of the results, model-independent upper limits are also provided for the number of signal events N_{sig} in single-bin signal regions obtained by varying the minimum m_T value m_T^{min} in the range between 130 (110) GeV and 5127 (5127) GeV in the electron (muon) channel. These limits are translated into limits on the visible cross section σ_{vis} computed as $N_{\text{sig}}/\mathcal{L}$, where \mathcal{L} is the

integrated luminosity. The visible cross section corresponds to the product of cross section times acceptance times efficiency and the observed 95% C.L. upper limits vary from 4.6 (15) pb at $m_T^{\text{min}} = 130$ (110) GeV to 22 (22) ab at

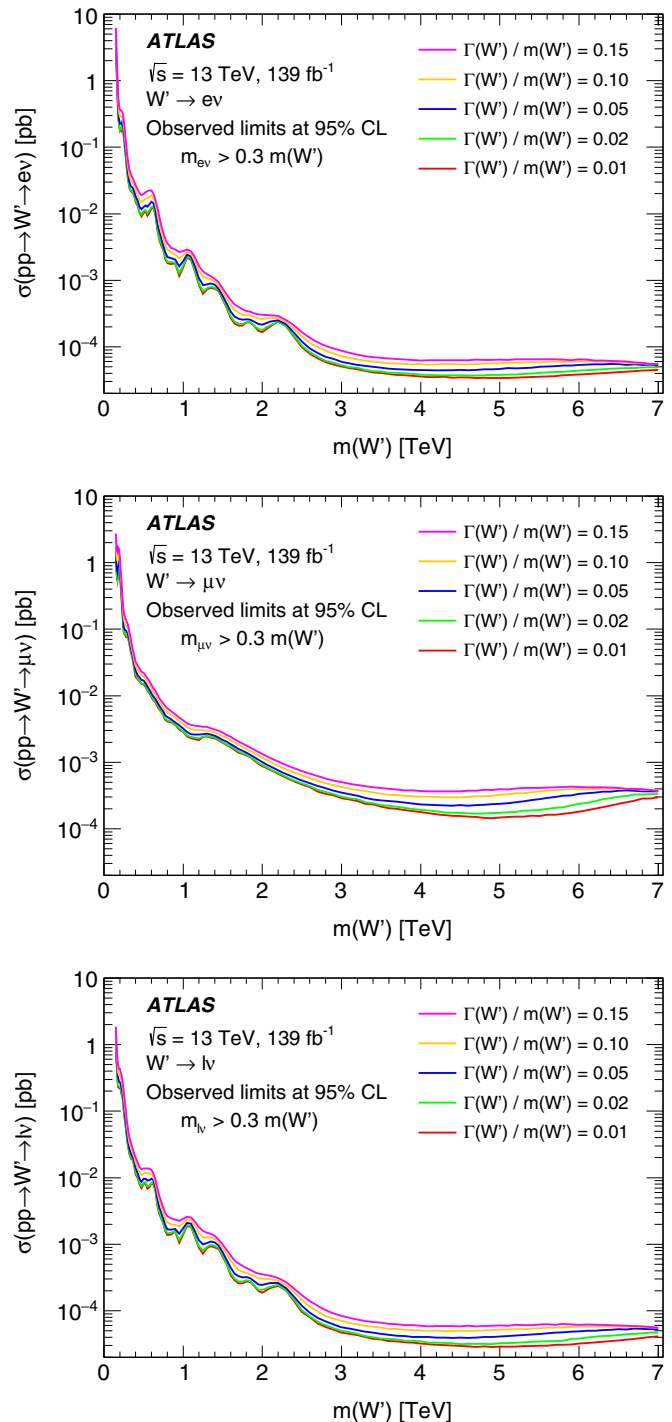


FIG. 3. Observed upper limits at the 95% C.L. on the fiducial cross section for $pp \rightarrow W' \rightarrow \ell\nu$ in the electron (top), muon (middle), and combined (bottom) channels as a function of W' mass for a number of different choices of $\Gamma(W')/m(W')$ ranging between 1% and 15%.

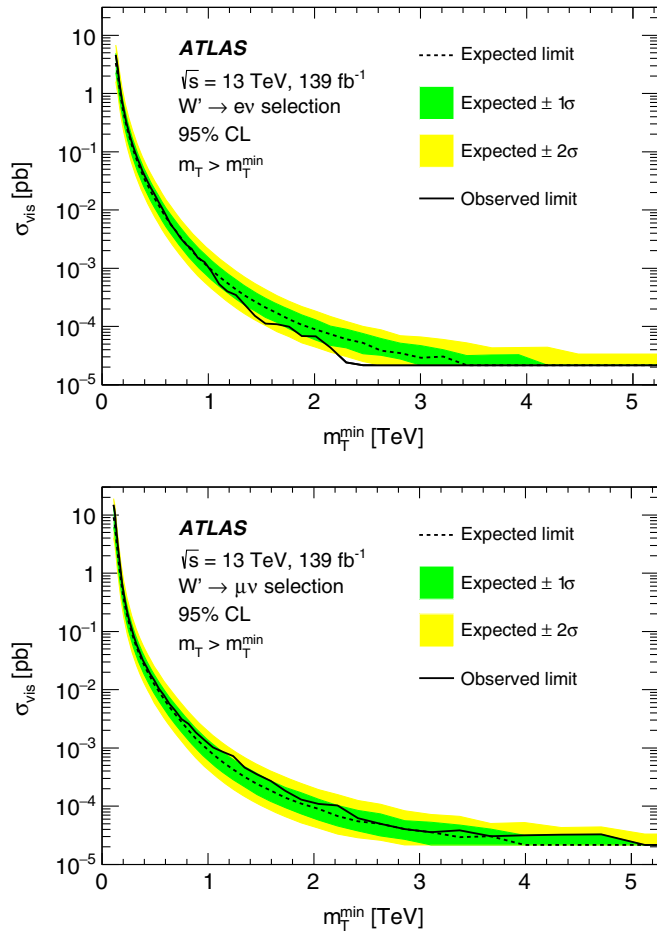


FIG. 4. Observed and expected model-independent upper limits at the 95% C.L. on the visible cross section in the electron (top) and muon (bottom) channels as a function of the m_T threshold m_T^{\min} . The limits are obtained at discrete m_T^{\min} values and are connected by a straight line for illustration purposes.

high m_T^{\min} in the electron (muon) channel as shown in Fig. 4. Further details about these model-independent limits are available in the Appendix.

VIII. CONCLUSION

A search for a heavy resonance decaying into a charged lepton and a neutrino is carried out in events with an isolated electron or muon and missing transverse momentum. The data sample corresponds to 139 fb^{-1} of pp collisions at $\sqrt{s} = 13 \text{ TeV}$ collected in 2015–2018 with the ATLAS detector at the LHC. Events are selected with single-electron and single-muon triggers, and the transverse mass computed from the lepton p_T and the missing transverse momentum is used as the discriminating variable between signal and background contributions. The latter is dominated by Drell-Yan production of W bosons. Monte Carlo simulation is used to estimate the normalization and shape of the m_T distributions for signal and background events, except for the multijet background, which is derived from the data.

The observed m_T distributions are found to be consistent with the background expectations, and upper limits are set on the cross section for $pp \rightarrow W' \rightarrow \ell \nu$, where the charged lepton is either an electron or a muon. Limits are also provided for the combination of the electron and muon channels. Lower limits of 6.0 and 5.1 TeV on the W' boson mass are set at 95% C.L. in the electron and muon channels, respectively, in the context of the sequential Standard Model. Fiducial cross-section limits are set on the production of resonances with different Γ/m values ranging from 1% to 15%. To allow for further interpretations of the results, a set of model-independent upper limits are presented for the number of signal events and for the visible cross section above a given transverse mass threshold. These vary from 4.6 (15) pb at $m_T^{\min} = 130$ (110) GeV to 22 (22) ab at high m_T^{\min} in the electron (muon) channel.

ACKNOWLEDGMENTS

We thank CERN for the very successful operation of the LHC, as well as the support staff from our institutions without whom ATLAS could not be operated efficiently. We acknowledge the support of ANPCyT, Argentina; YerPhI, Armenia; ARC, Australia; BMWFW and FWF, Austria; ANAS, Azerbaijan; SSTC, Belarus; CNPq and FAPESP, Brazil; NSERC, NRC, and CFI, Canada; CERN; CONICYT, Chile; CAS, MOST, and NSFC, China; COLCIENCIAS, Colombia; MSMT CR, MPO CR, and VSC CR, Czech Republic; DNRF and DNSRC, Denmark; IN2P3-CNRS, CEA-DRF/IRFU, France; SRNSFG, Georgia; BMBF, HGF, and MPG, Germany; GSRT, Greece; RGC, Hong Kong SAR, China; ISF and Benoziyo Center, Israel; INFN, Italy; MEXT and JSPS, Japan; CNRST, Morocco; NWO, Netherlands; RCN, Norway; MNiSW and NCN, Poland; FCT, Portugal; MNE/IFA, Romania; MES of Russia and NRC KI, Russian Federation; JINR; MESTD, Serbia; MSSR, Slovakia; ARRS and MIZŠ, Slovenia; DST/NRF, South Africa; MINECO, Spain; SRC and Wallenberg Foundation, Sweden; SERI, SNSF, and Cantons of Bern and Geneva, Switzerland; MOST, Taiwan; TAEK, Turkey; STFC, United Kingdom; DOE and NSF, United States of America. In addition, individual groups and members have received support from BCKDF, CANARIE, CRC, and Compute Canada, Canada; COST, ERC, ERDF, Horizon 2020, and Marie Skłodowska-Curie Actions, European Union; Investissements d’Avenir Labex and Idex, ANR, France; DFG and AvH Foundation, Germany; Herakleitos, Thales and Aristeia programmes cofinanced by EU-ESF and the Greek NSRF, Greece; BSF-NSF and GIF, Israel; CERCA Programme Generalitat de Catalunya, Spain; The Royal Society and Leverhulme Trust, United Kingdom. The crucial computing support from all WLCG partners is acknowledged gratefully, in particular from CERN, the ATLAS Tier-1 facilities at TRIUMF (Canada), NDGF (Denmark, Norway, Sweden), CC-IN2P3 (France), KIT/GridKA (Germany), INFN-CNAF (Italy), NL-T1 (Netherlands), PIC (Spain),

ASGC (Taiwan), RAL (UK), and BNL (USA), the Tier-2 facilities worldwide and large non-WLCG resource providers. Major contributors of computing resources are listed in Ref. [67].

APPENDIX

Model-independent upper limits are derived by applying the full event selection in a set of single-bin signal

regions defined by the minimum m_T value m_T^{\min} in the range between 130 (110) GeV and 5127 (5127) GeV, in the electron (muon) channel. These minimum values correspond to the bin boundaries of the m_T distributions shown in Fig. 1. The single-bin signal regions are defined in Tables IV and V. These tables also show the numbers of events observed in data and the expected numbers of background events.

TABLE IV. Observed and expected electron-channel model-independent limits at 95% C.L. on the number of signal events N_{sig} and corresponding visible cross section σ_{vis} after full event selection for different m_T thresholds m_T^{\min} . Also shown are the ingredients to the limit calculation, namely the number of observed events, the expected number of background events b , and the corresponding uncertainty Δ_b .

| m_T^{\min} [GeV] | N_{obs} | b | Δ_b | Upper limit at 95% C.L. | | | |
|--------------------|------------------|---------|------------|-------------------------------|-------------------------------|---|---|
| | | | | $N_{\text{sig}}^{\text{obs}}$ | $N_{\text{sig}}^{\text{exp}}$ | $\sigma_{\text{vis}}^{\text{obs}}$ [pb] | $\sigma_{\text{vis}}^{\text{exp}}$ [pb] |
| 130 | 3582164 | 3360000 | 250000 | 6.4×10^5 | 4.6×10^5 | 4.6 | 3.3 |
| 139 | 3018934 | 2850000 | 200000 | 5.1×10^5 | 3.8×10^5 | 3.7 | 2.7 |
| 149 | 2345269 | 2240000 | 150000 | 3.6×10^5 | 2.8×10^5 | 2.6 | 2.0 |
| 159 | 1784938 | 1720000 | 110000 | 2.5×10^5 | 2.0×10^5 | 1.8 | 1.4 |
| 170 | 1352988 | 1310000 | 80000 | 1.7×10^5 | 1.4×10^5 | 1.3 | 1.0 |
| 182 | 1028353 | 1000000 | 60000 | 1.2×10^5 | 1.1×10^5 | 0.90 | 0.76 |
| 194 | 784509 | 770000 | 40000 | 9.1×10^4 | 7.7×10^4 | 0.66 | 0.55 |
| 208 | 599989 | 588000 | 31000 | 6.7×10^4 | 5.8×10^4 | 0.48 | 0.42 |
| 222 | 459843 | 451000 | 23000 | 5.0×10^4 | 4.4×10^4 | 0.36 | 0.31 |
| 237 | 352825 | 347000 | 18000 | 3.8×10^4 | 3.4×10^4 | 0.27 | 0.24 |
| 254 | 270299 | 267000 | 14000 | 2.9×10^4 | 2.6×10^4 | 0.21 | 0.19 |
| 271 | 207728 | 204000 | 11000 | 2.3×10^4 | 2.0×10^4 | 0.16 | 0.15 |
| 290 | 159319 | 157000 | 8000 | 1.7×10^4 | 1.6×10^4 | 0.13 | 0.11 |
| 310 | 122150 | 120000 | 6000 | 1.4×10^4 | 1.2×10^4 | 0.10 | 0.088 |
| 331 | 93335 | 92000 | 5000 | 1.1×10^4 | 9.5×10^3 | 0.078 | 0.069 |
| 354 | 71416 | 70000 | 4000 | 8.6×10^3 | 7.4×10^3 | 0.062 | 0.053 |
| 379 | 54642 | 53500 | 3100 | 6.6×10^3 | 5.8×10^3 | 0.048 | 0.042 |
| 405 | 41745 | 40800 | 2400 | 5.3×10^3 | 4.5×10^3 | 0.038 | 0.033 |
| 433 | 31792 | 31100 | 1900 | 4.1×10^3 | 3.6×10^3 | 0.030 | 0.026 |
| 463 | 24257 | 23600 | 1500 | 3.3×10^3 | 2.8×10^3 | 0.023 | 0.020 |
| 495 | 18484 | 18000 | 1200 | 2.6×10^3 | 2.2×10^3 | 0.019 | 0.016 |
| 529 | 13937 | 13600 | 900 | 1.9×10^3 | 1.7×10^3 | 0.014 | 0.012 |
| 565 | 10548 | 10300 | 700 | 1.5×10^3 | 1.3×10^3 | 0.011 | 0.0096 |
| 604 | 7938 | 7800 | 500 | 1.1×10^3 | 1.0×10^3 | 0.0080 | 0.0074 |
| 646 | 5926 | 5900 | 400 | 7.8×10^2 | 8.0×10^2 | 0.0056 | 0.0057 |
| 691 | 4469 | 4470 | 330 | 6.2×10^2 | 6.2×10^2 | 0.0044 | 0.0044 |
| 739 | 3342 | 3360 | 250 | 4.6×10^2 | 4.8×10^2 | 0.0033 | 0.0034 |
| 790 | 2499 | 2510 | 190 | 3.6×10^2 | 3.7×10^2 | 0.0026 | 0.0026 |
| 844 | 1876 | 1850 | 140 | 3.0×10^2 | 2.8×10^2 | 0.0022 | 0.0020 |
| 902 | 1358 | 1370 | 110 | 2.1×10^2 | 2.2×10^2 | 0.0015 | 0.0016 |
| 965 | 1021 | 1010 | 80 | 1.8×10^2 | 1.7×10^2 | 0.0013 | 0.0012 |
| 1031 | 727 | 740 | 60 | 1.2×10^2 | 1.3×10^2 | 0.00088 | 0.00093 |
| 1103 | 495 | 540 | 50 | 74 | 1.0×10^2 | 0.00053 | 0.00072 |
| 1179 | 354 | 390 | 40 | 56 | 78 | 0.00040 | 0.00056 |
| 1260 | 260 | 278 | 27 | 48 | 60 | 0.00035 | 0.00043 |
| 1347 | 175 | 198 | 20 | 33 | 47 | 0.00024 | 0.00034 |
| 1441 | 113 | 140 | 15 | 21 | 37 | 0.00015 | 0.00027 |

(Table continued)

TABLE IV. (*Continued*)

| m_T^{\min} [GeV] | N_{obs} | b | Δ_b | Upper limit at 95% C.L. | | | |
|--------------------|------------------|------|------------|-------------------------------|-------------------------------|---|---|
| | | | | $N_{\text{sig}}^{\text{obs}}$ | $N_{\text{sig}}^{\text{exp}}$ | $\sigma_{\text{vis}}^{\text{obs}}$ [pb] | $\sigma_{\text{vis}}^{\text{exp}}$ [pb] |
| 1540 | 74 | 98 | 11 | 16 | 29 | 0.00011 | 0.00021 |
| 1647 | 55 | 68 | 8 | 15 | 24 | 0.00011 | 0.00017 |
| 1760 | 39 | 46 | 6 | 14 | 19 | 9.9×10^{-5} | 0.00013 |
| 1882 | 23 | 31 | 5 | 9.6 | 15 | 6.9×10^{-5} | 0.00011 |
| 2012 | 17 | 20.9 | 3.4 | 9.4 | 12 | 6.8×10^{-5} | 8.9×10^{-5} |
| 2151 | 8 | 13.7 | 2.5 | 6.0 | 10 | 4.3×10^{-5} | 7.4×10^{-5} |
| 2300 | 1 | 8.9 | 1.8 | 3.4 | 8.4 | 2.4×10^{-5} | 6.1×10^{-5} |
| 2458 | 0 | 5.7 | 1.4 | 3.0 | 7.3 | 2.2×10^{-5} | 5.2×10^{-5} |
| 2628 | 0 | 3.6 | 1.0 | 3.0 | 5.3 | 2.2×10^{-5} | 3.8×10^{-5} |
| 2810 | 0 | 2.2 | 0.8 | 3.0 | 4.9 | 2.2×10^{-5} | 3.5×10^{-5} |
| 3004 | 0 | 1.3 | 0.6 | 3.0 | 4.1 | 2.2×10^{-5} | 2.9×10^{-5} |
| 3212 | 0 | 0.8 | 0.5 | 3.0 | 4.2 | 2.2×10^{-5} | 3.1×10^{-5} |
| 3434 | 0 | 0.5 | 0.4 | 3.0 | 3.0 | 2.2×10^{-5} | 2.2×10^{-5} |
| 3671 | 0 | 0.28 | 0.28 | 3.0 | 3.0 | 2.2×10^{-5} | 2.2×10^{-5} |
| 3924 | 0 | 0.16 | 0.22 | 3.0 | 3.0 | 2.2×10^{-5} | 2.2×10^{-5} |
| 4196 | 0 | 0.09 | 0.17 | 3.0 | 3.0 | 2.2×10^{-5} | 2.2×10^{-5} |
| 4485 | 0 | 0.05 | 0.13 | 3.0 | 3.0 | 2.2×10^{-5} | 2.2×10^{-5} |
| 4795 | 0 | 0.03 | 0.10 | 3.0 | 3.0 | 2.2×10^{-5} | 2.2×10^{-5} |
| 5127 | 0 | 0.02 | 0.08 | 3.0 | 3.0 | 2.2×10^{-5} | 2.2×10^{-5} |

TABLE V. Observed and expected muon-channel model-independent limits at 95% C.L. on the number of signal events N_{sig} and corresponding visible cross section σ_{vis} after full event selection for different m_T^{\min} . Also shown are the ingredients to the limit calculation, namely the number of observed events, the expected number of background events b , and the corresponding uncertainty Δ_b .

| m_T^{\min} [GeV] | N_{obs} | b | Δ_b | Upper limit at 95% C.L. | | | |
|--------------------|------------------|---------|------------|-------------------------------|-------------------------------|---|---|
| | | | | $N_{\text{sig}}^{\text{obs}}$ | $N_{\text{sig}}^{\text{exp}}$ | $\sigma_{\text{vis}}^{\text{obs}}$ [pb] | $\sigma_{\text{vis}}^{\text{exp}}$ [pb] |
| 110 | 8783359 | 7800000 | 700000 | 2.1×10^6 | 1.3×10^6 | 15 | 9.1 |
| 120 | 6589361 | 5900000 | 500000 | 1.5×10^6 | 9.8×10^5 | 11 | 7.0 |
| 130 | 4353441 | 3900000 | 400000 | 9.9×10^5 | 6.5×10^5 | 7.1 | 4.7 |
| 141 | 2820607 | 2590000 | 220000 | 5.9×10^5 | 4.1×10^5 | 4.3 | 2.9 |
| 154 | 1840357 | 1720000 | 140000 | 3.5×10^5 | 2.5×10^5 | 2.5 | 1.8 |
| 167 | 1227452 | 1160000 | 80000 | 2.0×10^5 | 1.5×10^5 | 1.5 | 1.1 |
| 182 | 837724 | 800000 | 50000 | 1.2×10^5 | 9.3×10^4 | 0.88 | 0.67 |
| 197 | 581304 | 562000 | 32000 | 7.5×10^4 | 6.0×10^4 | 0.54 | 0.43 |
| 215 | 409019 | 398000 | 21000 | 4.8×10^4 | 4.0×10^4 | 0.35 | 0.29 |
| 233 | 289557 | 284000 | 15000 | 3.2×10^4 | 2.8×10^4 | 0.23 | 0.20 |
| 254 | 206096 | 202000 | 10000 | 2.3×10^4 | 2.0×10^4 | 0.16 | 0.14 |
| 276 | 146653 | 144000 | 7000 | 1.6×10^4 | 1.4×10^4 | 0.12 | 0.10 |
| 300 | 104516 | 103000 | 5000 | 1.1×10^4 | 1.0×10^4 | 0.083 | 0.073 |
| 326 | 74371 | 73000 | 4000 | 8.3×10^3 | 7.4×10^3 | 0.059 | 0.053 |
| 354 | 52871 | 52100 | 2900 | 6.1×10^3 | 5.5×10^3 | 0.044 | 0.039 |
| 385 | 37630 | 37100 | 2200 | 4.5×10^3 | 4.1×10^3 | 0.032 | 0.030 |
| 419 | 26878 | 26300 | 1600 | 3.5×10^3 | 3.1×10^3 | 0.025 | 0.022 |
| 455 | 19035 | 18700 | 1200 | 2.6×10^3 | 2.3×10^3 | 0.018 | 0.017 |
| 495 | 13578 | 13200 | 900 | 2.0×10^3 | 1.7×10^3 | 0.014 | 0.012 |

(Table continued)

TABLE V. (Continued)

| m_T^{\min} [GeV] | N_{obs} | b | Δ_b | Upper limit at 95% C.L. | | | |
|--------------------|------------------|------|------------|-------------------------------|-------------------------------|---|---|
| | | | | $N_{\text{sig}}^{\text{obs}}$ | $N_{\text{sig}}^{\text{exp}}$ | $\sigma_{\text{vis}}^{\text{obs}}$ [pb] | $\sigma_{\text{vis}}^{\text{exp}}$ [pb] |
| 538 | 9565 | 9400 | 700 | 1.4×10^3 | 1.3×10^3 | 0.010 | 0.0093 |
| 585 | 6804 | 6600 | 500 | 1.1×10^3 | 9.6×10^2 | 0.0080 | 0.0069 |
| 635 | 4754 | 4600 | 400 | 8.0×10^2 | 7.1×10^2 | 0.0058 | 0.0051 |
| 691 | 3353 | 3250 | 280 | 6.1×10^2 | 5.3×10^2 | 0.0044 | 0.0038 |
| 751 | 2297 | 2240 | 210 | 4.3×10^2 | 3.9×10^2 | 0.0031 | 0.0028 |
| 816 | 1624 | 1520 | 150 | 3.6×10^2 | 2.8×10^2 | 0.0026 | 0.0020 |
| 887 | 1093 | 1020 | 110 | 2.6×10^2 | 2.0×10^2 | 0.0018 | 0.0014 |
| 965 | 754 | 700 | 80 | 1.9×10^2 | 1.5×10^2 | 0.0014 | 0.0011 |
| 1049 | 517 | 470 | 60 | 1.4×10^2 | 1.1×10^2 | 0.0010 | 0.00078 |
| 1140 | 367 | 320 | 40 | 1.2×10^2 | 80 | 0.00086 | 0.00057 |
| 1239 | 262 | 215 | 29 | 1.0×10^2 | 60 | 0.00073 | 0.00043 |
| 1347 | 166 | 143 | 21 | 64 | 44 | 0.00046 | 0.00032 |
| 1465 | 113 | 95 | 15 | 49 | 33 | 0.00035 | 0.00024 |
| 1592 | 77 | 63 | 11 | 38 | 26 | 0.00027 | 0.00018 |
| 1731 | 48 | 41 | 8 | 25 | 19 | 0.00018 | 0.00014 |
| 1882 | 30 | 27 | 6 | 18 | 15 | 0.00013 | 0.00011 |
| 2046 | 21 | 18 | 4 | 15 | 13 | 0.00011 | 9.0×10^{-5} |
| 2224 | 16 | 11.4 | 3.1 | 14 | 9.5 | 0.00010 | 6.8×10^{-5} |
| 2418 | 8 | 7.4 | 2.2 | 8.6 | 7.7 | 6.2×10^{-5} | 5.5×10^{-5} |
| 2628 | 5 | 4.7 | 1.6 | 6.9 | 6.9 | 5.0×10^{-5} | 5.0×10^{-5} |
| 2857 | 3 | 3.0 | 1.1 | 5.6 | 5.6 | 4.1×10^{-5} | 4.1×10^{-5} |
| 3106 | 2 | 1.9 | 0.8 | 5.0 | 5.0 | 3.6×10^{-5} | 3.6×10^{-5} |
| 3377 | 2 | 1.2 | 0.5 | 5.3 | 4.1 | 3.8×10^{-5} | 2.9×10^{-5} |
| 3671 | 1 | 0.8 | 0.4 | 4.2 | 4.2 | 3.1×10^{-5} | 3.1×10^{-5} |
| 3990 | 1 | 0.47 | 0.25 | 4.4 | 3.0 | 3.2×10^{-5} | 2.2×10^{-5} |
| 4338 | 1 | 0.29 | 0.16 | 4.5 | 3.0 | 3.2×10^{-5} | 2.2×10^{-5} |
| 4716 | 1 | 0.18 | 0.11 | 4.6 | 3.0 | 3.3×10^{-5} | 2.2×10^{-5} |
| 5127 | 0 | 0.11 | 0.07 | 3.0 | 3.0 | 2.2×10^{-5} | 2.2×10^{-5} |

- [1] R. N. Mohapatra and J. C. Pati, Left-right gauge symmetry and an “isoconjugate” model of CP violation, *Phys. Rev. D* **11**, 566 (1975).
- [2] G. Senjanovic and R. N. Mohapatra, Exact left-right symmetry and spontaneous violation of parity, *Phys. Rev. D* **12**, 1502 (1975).
- [3] N. Arkani-Hamed, A. G. Cohen, E. Katz, and A. E. Nelson, The littlest Higgs, *J. High Energy Phys.* **07** (2002) 034.
- [4] T. Appelquist, H.-C. Cheng, and B. A. Dobrescu, Bounds on universal extra dimensions, *Phys. Rev. D* **64**, 035002 (2001).
- [5] K. Agashe, S. Gopalakrishna, T. Han, G.-Y. Huang, and A. Soni, LHC signals for warped electroweak charged gauge bosons, *Phys. Rev. D* **80**, 075007 (2009).
- [6] G. Altarelli, B. Mele, and M. Ruiz-Altaba, Searching for new heavy vector bosons in $p\bar{p}$ colliders, *Z. Phys. C* **45**, 109 (1989); Erratum, **47**, 676(E) (1990).
- [7] ATLAS Collaboration, Search for a new heavy gauge-boson resonance decaying into a lepton and missing transverse momentum in 36 fb^{-1} of pp collisions at $\sqrt{s} = 13 \text{ TeV}$ with the ATLAS experiment, *Eur. Phys. J. C* **78**, 401 (2018).
- [8] CMS Collaboration, Search for high-mass resonances in final states with a lepton and missing transverse momentum at $\sqrt{s} = 13 \text{ TeV}$, *J. High Energy Phys.* **06** (2018) 128.
- [9] ATLAS Collaboration, Electron and photon performance measurements with the ATLAS detector using the 2015–2017 LHC proton-proton collision data, [arXiv:1908.00005](https://arxiv.org/abs/1908.00005).
- [10] ATLAS Collaboration, The ATLAS experiment at the CERN large hadron collider, *J. Instrum.* **3**, S08003 (2008).
- [11] ATLAS Collaboration, ATLAS Insertable B -Layer Technical Design Report, CERN Report No. ATLAS-TDR-19, 2010, <https://cds.cern.ch/record/1291633>; Addendum, CERN Report No. ATLAS-TDR-19-ADD-1, 2012, <https://cds.cern.ch/record/1451888>.

- [12] B. Abbott *et al.*, Production and integration of the ATLAS Insertable B -Layer, *J. Instrum.* **13**, T05008 (2018).
- [13] ATLAS Collaboration, Performance of the ATLAS trigger system in 2015, *Eur. Phys. J. C* **77**, 317 (2017).
- [14] T. Sjöstrand, S. Mrenna, and P.Z. Skands, A brief introduction to PYTHIA 8.1, *Comput. Phys. Commun.* **178**, 852 (2008).
- [15] R. D. Ball *et al.*, Parton distributions with LHC data, *Nucl. Phys.* **B867**, 244 (2013).
- [16] ATLAS Collaboration, ATLAS PYTHIA 8 tunes to 7 TeV data, CERN Report No. ATL-PHYS-PUB-2014-021, 2014, <https://cds.cern.ch/record/1966419>.
- [17] ATLAS Collaboration, ATLAS search for a heavy gauge boson decaying to a charged lepton and a neutrino in pp collisions at $\sqrt{s} = 7$ TeV, *Eur. Phys. J. C* **72**, 2241 (2012).
- [18] P. Nason, A new method for combining NLO QCD with shower Monte Carlo algorithms, *J. High Energy Phys.* **11** (2004) 040.
- [19] S. Frixione, P. Nason, and C. Oleari, Matching NLO QCD computations with parton shower simulations: The POWHEG method, *J. High Energy Phys.* **11** (2007) 070.
- [20] S. Alioli, P. Nason, C. Oleari, and E. Re, NLO vector-boson production matched with shower in POWHEG, *J. High Energy Phys.* **07** (2008) 060.
- [21] S. Alioli, P. Nason, C. Oleari, and E. Re, A general framework for implementing NLO calculations in shower Monte Carlo programs: The POWHEG BOX, *J. High Energy Phys.* **06** (2010) 043.
- [22] H.-L. Lai, M. Guzzi, J. Huston, Z. Li, P. M. Nadolsky, J. Pumplin, and C.-P. Yuan, New parton distributions for collider physics, *Phys. Rev. D* **82**, 074024 (2010).
- [23] ATLAS Collaboration, Measurement of the Z/γ^* boson transverse momentum distribution in pp collisions at $\sqrt{s} = 7$ TeV with the ATLAS detector, *J. High Energy Phys.* **09** (2014) 145.
- [24] C. Anastasiou, L. Dixon, K. Melnikov, and F. Petriello, High-precision QCD at hadron colliders: Electroweak gauge boson rapidity distributions at next-to-next-to leading order, *Phys. Rev. D* **69**, 094008 (2004).
- [25] S. Dulat, T.-J. Hou, J. Gao, M. Guzzi, J. Huston, P. Nadolsky, J. Pumplin, C. Schmidt, D. Stump, and C.-P. Yuan, New parton distribution functions from a global analysis of quantum chromodynamics, *Phys. Rev. D* **93**, 033006 (2016).
- [26] A. Arbuzov, D. Bardin, S. Bondarenko, P. Christova, L. Kalinovskaya, U. Klein, V. Kolesnikov, L. Romyantsev, R. Sadykov, and A. Saproinov, Update of the MCSANC Monte Carlo integrator, v. 1.20, *JETP Lett.* **103**, 131 (2016).
- [27] P. Golonka and Z. Was, PHOTOS Monte Carlo: A precision tool for QED corrections in Z and W decays, *Eur. Phys. J. C* **45**, 97 (2006).
- [28] T. Gleisberg, S. Höche, F. Krauss, M. Schönherr, S. Schumann, F. Siegert, and J. Winter, Event generation with SHERPA 1.1, *J. High Energy Phys.* **02** (2009) 007.
- [29] R. D. Ball *et al.*, Parton distributions for the LHC Run II, *J. High Energy Phys.* **04** (2015) 040.
- [30] S. Frixione, P. Nason, and G. Ridolfi, A positive-weight next-to-leading-order Monte Carlo for heavy flavour hadroproduction, *J. High Energy Phys.* **09** (2007) 126.
- [31] S. Alioli, P. Nason, C. Oleari, and E. Re, NLO single-top production matched with shower in POWHEG: s - and t -channel contributions, *J. High Energy Phys.* **09** (2009) 111.
- [32] E. Re, Single-top W -channel production matched with parton showers using the POWHEG method, *Eur. Phys. J. C* **71**, 1547 (2011).
- [33] M. Cacciari, M. Czakon, M. Mangano, A. Mitov, and P. Nason, Top-pair production at hadron colliders with next-to-next-to-leading logarithmic soft-gluon resummation, *Phys. Lett. B* **710**, 612 (2012).
- [34] M. Beneke, P. Falgari, S. Klein, and C. Schwinn, Hadronic top-quark pair production with NNLL threshold resummation, *Nucl. Phys.* **B855**, 695 (2012).
- [35] P. Bärnreuther, M. Czakon, and A. Mitov, Percent-Level-Precision Physics at the Tevatron: Next-to-Next-to-Leading Order QCD Corrections to $q\bar{q} \rightarrow t\bar{t} + X$, *Phys. Rev. Lett.* **109**, 132001 (2012).
- [36] M. Czakon and A. Mitov, NNLO corrections to top-pair production at hadron colliders: The all-fermionic scattering channels, *J. High Energy Phys.* **12** (2012) 054.
- [37] M. Czakon and A. Mitov, NNLO corrections to top pair production at hadron colliders: The quark-gluon reaction, *J. High Energy Phys.* **01** (2013) 080.
- [38] M. Czakon, P. Fiedler, and A. Mitov, Total Top-Quark Pair-Production Cross Section at Hadron Colliders Through $O(\alpha_s^4)$, *Phys. Rev. Lett.* **110**, 252004 (2013).
- [39] M. Czakon and A. Mitov, TOP++: A program for the calculation of the top-pair cross-section at hadron colliders, *Comput. Phys. Commun.* **185**, 2930 (2014).
- [40] M. Czakon, D. Heymes, A. Mitov, D. Pagani, I. Tsinikos, and M. Zaro, Top-pair production at the LHC through NNLO QCD and NLO EW, *J. High Energy Phys.* **10** (2017) 186.
- [41] N. Kidonakis, Next-to-next-to-leading-order collinear and soft gluon corrections for t -channel single top quark production, *Phys. Rev. D* **83**, 091503 (2011).
- [42] N. Kidonakis, Next-to-next-to-leading logarithm resummation for s -channel single top quark production, *Phys. Rev. D* **81**, 054028 (2010).
- [43] N. Kidonakis, Two-loop soft anomalous dimensions for single top quark associated production with a W^- or H^- , *Phys. Rev. D* **82**, 054018 (2010).
- [44] D. J. Lange, The EVTGEN particle decay simulation package, *Nucl. Instrum. Methods Phys. Res., Sect. A* **462**, 152 (2001).
- [45] ATLAS Collaboration, The PYTHIA 8 A3 tune description of ATLAS minimum bias and inelastic measurements incorporating the Donnachie-Landshoff diffractive model, CERN Report No. ATL-PHYS-PUB-2016-017, 2016, <https://cds.cern.ch/record/2206965>.
- [46] S. Agostinelli *et al.*, GEANT4—A simulation toolkit, *Nucl. Instrum. Methods Phys. Res., Sect. A* **506**, 250 (2003).
- [47] ATLAS Collaboration, The ATLAS simulation infrastructure, *Eur. Phys. J. C* **70**, 823 (2010).
- [48] ATLAS Collaboration, Muon reconstruction performance of the ATLAS detector in proton-proton collision data at $\sqrt{s} = 13$ TeV, *Eur. Phys. J. C* **76**, 292 (2016).
- [49] ATLAS Collaboration, Topological cell clustering in the ATLAS calorimeters and its performance in LHC Run 1, *Eur. Phys. J. C* **77**, 490 (2017).

- [50] M. Cacciari, G.P. Salam, and G. Soyez, The anti- k_t jet clustering algorithm, *J. High Energy Phys.* **04** (2008) 063.
- [51] M. Cacciari, G.P. Salam, and G. Soyez, FASTJET user manual, *Eur. Phys. J. C* **72**, 1896 (2012).
- [52] ATLAS Collaboration, Jet energy scale measurements and their systematic uncertainties in proton-proton collisions at $\sqrt{s} = 13$ TeV with the ATLAS detector, *Phys. Rev. D* **96**, 072002 (2017).
- [53] ATLAS Collaboration, Performance of pile-up mitigation techniques for jets in pp collisions at $\sqrt{s} = 8$ TeV using the ATLAS detector, *Eur. Phys. J. C* **76**, 581 (2016).
- [54] ATLAS Collaboration, Performance of missing transverse momentum reconstruction with the ATLAS detector using proton-proton collisions at $\sqrt{s} = 13$ TeV, *Eur. Phys. J. C* **78**, 903 (2018).
- [55] ATLAS Collaboration, Selection of jets produced in 13 TeV proton-proton collisions with the ATLAS detector, CERN Report No. ATLAS-CONF-2015-029, 2015, <https://cds.cern.ch/record/2037702>.
- [56] ATLAS Collaboration, Search for new phenomena in dijet events using 37 fb $^{-1}$ of pp collision data collected at $\sqrt{s} = 13$ TeV with the ATLAS detector, *Phys. Rev. D* **96**, 052004 (2017).
- [57] CMS Collaboration, Search for narrow and broad dijet resonances in proton-proton collisions at $\sqrt{s} = 13$ TeV and constraints on dark matter mediators and other new particles, *J. High Energy Phys.* **08** (2018) 130.
- [58] ATLAS Collaboration, Search for new resonances in events with one lepton and missing transverse momentum in pp collisions at $\sqrt{s} = 13$ TeV with the ATLAS detector, *Phys. Lett. B* **762**, 334 (2016).
- [59] S. Alekhin, J. Blümlein, and S. Moch, The ABM parton distributions tuned to LHC data, *Phys. Rev. D* **89**, 054028 (2014).
- [60] L. A. Harland-Lang, A. D. Martin, P. Motylinski, and R. S. Thorne, Parton distributions in the LHC era: MMHT 2014 PDFs, *Eur. Phys. J. C* **75**, 204 (2015).
- [61] P. Jimenez-Delgado and E. Reya, Delineating parton distributions and the strong coupling, *Phys. Rev. D* **89**, 074049 (2014).
- [62] ATLAS Collaboration, Studies on top-quark Monte Carlo modelling for Top2016, CERN Report No. ATL-PHYS-PUB-2016-020, 2016, <https://cds.cern.ch/record/2216168>.
- [63] ATLAS Collaboration, Luminosity determination in pp collisions at $\sqrt{s} = 13$ TeV using the ATLAS detector at the LHC, CERN Report No. ATLAS-CONF-2019-021, 2019, <https://cds.cern.ch/record/2677054>.
- [64] G. Cowan, K. Cranmer, E. Gross, and O. Vitells, Asymptotic formulae for likelihood-based tests of new physics, *Eur. Phys. J. C* **71**, 1554 (2011); **73**, 2501 (2013).
- [65] A. Caldwell, D. Kollár, and K. Kröninger, BAT-The Bayesian analysis toolkit, *Comput. Phys. Commun.* **180**, 2197 (2009).
- [66] J. Alwall, M. Herquet, F. Maltoni, O. Mattelaer, and T. Stelzer, MADGRAPH 5: Going beyond, *J. High Energy Phys.* **06** (2011) 128.
- [67] ATLAS Collaboration, ATLAS Computing Acknowledgements, CERN Report No. ATL-GEN-PUB-2016-002, 2016, <https://cds.cern.ch/record/2202407>.

G. Aad,¹⁰¹ B. Abbott,¹²⁸ D. C. Abbott,¹⁰² O. Abidinov,^{13,a} A. Abed Abud,^{70a,70b} K. Abeling,⁵³ D. K. Abhayasinghe,⁹³ S. H. Abidi,¹⁶⁷ O. S. AbouZeid,⁴⁰ N. L. Abraham,¹⁵⁶ H. Abramowicz,¹⁶¹ H. Abreu,¹⁶⁰ Y. Abulaiti,⁶ B. S. Acharya,^{66a,66b,b} B. Achkar,⁵³ S. Adachi,¹⁶³ L. Adam,⁹⁹ C. Adam Bourdarios,¹³² L. Adamczyk,^{83a} L. Adamek,¹⁶⁷ J. Adelman,¹²¹ M. Adersberger,¹¹⁴ A. Adiguzel,^{12c,c} S. Adorni,⁵⁴ T. Adye,¹⁴⁴ A. A. Affolder,¹⁴⁶ Y. Afik,¹⁶⁰ C. Agapopoulou,¹³² M. N. Agaras,³⁸ A. Aggarwal,¹¹⁹ C. Agheorghiesei,^{27c} J. A. Aguilar-Saavedra,^{140f,140a,d} F. Ahmadov,⁷⁹ W. S. Ahmed,¹⁰³ X. Ai,^{15a} G. Aielli,^{73a,73b} S. Akatsuka,⁸⁵ T. P. A. Åkesson,⁹⁶ E. Akilli,⁵⁴ A. V. Akimov,¹¹⁰ K. Al Khoury,¹³² G. L. Alberghi,^{23b,23a} J. Albert,¹⁷⁶ M. J. Alconada Verzini,⁸⁸ S. Alderweireldt,³⁶ M. Aleksa,³⁶ I. N. Aleksandrov,⁷⁹ C. Alexa,^{27b} D. Alexandre,¹⁹ T. Alexopoulos,¹⁰ A. Alfonsi,¹²⁰ M. Alhroob,¹²⁸ B. Ali,¹⁴² G. Alimonti,^{68a} J. Alison,³⁷ S. P. Alkire,¹⁴⁸ C. Allaire,¹³² B. M. M. Allbrooke,¹⁵⁶ B. W. Allen,¹³¹ P. P. Allport,²¹ A. Aloisio,^{69a,69b} A. Alonso,⁴⁰ F. Alonso,⁸⁸ C. Alpigiani,¹⁴⁸ A. A. Alshehri,⁵⁷ M. Alvarez Estevez,⁹⁸ D. Álvarez Piqueras,¹⁷⁴ M. G. Alviggi,^{69a,69b} Y. Amaral Coutinho,^{80b} A. Ambler,¹⁰³ L. Ambroz,¹³⁵ C. Amelung,²⁶ D. Amidei,¹⁰⁵ S. P. Amor Dos Santos,^{140a} S. Amoroso,⁴⁶ C. S. Amrouche,⁵⁴ F. An,⁷⁸ C. Anastopoulos,¹⁴⁹ N. Andari,¹⁴⁵ T. Andeen,¹¹ C. F. Anders,^{61b} J. K. Anders,²⁰ A. Andreazza,^{68a,68b} V. Andrei,^{61a} C. R. Anelli,¹⁷⁶ S. Angelidakis,³⁸ A. Angerami,³⁹ A. V. Anisenkov,^{122b,122a} A. Annovi,^{71a} C. Antel,^{61a} M. T. Anthony,¹⁴⁹ M. Antonelli,⁵¹ D. J. A. Antrim,¹⁷¹ F. Anulli,^{72a} M. Aoki,⁸¹ J. A. Aparisi Pozo,¹⁷⁴ L. Aperio Bella,³⁶ G. Arabidze,¹⁰⁶ J. P. Araque,^{140a} V. Araujo Ferraz,^{80b} R. Araujo Pereira,^{80b} C. Arcangeletti,⁵¹ A. T. H. Arce,⁴⁹ F. A. Arduh,⁸⁸ J-F. Arguin,¹⁰⁹ S. Argyropoulos,⁷⁷ J.-H. Arling,⁴⁶ A. J. Armbruster,³⁶ A. Armstrong,¹⁷¹ O. Arnaez,¹⁶⁷ H. Arnold,¹²⁰ A. Artamonov,^{111,a} G. Artoni,¹³⁵ S. Artz,⁹⁹ S. Asai,¹⁶³ N. Asbah,⁵⁹ E. M. Asimakopoulou,¹⁷² L. Asquith,¹⁵⁶ K. Assamagan,²⁹ R. Astalos,^{28a} R. J. Atkin,^{33a} M. Atkinson,¹⁷³ N. B. Atlay,¹⁹ H. Atmani,¹³² K. Augsten,¹⁴² G. Avolio,³⁶ R. Avramidou,^{60a} M. K. Ayoub,^{15a} A. M. Azoulay,^{168b} G. Azuelos,^{109,e} M. J. Baca,²¹ H. Bachacou,¹⁴⁵ K. Bachas,^{67a,67b} M. Backes,¹³⁵ F. Backman,^{45a,45b} P. Bagnaia,^{72a,72b} M. Bahmani,⁸⁴ H. Bahrasemani,¹⁵² A. J. Bailey,¹⁷⁴ V. R. Bailey,¹⁷³ J. T. Baines,¹⁴⁴ M. Bajic,⁴⁰ C. Bakalis,¹⁰ O. K. Baker,¹⁸³ P. J. Bakker,¹²⁰ D. Bakshi Gupta,⁸ S. Balaji,¹⁵⁷

E. M. Baldin,^{122b,122a} P. Balek,¹⁸⁰ F. Balli,¹⁴⁵ W. K. Balunas,¹³⁵ J. Balz,⁹⁹ E. Banas,⁸⁴ A. Bandyopadhyay,²⁴ Sw. Banerjee,^{181,f}
A. A. E. Bannoura,¹⁸² L. Barak,¹⁶¹ W. M. Barbe,³⁸ E. L. Barberio,¹⁰⁴ D. Barberis,^{55b,55a} M. Barbero,¹⁰¹ T. Barillari,¹¹⁵
M-S. Barisits,³⁶ J. Barkeloo,¹³¹ T. Barklow,¹⁵³ R. Barnea,¹⁶⁰ S. L. Barnes,^{60c} B. M. Barnett,¹⁴⁴ R. M. Barnett,¹⁸
Z. Barnovska-Blenessy,^{60a} A. Baroncelli,^{60a} G. Barone,²⁹ A. J. Barr,¹³⁵ L. Barranco Navarro,^{45a,45b} F. Barreiro,⁹⁸
J. Barreiro Guimarães da Costa,^{15a} S. Barsov,¹³⁸ R. Bartoldus,¹⁵³ G. Bartolini,¹⁰¹ A. E. Barton,⁸⁹ P. Bartos,^{28a} A. Basalaev,⁴⁶
A. Bassalat,^{132,g} R. L. Bates,⁵⁷ S. J. Batista,¹⁶⁷ S. Batlamous,^{35e} J. R. Batley,³² B. Batool,¹⁵¹ M. Battaglia,¹⁴⁶ M. Bauce,^{72a,72b}
F. Bauer,¹⁴⁵ K. T. Bauer,¹⁷¹ H. S. Bawa,^{31,h} J. B. Beacham,⁴⁹ T. Beau,¹³⁶ P. H. Beauchemin,¹⁷⁰ F. Becherer,⁵² P. Bechtle,²⁴
H. C. Beck,⁵³ H. P. Beck,^{20,i} K. Becker,⁵² M. Becker,⁹⁹ C. Becot,⁴⁶ A. Beddall,^{12d} A. J. Beddall,^{12a} V. A. Bednyakov,⁷⁹
M. Bedognetti,¹²⁰ C. P. Bee,¹⁵⁵ T. A. Beermann,⁷⁶ M. Begalli,^{80b} M. Begel,²⁹ A. Behera,¹⁵⁵ J. K. Behr,⁴⁶ F. Beisiegel,²⁴
A. S. Bell,⁹⁴ G. Bella,¹⁶¹ L. Bellagamba,^{23b} A. Bellerive,³⁴ P. Bellos,⁹ K. Beloborodov,^{122b,122a} K. Belotskiy,¹¹²
N. L. Belyaev,¹¹² D. Benckekroun,^{35a} N. Benekos,¹⁰ Y. Benhammou,¹⁶¹ D. P. Benjamin,⁶ M. Benoit,⁵⁴ J. R. Bensinger,²⁶
S. Bentvelsen,¹²⁰ L. Beresford,¹³⁵ M. Beretta,⁵¹ D. Berge,⁴⁶ E. Bergeaas Kuutmann,¹⁷² N. Berger,⁵ B. Bergmann,¹⁴²
L. J. Bergsten,²⁶ J. Beringer,¹⁸ S. Berlendis,⁷ N. R. Bernard,¹⁰² G. Bernardi,¹³⁶ C. Bernius,¹⁵³ T. Berry,⁹³ P. Berta,⁹⁹
C. Bertella,^{15a} I. A. Bertram,⁸⁹ G. J. Besjes,⁴⁰ O. Bessidskaia Bylund,¹⁸² N. Besson,¹⁴⁵ A. Bethani,¹⁰⁰ S. Bethke,¹¹⁵
A. Betti,²⁴ A. J. Bevan,⁹² J. Beyer,¹¹⁵ R. Bi,¹³⁹ R. M. Bianchi,¹³⁹ O. Biebel,¹¹⁴ D. Biedermann,¹⁹ R. Bielski,³⁶
K. Bierwagen,⁹⁹ N. V. Biesuz,^{71a,71b} M. Biglietti,^{74a} T. R. V. Billoud,¹⁰⁹ M. Bindi,⁵³ A. Bingul,^{12d} C. Bini,^{72a,72b}
S. Biondi,^{23b,23a} M. Birman,¹⁸⁰ T. Bisanz,⁵³ J. P. Biswal,¹⁶¹ D. Biswas,¹⁸¹ A. Bitadze,¹⁰⁰ C. Bittrich,⁴⁸ K. Bjørke,¹³⁴
K. M. Black,²⁵ T. Blazek,^{28a} I. Bloch,⁴⁶ C. Blocker,²⁶ A. Blue,⁵⁷ U. Blumenschein,⁹² G. J. Bobbink,¹²⁰
V. S. Bobrovnikov,^{122b,122a} S. S. Bocchetta,⁹⁶ A. Bocci,⁴⁹ D. Boerner,⁴⁶ D. Bogavac,¹⁴ A. G. Bogdanchikov,^{122b,122a}
C. Bohm,^{45a} V. Boisvert,⁹³ P. Bokan,^{53,172} T. Bold,^{83a} A. S. Boldyrev,¹¹³ A. E. Bolz,^{61b} M. Bomben,¹³⁶ M. Bona,⁹²
J. S. Bonilla,¹³¹ M. Boonekamp,¹⁴⁵ H. M. Borecka-Bielska,⁹⁰ A. Borisov,¹²³ G. Borissov,⁸⁹ J. Bortfeldt,³⁶ D. Bortoletto,¹³⁵
V. Bortolotto,^{73a,73b} D. Boscherini,^{23b} M. Bosman,¹⁴ J. D. Bossio Sola,¹⁰³ K. Bouaouda,^{35a} J. Boudreau,¹³⁹
E. V. Bouhova-Thacker,⁸⁹ D. Boumediene,³⁸ S. K. Boutle,⁵⁷ A. Boveia,¹²⁶ J. Boyd,³⁶ D. Boye,^{33b,j} I. R. Boyko,⁷⁹
A. J. Bozson,⁹³ J. Bracinik,²¹ N. Brahimy,¹⁰¹ G. Brandt,¹⁸² O. Brandt,³² F. Braren,⁴⁶ U. Bratzler,¹⁶⁴ B. Brau,¹⁰² J. E. Brau,¹³¹
W. D. Breaden Madden,⁵⁷ K. Brendlinger,⁴⁶ L. Brenner,⁴⁶ R. Brenner,¹⁷² S. Bressler,¹⁸⁰ B. Brickwedde,⁹⁹ D. L. Briglin,²¹
D. Britton,⁵⁷ D. Britzger,¹¹⁵ I. Brock,²⁴ R. Brock,¹⁰⁶ G. Brooijmans,³⁹ W. K. Brooks,^{147b} E. Brost,¹²¹ J. H. Broughton,²¹
P. A. Bruckman de Renstrom,⁸⁴ D. Bruncko,^{28b} A. Bruni,^{23b} G. Bruni,^{23b} L. S. Bruni,¹²⁰ S. Bruno,^{73a,73b} B. H. Brunt,³²
M. Bruschi,^{23b} N. Bruscinio,¹³⁹ P. Bryant,³⁷ L. Bryngemark,⁹⁶ T. Buanes,¹⁷ Q. Buat,³⁶ P. Buchholz,¹⁵¹ A. G. Buckley,⁵⁷
I. A. Budagov,⁷⁹ M. K. Bugge,¹³⁴ F. Bühner,⁵² O. Bulekov,¹¹² T. J. Burch,¹²¹ S. Burdin,⁹⁰ C. D. Burgard,¹²⁰ A. M. Burger,¹²⁹
B. Burghgrave,⁸ K. Burka,⁸⁴ J. T. P. Burr,⁴⁶ J. C. Burzynski,¹⁰² V. Büscher,⁹⁹ E. Buschmann,⁵³ P. J. Bussey,⁵⁷ J. M. Butler,²⁵
C. M. Buttar,⁵⁷ J. M. Butterworth,⁹⁴ P. Butti,³⁶ W. Buttinger,³⁶ A. Buzatu,¹⁵⁸ A. R. Buzykaev,^{122b,122a} G. Cabras,^{23b,23a}
S. Cabrera Urbán,¹⁷⁴ D. Caforio,⁵⁶ H. Cai,¹⁷³ V. M. M. Cairo,¹⁵³ O. Cakir,^{4a} N. Calace,³⁶ P. Calafiura,¹⁸ A. Calandri,¹⁰¹
G. Calderini,¹³⁶ P. Calfayan,⁶⁵ G. Callea,⁵⁷ L. P. Caloba,^{80b} S. Calvente Lopez,⁹⁸ D. Calvet,³⁸ S. Calvet,³⁸ T. P. Calvet,¹⁵⁵
M. Calvetti,^{71a,71b} R. Camacho Toro,¹³⁶ S. Camarda,³⁶ D. Camarero Munoz,⁹⁸ P. Camarri,^{73a,73b} D. Cameron,¹³⁴
R. Caminal Armadans,¹⁰² C. Camincher,³⁶ S. Campana,³⁶ M. Campanelli,⁹⁴ A. Camplani,⁴⁰ A. Campoverde,¹⁵¹
V. Canale,^{69a,69b} A. Canesse,¹⁰³ M. Cano Bret,^{60c} J. Cantero,¹²⁹ T. Cao,¹⁶¹ Y. Cao,¹⁷³ M. D. M. Capeans Garrido,³⁶
M. Capua,^{41b,41a} R. Cardarelli,^{73a} F. C. Cardillo,¹⁴⁹ G. Carducci,^{41b,41a} I. Carli,¹⁴³ T. Carli,³⁶ G. Carlino,^{69a} B. T. Carlson,¹³⁹
L. Carminati,^{68a,68b} R. M. D. Carney,^{45a,45b} S. Caron,¹¹⁹ E. Carquin,^{147b} S. Carrá,⁴⁶ J. W. S. Carter,¹⁶⁷ M. P. Casado,^{14,k}
A. F. Casha,¹⁶⁷ D. W. Casper,¹⁷¹ R. Castelijin,¹²⁰ F. L. Castillo,¹⁷⁴ V. Castillo Gimenez,¹⁷⁴ N. F. Castro,^{140a,140e}
A. Catinaccio,³⁶ J. R. Catmore,¹³⁴ A. Cattai,³⁶ J. Caudron,²⁴ V. Cavaliere,²⁹ E. Cavallaro,¹⁴ M. Cavalli-Sforza,¹⁴
V. Cavasinni,^{71a,71b} E. Celebi,^{12b} F. Ceradini,^{74a,74b} L. Cerda Alberich,¹⁷⁴ K. Cerny,¹³⁰ A. S. Cerqueira,^{80a} A. Cerri,¹⁵⁶
L. Cerrito,^{73a,73b} F. Cerutti,¹⁸ A. Cervelli,^{23b,23a} S. A. Cetin,^{12b} Z. Chadi,^{35a} D. Chakraborty,¹²¹ S. K. Chan,⁵⁹ W. S. Chan,¹²⁰
W. Y. Chan,⁹⁰ J. D. Chapman,³² B. Chargeishvili,^{159b} D. G. Charlton,²¹ T. P. Charman,⁹² C. C. Chau,³⁴ S. Che,¹²⁶
A. Chegwidden,¹⁰⁶ S. Chekanov,⁶ S. V. Chekulaev,^{168a} G. A. Chelkov,^{79,1} M. A. Chelstowska,³⁶ B. Chen,⁷⁸ C. Chen,^{60a}
C. H. Chen,⁷⁸ H. Chen,²⁹ J. Chen,^{60a} J. Chen,³⁹ S. Chen,¹³⁷ S. J. Chen,^{15c} X. Chen,^{15b,m} Y. Chen,⁸² Y-H. Chen,⁴⁶
H. C. Cheng,^{63a} H. J. Cheng,^{15a,15d} A. Cheplakov,⁷⁹ E. Cheremushkina,¹²³ R. Cherkaoui El Moursli,^{35e} E. Cheu,⁷
K. Cheung,⁶⁴ T. J. A. Chevalérias,¹⁴⁵ L. Chevalier,¹⁴⁵ V. Chiarella,⁵¹ G. Chiarelli,^{71a} G. Chiodini,^{67a} A. S. Chisholm,^{36,21}
A. Chitan,^{27b} I. Chiu,¹⁶³ Y. H. Chiu,¹⁷⁶ M. V. Chizhov,⁷⁹ K. Choi,⁶⁵ A. R. Chomont,^{72a,72b} S. Chouridou,¹⁶² Y. S. Chow,¹²⁰
M. C. Chu,^{63a} X. Chu,^{15a} J. Chudoba,¹⁴¹ A. J. Chuinard,¹⁰³ J. J. Chwastowski,⁸⁴ L. Chytka,¹³⁰ K. M. Ciesla,⁸⁴ D. Cinca,⁴⁷

V. Cindro,⁹¹ I. A. Cioară,^{27b} A. Ciocio,¹⁸ F. Ciroto,^{69a,69b} Z. H. Citron,¹⁸⁰ M. Citterio,^{68a} D. A. Ciubotaru,^{27b} B. M. Ciungu,¹⁶⁷ A. Clark,⁵⁴ M. R. Clark,³⁹ P. J. Clark,⁵⁰ C. Clement,^{45a,45b} Y. Coadou,¹⁰¹ M. Cobal,^{66a,66c} A. Coccaro,^{55b} J. Cochran,⁷⁸ H. Cohen,¹⁶¹ A. E. C. Coimbra,³⁶ L. Colasurdo,¹¹⁹ B. Cole,³⁹ A. P. Colijn,¹²⁰ J. Collot,⁵⁸ P. Conde Muino,^{140a,n} E. Coniavitis,⁵² S. H. Connell,^{33b} I. A. Connelly,⁵⁷ S. Constantinescu,^{27b} F. Conventi,^{69a,o} A. M. Cooper-Sarkar,¹³⁵ F. Cormier,¹⁷⁵ K. J. R. Cormier,¹⁶⁷ L. D. Corpe,⁹⁴ M. Corradi,^{72a,72b} E. E. Corrigan,⁹⁶ F. Corriveau,^{103,p} A. Cortes-Gonzalez,³⁶ M. J. Costa,¹⁷⁴ F. Costanza,⁵ D. Costanzo,¹⁴⁹ G. Cowan,⁹³ J. W. Cowley,³² J. Crane,¹⁰⁰ K. Cranmer,¹²⁴ S. J. Crawley,⁵⁷ R. A. Creager,¹³⁷ S. Crépé-Renaudin,⁵⁸ F. Crescioli,¹³⁶ M. Cristinziani,²⁴ V. Croft,¹²⁰ G. Crosetti,^{41b,41a} A. Cueto,⁵ T. Cuhadar Donszelmann,¹⁴⁹ A. R. Cukierman,¹⁵³ S. Czekierda,⁸⁴ P. Czodrowski,³⁶ M. J. Da Cunha Sargedas De Sousa,^{60b} J. V. Da Fonseca Pinto,^{80b} C. Da Via,¹⁰⁰ W. Dabrowski,^{83a} T. Dado,^{28a} S. Dahbi,^{35e} T. Dai,¹⁰⁵ C. Dallapiccola,¹⁰² M. Dam,⁴⁰ G. D'amen,^{23b,23a} V. D'Amico,^{74a,74b} J. Damp,⁹⁹ J. R. Dandoy,¹³⁷ M. F. Daneri,³⁰ N. P. Dang,¹⁸¹ N. D. Dann,¹⁰⁰ M. Danninger,¹⁷⁵ V. Dao,³⁶ G. Darbo,^{55b} O. Darsi,⁵ A. Dattagupta,¹³¹ T. Daubney,⁴⁶ S. D'Auria,^{68a,68b} W. Davey,²⁴ C. David,⁴⁶ T. Davidek,¹⁴³ D. R. Davis,⁴⁹ I. Dawson,¹⁴⁹ K. De,⁸ R. De Asmundis,^{69a} M. De Beurs,¹²⁰ S. De Castro,^{23b,23a} S. De Cecco,^{72a,72b} N. De Groot,¹¹⁹ P. de Jong,¹²⁰ H. De la Torre,¹⁰⁶ A. De Maria,^{15c} D. De Pedis,^{72a} A. De Salvo,^{72a} U. De Sanctis,^{73a,73b} M. De Santis,^{73a,73b} A. De Santo,¹⁵⁶ K. De Vasconcelos Corga,¹⁰¹ J. B. De Vivie De Regie,¹³² C. Debenedetti,¹⁴⁶ D. V. Dedovich,⁷⁹ A. M. Deiana,⁴² M. Del Gaudio,^{41b,41a} J. Del Peso,⁹⁸ Y. Delabat Diaz,⁴⁶ D. Delgove,¹³² F. Deliot,^{145,q} C. M. Delitzsch,⁷ M. Della Pietra,^{69a,69b} D. Della Volpe,⁵⁴ A. Dell'Acqua,³⁶ L. Dell'Asta,^{73a,73b} M. Delmastro,⁵ C. Delporte,¹³² P. A. Delsart,⁵⁸ D. A. DeMarco,¹⁶⁷ S. Demers,¹⁸³ M. Demichev,⁷⁹ G. Demontigny,¹⁰⁹ S. P. Denisov,¹²³ D. Denysiuk,¹²⁰ L. D'Eramo,¹³⁶ D. Derendarz,⁸⁴ J. E. Derkaoui,^{35d} F. Derue,¹³⁶ P. Dervan,⁹⁰ K. Desch,²⁴ C. Deterre,⁴⁶ K. Dette,¹⁶⁷ C. Deutsch,²⁴ M. R. Devesa,³⁰ P. O. Deviveiros,³⁶ A. Dewhurst,¹⁴⁴ S. Dhaliwal,²⁶ F. A. Di Bello,⁵⁴ A. Di Ciaccio,^{73a,73b} L. Di Ciaccio,⁵ W. K. Di Clemente,¹³⁷ C. Di Donato,^{69a,69b} A. Di Girolamo,³⁶ G. Di Gregorio,^{71a,71b} B. Di Micco,^{74a,74b} R. Di Nardo,¹⁰² K. F. Di Petrillo,⁵⁹ R. Di Sipio,¹⁶⁷ D. Di Valentino,³⁴ C. Diaconu,¹⁰¹ F. A. Dias,⁴⁰ T. Dias Do Vale,^{140a} M. A. Diaz,^{147a} J. Dickinson,¹⁸ E. B. Diehl,¹⁰⁵ J. Dietrich,¹⁹ S. Díez Cornell,⁴⁶ A. Dimitrievska,¹⁸ W. Ding,^{15b} J. Dingfelder,²⁴ F. Dittus,³⁶ F. Djama,¹⁰¹ T. Djobava,^{159b} J. I. Djuvsland,¹⁷ M. A. B. Do Vale,^{80c} M. Dobre,^{27b} D. Dodsworth,²⁶ C. Doglioni,⁹⁶ J. Dolejsi,¹⁴³ Z. Dolezal,¹⁴³ M. Donadelli,^{80d} B. Dong,^{60c} J. Donini,³⁸ A. D'onofrio,⁹² M. D'Onofrio,⁹⁰ J. Dopke,¹⁴⁴ A. Doria,^{69a} M. T. Dova,⁸⁸ A. T. Doyle,⁵⁷ E. Drechsler,¹⁵² E. Dreyer,¹⁵² T. Dreyer,⁵³ A. S. Drobac,¹⁷⁰ Y. Duan,^{60b} F. Dubinin,¹¹⁰ M. Dubovsky,^{28a} A. Dubreuil,⁵⁴ E. Duchovni,¹⁸⁰ G. Duckeck,¹¹⁴ A. Ducourthial,¹³⁶ O. A. Ducu,¹⁰⁹ D. Duda,¹¹⁵ A. Dudarev,³⁶ A. C. Dudder,⁹⁹ E. M. Duffield,¹⁸ L. Dufлот,¹³² M. Dührssen,³⁶ C. Dülsen,¹⁸² M. Dumancic,¹⁸⁰ A. E. Dumitriu,^{27b} A. K. Duncan,⁵⁷ M. Dunford,^{61a} A. Duperrin,¹⁰¹ H. Duran Yildiz,^{4a} M. Düren,⁵⁶ A. Durglishvili,^{159b} D. Duschinger,⁴⁸ B. Dutta,⁴⁶ D. Duvnjak,¹ G. I. Dyckes,¹³⁷ M. Dyndal,³⁶ S. Dysch,¹⁰⁰ B. S. Dziejdzic,⁸⁴ K. M. Ecker,¹¹⁵ R. C. Edgar,¹⁰⁵ M. G. Eggleston,⁴⁹ T. Eifert,³⁶ G. Eigen,¹⁷ K. Einsweiler,¹⁸ T. Ekelof,¹⁷² H. El Jarrari,^{35e} M. El Kacimi,^{35c} R. El Kosseifi,¹⁰¹ V. Ellajosyula,¹⁷² M. Ellert,¹⁷² F. Ellinghaus,¹⁸² A. A. Elliot,⁹² N. Ellis,³⁶ J. Elmsheuser,²⁹ M. Elsing,³⁶ D. Emelianov,¹⁴⁴ A. Emerman,³⁹ Y. Enari,¹⁶³ M. B. Epland,⁴⁹ J. Erdmann,⁴⁷ A. Ereditato,²⁰ M. Errenst,³⁶ M. Escalier,¹³² C. Escobar,¹⁷⁴ O. Estrada Pastor,¹⁷⁴ E. Etzion,¹⁶¹ H. Evans,⁶⁵ A. Ezhilov,¹³⁸ F. Fabbri,⁵⁷ L. Fabbri,^{23b,23a} V. Fabiani,¹¹⁹ G. Facini,⁹⁴ R. M. Faisca Rodrigues Pereira,^{140a} R. M. Fakhruddinov,¹²³ S. Falciano,^{72a} P. J. Falke,⁵ S. Falke,⁵ J. Faltova,¹⁴³ Y. Fang,^{15a} Y. Fang,^{15a} G. Fanourakis,⁴⁴ M. Fanti,^{68a,68b} M. Faraj,^{66a,66c} A. Farbin,⁸ A. Farilla,^{74a} E. M. Farina,^{70a,70b} T. Farooque,¹⁰⁶ S. Farrell,¹⁸ S. M. Farrington,⁵⁰ P. Farthouat,³⁶ F. Fassi,^{35e} P. Fassnacht,³⁶ D. Fassouliotis,⁹ M. Faucci Giannelli,⁵⁰ W. J. Fawcett,³² L. Fayard,¹³² O. L. Fedin,^{138,r} W. Fedorko,¹⁷⁵ M. Feickert,⁴² S. Feigl,¹³⁴ L. Feligioni,¹⁰¹ A. Fell,¹⁴⁹ C. Feng,^{60b} E. J. Feng,³⁶ M. Feng,⁴⁹ M. J. Fenton,⁵⁷ A. B. Fenyuk,¹²³ J. Ferrando,⁴⁶ A. Ferrante,¹⁷³ A. Ferrari,¹⁷² P. Ferrari,¹²⁰ R. Ferrari,^{70a} D. E. Ferreira de Lima,^{61b} A. Ferrer,¹⁷⁴ D. Ferrere,⁵⁴ C. Ferretti,¹⁰⁵ F. Fiedler,⁹⁹ A. Filipčić,⁹¹ F. Filthaut,¹¹⁹ K. D. Finelli,²⁵ M. C. N. Fiolhais,^{140a} L. Fiorini,¹⁷⁴ F. Fischer,¹¹⁴ W. C. Fisher,¹⁰⁶ I. Fleck,¹⁵¹ P. Fleischmann,¹⁰⁵ R. R. M. Fletcher,¹³⁷ T. Flick,¹⁸² B. M. Flierl,¹¹⁴ L. F. Flores,¹³⁷ L. R. Flores Castillo,^{63a} F. M. Follega,^{75a,75b} N. Fomin,¹⁷ J. H. Foo,¹⁶⁷ G. T. Forcolin,^{75a,75b} A. Formica,¹⁴⁵ F. A. Förster,¹⁴ A. C. Forti,¹⁰⁰ A. G. Foster,²¹ M. G. Foti,¹³⁵ D. Fournier,¹³² H. Fox,⁸⁹ P. Francavilla,^{71a,71b} S. Francescato,^{72a,72b} M. Franchini,^{23b,23a} S. Franchino,^{61a} D. Francis,³⁶ L. Franconi,²⁰ M. Franklin,⁵⁹ A. N. Fray,⁹² B. Freund,¹⁰⁹ W. S. Freund,^{80b} E. M. Freundlich,⁴⁷ D. C. Frizzell,¹²⁸ D. Froidevaux,³⁶ J. A. Frost,¹³⁵ C. Fukunaga,¹⁶⁴ E. Fullana Torregrosa,¹⁷⁴ E. Fumagalli,^{55b,55a} T. Fusayasu,¹¹⁶ J. Fuster,¹⁷⁴ A. Gabrielli,^{23b,23a} A. Gabrielli,¹⁸ G. P. Gach,^{83a} S. Gadatsch,⁵⁴ P. Gadow,¹¹⁵ G. Gagliardi,^{55b,55a} L. G. Gagnon,¹⁰⁹ C. Galea,^{27b} B. Galhardo,^{140a} G. E. Gallardo,¹³⁵ E. J. Gallas,¹³⁵ B. J. Gallop,¹⁴⁴ G. Galster,⁴⁰ R. Gamboa Goni,⁹² K. K. Gan,¹²⁶ S. Ganguly,¹⁸⁰ J. Gao,^{60a} Y. Gao,⁵⁰ Y. S. Gao,^{31,h} C. García,¹⁷⁴ J. E. García Navarro,¹⁷⁴ J. A. García Pascual,^{15a} C. Garcia-Argos,⁵²

M. Garcia-Sciveres,¹⁸ R. W. Gardner,³⁷ N. Garelli,¹⁵³ S. Gargiulo,⁵² V. Garonne,¹³⁴ A. Gaudiello,^{55b,55a} G. Gaudio,^{70a}
 I. L. Gavrilenko,¹¹⁰ A. Gavriluk,¹¹¹ C. Gay,¹⁷⁵ G. Gaycken,⁴⁶ E. N. Gazis,¹⁰ A. A. Geanta,^{27b} C. N. P. Gee,¹⁴⁴ J. Geisen,⁵³
 M. Geisen,⁹⁹ M. P. Geisler,^{61a} C. Gemme,^{55b} M. H. Genest,⁵⁸ C. Geng,¹⁰⁵ S. Gentile,^{72a,72b} S. George,⁹³ T. Geralis,⁴⁴
 L. O. Gerlach,⁵³ P. Gessinger-Befurt,⁹⁹ G. Gessner,⁴⁷ S. Ghasemi,¹⁵¹ M. Ghasemi Bostanabad,¹⁷⁶ M. Ghneimat,²⁴
 A. Ghosh,¹³² A. Ghosh,⁷⁷ B. Giacobbe,^{23b} S. Giagu,^{72a,72b} N. Giangiacomi,^{23b,23a} P. Giannetti,^{71a} A. Giannini,^{69a,69b}
 G. Giannini,¹⁴ S. M. Gibson,⁹³ M. Gignac,¹⁴⁶ D. Gillberg,³⁴ G. Gilles,¹⁸² D. M. Gingrich,^{3,e} M. P. Giordani,^{66a,66c}
 F. M. Giorgi,^{23b} P. F. Giraud,¹⁴⁵ G. Giugliarelli,^{66a,66c} D. Giugni,^{68a} F. Giuli,^{73a,73b} S. Gkaitatzis,¹⁶² I. Gkialas,^{9,s}
 E. L. Gkougkousis,¹⁴ P. Gkoutoumis,¹⁰ L. K. Gladilin,¹¹³ C. Glasman,⁹⁸ J. Glatzer,¹⁴ P. C. F. Glaysheer,⁴⁶ A. Glazov,⁴⁶
 M. Goblirsch-Kolb,²⁶ S. Goldfarb,¹⁰⁴ T. Golling,⁵⁴ D. Golubkov,¹²³ A. Gomes,^{140a,140b} R. Goncalves Gama,⁵³
 R. Gonçalo,^{140a,140b} G. Gonella,⁵² L. Gonella,²¹ A. Gongadze,⁷⁹ F. Gonnella,²¹ J. L. Gonski,⁵⁹ S. González de la Hoz,¹⁷⁴
 S. Gonzalez-Sevilla,⁵⁴ G. R. Gonzalvo Rodriguez,¹⁷⁴ L. Goossens,³⁶ P. A. Gorbounov,¹¹¹ H. A. Gordon,²⁹ B. Gorini,³⁶
 E. Gorini,^{67a,67b} A. Gorišek,⁹¹ A. T. Goshaw,⁴⁹ C. Gössling,⁴⁷ M. I. Gostkin,⁷⁹ C. A. Gottardo,¹¹⁹ M. Gouighri,^{35b}
 D. Goujdami,^{35c} A. G. Goussiou,¹⁴⁸ N. Govender,^{33b} C. Goy,⁵ E. Gozani,¹⁶⁰ I. Grabowska-Bold,^{83a} E. C. Graham,⁹⁰
 J. Gramling,¹⁷¹ E. Gramstad,¹³⁴ S. Grancagnolo,¹⁹ M. Grandi,¹⁵⁶ V. Gratchev,¹³⁸ P. M. Gravila,^{27f} F. G. Gravili,^{67a,67b}
 C. Gray,⁵⁷ H. M. Gray,¹⁸ C. Greife,²⁴ K. Gregersen,⁹⁶ I. M. Gregor,⁴⁶ P. Grenier,¹⁵³ K. Grevtsov,⁴⁶ C. Grieco,¹⁴
 N. A. Grieser,¹²⁸ J. Griffiths,⁸ A. A. Grillo,¹⁴⁶ K. Grimm,^{31,t} S. Grinstein,^{14,u} J.-F. Grivaz,¹³² S. Groh,⁹⁹ E. Gross,¹⁸⁰
 J. Grosse-Knetter,⁵³ Z. J. Grout,⁹⁴ C. Grud,¹⁰⁵ A. Grummer,¹¹⁸ L. Guan,¹⁰⁵ W. Guan,¹⁸¹ J. Guenther,³⁶ A. Guerguichon,¹³²
 J. G. R. Guerrero Rojas,¹⁷⁴ F. Guescini,¹¹⁵ D. Guest,¹⁷¹ R. Gugel,⁵² T. Guillemain,⁵ S. Guindon,³⁶ U. Gul,⁵⁷ J. Guo,^{60c}
 W. Guo,¹⁰⁵ Y. Guo,^{60a,v} Z. Guo,¹⁰¹ R. Gupta,⁴⁶ S. Gurbuz,^{12c} G. Gustavino,¹²⁸ P. Gutierrez,¹²⁸ C. Gutsche,⁹⁴ C. Guyot,¹⁴⁵
 C. Gwenlan,¹³⁵ C. B. Gwilliam,⁹⁰ A. Haas,¹²⁴ C. Haber,¹⁸ H. K. Hadavand,⁸ N. Haddad,^{35e} A. Hadeif,^{60a} S. Hageböck,³⁶
 M. Hagihara,¹⁶⁹ M. Haleem,¹⁷⁷ J. Haley,¹²⁹ G. Halladjian,¹⁰⁶ G. D. Hallewell,¹⁰¹ K. Hamacher,¹⁸² P. Hamal,¹³⁰
 K. Hamano,¹⁷⁶ H. Hamdaoui,^{35e} G. N. Hamity,¹⁴⁹ K. Han,^{60a,w} L. Han,^{60a} S. Han,^{15a,15d} K. Hanagaki,^{81,x} M. Hance,¹⁴⁶
 D. M. Handl,¹¹⁴ B. Haney,¹³⁷ R. Hankache,¹³⁶ P. Hanke,^{61a} E. Hansen,⁹⁶ J. B. Hansen,⁴⁰ J. D. Hansen,⁴⁰ M. C. Hansen,²⁴
 P. H. Hansen,⁴⁰ E. C. Hanson,¹⁰⁰ K. Hara,¹⁶⁹ A. S. Hard,¹⁸¹ T. Harenberg,¹⁸² S. Harkusha,¹⁰⁷ P. F. Harrison,¹⁷⁸
 N. M. Hartmann,¹¹⁴ Y. Hasegawa,¹⁵⁰ A. Hasib,⁵⁰ S. Hassani,¹⁴⁵ S. Haug,²⁰ R. Hauser,¹⁰⁶ L. B. Havener,³⁹ M. Havranek,¹⁴²
 C. M. Hawkes,²¹ R. J. Hawkings,³⁶ D. Hayden,¹⁰⁶ C. Hayes,¹⁵⁵ R. L. Hayes,¹⁷⁵ C. P. Hays,¹³⁵ J. M. Hays,⁹² H. S. Hayward,⁹⁰
 S. J. Haywood,¹⁴⁴ F. He,^{60a} M. P. Heath,⁵⁰ V. Hedberg,⁹⁶ L. Heelan,⁸ S. Heer,²⁴ K. K. Heidegger,⁵² W. D. Heidorn,⁷⁸
 J. Heilman,³⁴ S. Heim,⁴⁶ T. Heim,¹⁸ B. Heinemann,^{46,y} J. J. Heinrich,¹³¹ L. Heinrich,³⁶ C. Heinz,⁵⁶ J. Hejbal,¹⁴¹ L. Helary,^{61b}
 A. Held,¹⁷⁵ S. Hellesund,¹³⁴ C. M. Helling,¹⁴⁶ S. Hellman,^{45a,45b} C. Helsen,³⁶ R. C. W. Henderson,⁸⁹ Y. Heng,¹⁸¹
 S. Henkelmann,¹⁷⁵ A. M. Henriques Correia,³⁶ G. H. Herbert,¹⁹ H. Herde,²⁶ V. Herget,¹⁷⁷ Y. Hernández Jiménez,^{33c}
 H. Herr,⁹⁹ M. G. Herrmann,¹¹⁴ T. Herrmann,⁴⁸ G. Herten,⁵² R. Hertenberger,¹¹⁴ L. Hervas,³⁶ T. C. Herwig,¹³⁷
 G. G. Hesketh,⁹⁴ N. P. Hessey,^{168a} A. Higashida,¹⁶³ S. Higashino,⁸¹ E. Higón-Rodríguez,¹⁷⁴ K. Hildebrand,³⁷ E. Hill,¹⁷⁶
 J. C. Hill,³² K. K. Hill,²⁹ K. H. Hiller,⁴⁶ S. J. Hillier,²¹ M. Hils,⁴⁸ I. Hinchliffe,¹⁸ F. Hinterkeuser,²⁴ M. Hirose,¹³³ S. Hirose,⁵²
 D. Hirschbuehl,¹⁸² B. Hiti,⁹¹ O. Hladik,¹⁴¹ D. R. Hlaluku,^{33c} X. Hoad,⁵⁰ J. Hobbs,¹⁵⁵ N. Hod,¹⁸⁰ M. C. Hodgkinson,¹⁴⁹
 A. Hoecker,³⁶ F. Hoenig,¹¹⁴ D. Hohn,⁵² D. Hohov,¹³² T. R. Holmes,³⁷ M. Holzbock,¹¹⁴ L. B. A. H. Hommels,³² S. Honda,¹⁶⁹
 T. Honda,⁸¹ T. M. Hong,¹³⁹ A. Hönle,¹¹⁵ B. H. Hooberman,¹⁷³ W. H. Hopkins,⁶ Y. Horii,¹¹⁷ P. Horn,⁴⁸ L. A. Horyn,³⁷
 A. Hostiuc,¹⁴⁸ S. Hou,¹⁵⁸ A. Hoummada,^{35a} J. Howarth,¹⁰⁰ J. Hoya,⁸⁸ M. Hrabovsky,¹³⁰ J. Hrdinka,⁷⁶ I. Hristova,¹⁹
 J. Hrivnac,¹³² A. Hrynevich,¹⁰⁸ T. Hryn'ova,⁵ P. J. Hsu,⁶⁴ S.-C. Hsu,¹⁴⁸ Q. Hu,²⁹ S. Hu,^{60c} D. P. Huang,⁹⁴ Y. Huang,^{15a}
 Z. Hubacek,¹⁴² F. Hubaut,¹⁰¹ M. Huebner,²⁴ F. Huegging,²⁴ T. B. Huffman,¹³⁵ M. Huhtinen,³⁶ R. F. H. Hunter,³⁴ P. Huo,¹⁵⁵
 A. M. Hupe,³⁴ N. Huseynov,^{79,z} J. Huston,¹⁰⁶ J. Huth,⁵⁹ R. Hyneman,¹⁰⁵ S. Hyrych,^{28a} G. Iacobucci,⁵⁴ G. Iakovidis,²⁹
 I. Ibragimov,¹⁵¹ L. Iconomidou-Fayard,¹³² Z. Idrissi,^{35e} P. I. Iengo,³⁶ R. Ignazzi,⁴⁰ O. Igonkina,^{120,a,aa} R. Iguchi,¹⁶³
 T. Iizawa,⁵⁴ Y. Ikegami,⁸¹ M. Ikeno,⁸¹ D. Iliadis,¹⁶² N. Ilic,¹¹⁹ F. Iltzsche,⁴⁸ G. Introzzi,^{70a,70b} M. Iodice,^{74a} K. Iordanidou,^{168a}
 V. Ippolito,^{72a,72b} M. F. Isacson,¹⁷² M. Ishino,¹⁶³ M. Ishitsuka,¹⁶⁵ W. Islam,¹²⁹ C. Issever,¹³⁵ S. Istin,¹⁶⁰ F. Ito,¹⁶⁹
 J. M. Iturbe Ponce,^{63a} R. Iuppa,^{75a,75b} A. Ivina,¹⁸⁰ H. Iwasaki,⁸¹ J. M. Izen,⁴³ V. Izzo,^{69a} P. Jacka,¹⁴¹ P. Jackson,¹
 R. M. Jacobs,²⁴ B. P. Jaeger,¹⁵² V. Jain,² G. Jäkel,¹⁸² K. B. Jakobi,⁹⁹ K. Jakobs,⁵² S. Jakobsen,⁷⁶ T. Jakoubek,¹⁴¹
 J. Jamieson,⁵⁷ K. W. Janas,^{83a} R. Jansky,⁵⁴ J. Janssen,²⁴ M. Janus,⁵³ P. A. Janus,^{83a} G. Jarlskog,⁹⁶ N. Javadov,^{79,z} T. Javůrek,³⁶
 M. Javurkova,⁵² F. Jeanneau,¹⁴⁵ L. Jeanty,¹³¹ J. Jejelava,^{159a,bb} A. Jelinskas,¹⁷⁸ P. Jenni,^{52,cc} J. Jeong,⁴⁶ N. Jeong,⁴⁶
 S. Jézéquel,⁵ H. Ji,¹⁸¹ J. Jia,¹⁵⁵ H. Jiang,⁷⁸ Y. Jiang,^{60a} Z. Jiang,^{153,dd} S. Jiggins,⁵² F. A. Jimenez Morales,³⁸
 J. Jimenez Pena,¹¹⁵ S. Jin,^{15c} A. Jinaru,^{27b} O. Jinnouchi,¹⁶⁵ H. Jivan,^{33c} P. Johansson,¹⁴⁹ K. A. Johns,⁷ C. A. Johnson,⁶⁵

K. Jon-And,^{45a,45b} R. W. L. Jones,⁸⁹ S. D. Jones,¹⁵⁶ S. Jones,⁷ T. J. Jones,⁹⁰ J. Jongmanns,^{61a} P. M. Jorge,^{140a} J. Jovicevic,³⁶
 X. Ju,¹⁸ J. J. Junggeburth,¹¹⁵ A. Juste Rozas,^{14,u} A. Kaczmarek,⁸⁴ M. Kado,^{72a,72b} H. Kagan,¹²⁶ M. Kagan,¹⁵³ C. Kahra,⁹⁹
 T. Kaji,¹⁷⁹ E. Kajomovitz,¹⁶⁰ C. W. Kalderon,⁹⁶ A. Kaluza,⁹⁹ A. Kamenshchikov,¹²³ L. Kanjir,⁹¹ Y. Kano,¹⁶³
 V. A. Kantserov,¹¹² J. Kanzaki,⁸¹ L. S. Kaplan,¹⁸¹ D. Kar,^{33c} M. J. Kareem,^{168b} S. N. Karpov,⁷⁹ Z. M. Karpova,⁷⁹
 V. Kartvelishvili,⁸⁹ A. N. Karyukhin,¹²³ L. Kashif,¹⁸¹ R. D. Kass,¹²⁶ A. Kastanas,^{45a,45b} Y. Kataoka,¹⁶³ C. Kato,^{60d,60c}
 J. Katzy,⁴⁶ K. Kawade,⁸² K. Kawagoe,⁸⁷ T. Kawaguchi,¹¹⁷ T. Kawamoto,¹⁶³ G. Kawamura,⁵³ E. F. Kay,¹⁷⁶
 V. F. Kazanin,^{122b,122a} R. Keeler,¹⁷⁶ R. Kehoe,⁴² J. S. Keller,³⁴ E. Kellermann,⁹⁶ D. Kelsey,¹⁵⁶ J. J. Kempster,²¹ J. Kendrick,²¹
 O. Kepka,¹⁴¹ S. Kersten,¹⁸² B. P. Kerševan,⁹¹ S. Ketabchi Haghighat,¹⁶⁷ M. Khader,¹⁷³ F. Khalil-Zada,¹³ M. Khandoga,¹⁴⁵
 A. Khanov,¹²⁹ A. G. Kharlamov,^{122b,122a} T. Kharlamova,^{122b,122a} E. E. Khoda,¹⁷⁵ A. Khodinov,¹⁶⁶ T. J. Khoo,⁵⁴ E. Khramov,⁷⁹
 J. Khubua,^{159b} S. Kido,⁸² M. Kiehn,⁵⁴ C. R. Kilby,⁹³ Y. K. Kim,³⁷ N. Kimura,^{66a,66c} O. M. Kind,¹⁹ B. T. King,^{90,a}
 D. Kirchmeier,⁴⁸ J. Kirk,¹⁴⁴ A. E. Kiryunin,¹¹⁵ T. Kishimoto,¹⁶³ D. P. Kisliuk,¹⁶⁷ V. Kitali,⁴⁶ O. Kivernyk,⁵ E. Kladiva,^{28b,a}
 T. Klapdor-Kleingrothaus,⁵² M. Klassen,^{61a} M. H. Klein,¹⁰⁵ M. Klein,⁹⁰ U. Klein,⁹⁰ K. Kleinknecht,⁹⁹ P. Klimek,¹²¹
 A. Klimentov,²⁹ T. Klingl,²⁴ T. Klioutchnikova,³⁶ F. F. Klitzner,¹¹⁴ P. Kluit,¹²⁰ S. Kluth,¹¹⁵ E. Kneringer,⁷⁶
 E. B. F. G. Knoop,¹⁰¹ A. Knue,⁵² D. Kobayashi,⁸⁷ T. Kobayashi,¹⁶³ M. Kobel,⁴⁸ M. Kocian,¹⁵³ P. Kodys,¹⁴³ P. T. Koenig,²⁴
 T. Koffas,³⁴ N. M. Köhler,³⁶ T. Koi,¹⁵³ M. Kolb,^{61b} I. Koletsou,⁵ T. Komarek,¹³⁰ T. Kondo,⁸¹ N. Kondrashova,^{60c}
 K. Köneke,⁵² A. C. König,¹¹⁹ T. Kono,¹²⁵ R. Konoplich,^{124,ee} V. Konstantinides,⁹⁴ N. Konstantinidis,⁹⁴ B. Konya,⁹⁶
 R. Kopeliainsky,⁶⁵ S. Koperny,^{83a} K. Korcyl,⁸⁴ K. Kordas,¹⁶² G. Koren,¹⁶¹ A. Korn,⁹⁴ I. Korolkov,¹⁴ E. V. Korolkova,¹⁴⁹
 N. Korotkova,¹¹³ O. Kortner,¹¹⁵ S. Kortner,¹¹⁵ T. Kosek,¹⁴³ V. V. Kostyukhin,²⁴ A. Kotwal,⁴⁹ A. Koulouris,¹⁰
 A. Kourkoumeli-Charalampidi,^{70a,70b} C. Kourkoumelis,⁹ E. Kourlitis,¹⁴⁹ V. Kouskoura,²⁹ A. B. Kowalewska,⁸⁴
 R. Kowalewski,¹⁷⁶ C. Kozakai,¹⁶³ W. Kozanecki,¹⁴⁵ A. S. Kozhin,¹²³ V. A. Kramarenko,¹¹³ G. Kramberger,⁹¹
 D. Krasnopevtsev,^{60a} M. W. Krasny,¹³⁶ A. Krasznahorkay,³⁶ D. Krauss,¹¹⁵ J. A. Kremer,^{83a} J. Kretzschmar,⁹⁰ P. Krieger,¹⁶⁷
 F. Krieter,¹¹⁴ A. Krishnan,^{61b} K. Krizka,¹⁸ K. Kroeninger,⁴⁷ H. Kroha,¹¹⁵ J. Kroll,¹⁴¹ J. Kroll,¹³⁷ J. Krstic,¹⁶ U. Kruchonak,⁷⁹
 H. Krüger,²⁴ N. Krumnack,⁷⁸ M. C. Kruse,⁴⁹ J. A. Krzysiak,⁸⁴ T. Kubota,¹⁰⁴ O. Kuchinskaia,¹⁶⁶ S. Kuday,^{4b} J. T. Kuechler,⁴⁶
 S. Kuehn,³⁶ A. Kugel,^{61a} T. Kuhl,⁴⁶ V. Kukhtin,⁷⁹ R. Kukla,¹⁰¹ Y. Kulchitsky,^{107,ff} S. Kuleshov,^{147b} Y. P. Kulinich,¹⁷³
 M. Kuna,⁵⁸ T. Kunigo,⁸⁵ A. Kupco,¹⁴¹ T. Kupfer,⁴⁷ O. Kuprash,⁵² H. Kurashige,⁸² L. L. Kurchaninov,^{168a}
 Y. A. Kurochkin,¹⁰⁷ A. Kurova,¹¹² M. G. Kurth,^{15a,15d} E. S. Kuwertz,³⁶ M. Kuze,¹⁶⁵ A. K. Kvam,¹⁴⁸ J. Kvita,¹³⁰ T. Kwan,¹⁰³
 A. La Rosa,¹¹⁵ L. La Rotonda,^{41b,41a} F. La Ruffa,^{41b,41a} C. Lacasta,¹⁷⁴ F. Lacava,^{72a,72b} D. P. J. Lack,¹⁰⁰ H. Lacker,¹⁹
 D. Lacour,¹³⁶ E. Ladygin,⁷⁹ R. Lafaye,⁵ B. Laforge,¹³⁶ T. Lagouri,^{33c} S. Lai,⁵³ S. Lammers,⁶⁵ W. Lampl,⁷ C. Lampoudis,¹⁶²
 E. Lançon,²⁹ U. Landgraf,⁵² M. P. J. Landon,⁹² M. C. Lanfermann,⁵⁴ V. S. Lang,⁴⁶ J. C. Lange,⁵³ R. J. Langenberg,³⁶
 A. J. Lankford,¹⁷¹ F. Lanni,²⁹ K. Lantzsch,²⁴ A. Lanza,^{70a} A. Lapertosa,^{55b,55a} S. Laplace,¹³⁶ J. F. Laporte,¹⁴⁵ T. Lari,^{68a}
 F. Lasagni Manghi,^{23b,23a} M. Lassnig,³⁶ T. S. Lau,^{63a} A. Laudrain,¹³² A. Laurier,³⁴ M. Lavorgna,^{69a,69b} M. Lazzaroni,^{68a,68b}
 B. Le,¹⁰⁴ O. Le Dortz,¹³⁶ E. Le Guirriec,¹⁰¹ M. LeBlanc,⁷ T. LeCompte,⁶ F. Ledroit-Guillon,⁵⁸ C. A. Lee,²⁹ G. R. Lee,¹⁷
 L. Lee,⁵⁹ S. C. Lee,¹⁵⁸ S. J. Lee,³⁴ B. Lefebvre,^{168a} M. Lefebvre,¹⁷⁶ F. Legger,¹¹⁴ C. Leggett,¹⁸ K. Lehmann,¹⁵²
 N. Lehmann,¹⁸² G. Lehmann Miotto,³⁶ W. A. Leight,⁴⁶ A. Leisos,^{162,gg} M. A. L. Leite,^{80d} C. E. Leitgeb,¹¹⁴ R. Leitner,¹⁴³
 D. Lellouch,^{180,a} K. J. C. Leney,⁴² T. Lenz,²⁴ B. Lenzi,³⁶ R. Leone,⁷ S. Leone,^{71a} C. Leonidopoulos,⁵⁰ A. Leopold,¹³⁶
 G. Lerner,¹⁵⁶ C. Leroy,¹⁰⁹ R. Les,¹⁶⁷ C. G. Lester,³² M. Levchenko,¹³⁸ J. Levêque,⁵ D. Levin,¹⁰⁵ L. J. Levinson,¹⁸⁰
 D. J. Lewis,²¹ B. Li,^{15b} B. Li,¹⁰⁵ C-Q. Li,^{60a} F. Li,^{60c} H. Li,^{60a} H. Li,^{60b} J. Li,^{60c} K. Li,¹⁵³ L. Li,^{60c} M. Li,^{15a} Q. Li,^{15a,15d}
 Q. Y. Li,^{60a} S. Li,^{60d,60c} X. Li,⁴⁶ Y. Li,⁴⁶ Z. Li,^{60b} Z. Liang,^{15a} B. Liberti,^{73a} A. Liblong,¹⁶⁷ K. Lie,^{63c} S. Liem,¹²⁰ C. Y. Lin,³²
 K. Lin,¹⁰⁶ T. H. Lin,⁹⁹ R. A. Linck,⁶⁵ J. H. Lindon,²¹ A. L. Lioni,⁵⁴ E. Lipeles,¹³⁷ A. Lipniacka,¹⁷ M. Lisovsky,^{61b}
 T. M. Liss,^{173,hh} A. Lister,¹⁷⁵ A. M. Litke,¹⁴⁶ J. D. Little,⁸ B. Liu,^{78,ii} B. L. Liu,⁶ H. B. Liu,²⁹ H. Liu,¹⁰⁵ J. B. Liu,^{60a}
 J. K. K. Liu,¹³⁵ K. Liu,¹³⁶ M. Liu,^{60a} P. Liu,¹⁸ Y. Liu,^{15a,15d} Y. L. Liu,¹⁰⁵ Y. W. Liu,^{60a} M. Livan,^{70a,70b} A. Lleres,⁵⁸
 J. Llorente Merino,^{15a} S. L. Lloyd,⁹² C. Y. Lo,^{63b} F. Lo Sterzo,⁴² E. M. Lobodzinska,⁴⁶ P. Loch,⁷ S. Loffredo,^{73a,73b}
 T. Lohse,¹⁹ K. Lohwasser,¹⁴⁹ M. Lokajicek,¹⁴¹ J. D. Long,¹⁷³ R. E. Long,⁸⁹ L. Longo,³⁶ K. A. Looper,¹²⁶ J. A. Lopez,^{147b}
 I. Lopez Paz,¹⁰⁰ A. Lopez Solis,¹⁴⁹ J. Lorenz,¹¹⁴ N. Lorenzo Martinez,⁵ M. Losada,²² P. J. Lösel,¹¹⁴ A. Lösle,⁵² X. Lou,⁴⁶
 X. Lou,^{15a} A. Lounis,¹³² J. Love,⁶ P. A. Love,⁸⁹ J. J. Lozano Bahilo,¹⁷⁴ M. Lu,^{60a} Y. J. Lu,⁶⁴ H. J. Lubatti,¹⁴⁸ C. Luci,^{72a,72b}
 A. Lucotte,⁵⁸ C. Luedtke,⁵² F. Luehring,⁶⁵ I. Luise,¹³⁶ L. Luminari,^{72a} B. Lund-Jensen,¹⁵⁴ M. S. Lutz,¹⁰² D. Lynn,²⁹
 R. Lysak,¹⁴¹ E. Lytken,⁹⁶ F. Lyu,^{15a} V. Lyubushkin,⁷⁹ T. Lyubushkina,⁷⁹ H. Ma,²⁹ L. L. Ma,^{60b} Y. Ma,^{60b} G. Maccarrone,⁵¹
 A. Macchiolo,¹¹⁵ C. M. Macdonald,¹⁴⁹ J. Machado Miguens,¹³⁷ D. Madaffari,¹⁷⁴ R. Madar,³⁸ W. F. Mader,⁴⁸ N. Madysa,⁴⁸
 J. Maeda,⁸² K. Maekawa,¹⁶³ S. Maeland,¹⁷ T. Maeno,²⁹ M. Maerker,⁴⁸ A. S. Maevskiy,¹¹³ V. Magerl,⁵² N. Magini,⁷⁸

D. J. Mahon,³⁹ C. Maidantchik,^{80b} T. Maier,¹¹⁴ A. Maio,^{140a,140b,140d} O. Majersky,^{28a} S. Majewski,¹³¹ Y. Makida,⁸¹ N. Makovec,¹³² B. Malaescu,¹³⁶ Pa. Malecki,⁸⁴ V. P. Maleev,¹³⁸ F. Malek,⁵⁸ U. Mallik,⁷⁷ D. Malon,⁶ C. Malone,³² S. Maltezos,¹⁰ S. Malyukov,³⁶ J. Mamuzic,¹⁷⁴ G. Mancini,⁵¹ I. Mandić,⁹¹ L. Manhaes de Andrade Filho,^{80a} I. M. Maniatis,¹⁶² J. Manjarres Ramos,⁴⁸ K. H. Mankinen,⁹⁶ A. Mann,¹¹⁴ A. Manousos,⁷⁶ B. Mansoulie,¹⁴⁵ I. Manthos,¹⁶² S. Manzoni,¹²⁰ A. Marantis,¹⁶² G. Marceca,³⁰ L. Marchese,¹³⁵ G. Marchiori,¹³⁶ M. Marcisovsky,¹⁴¹ C. Marcon,⁹⁶ C. A. Marin Tobon,³⁶ M. Marjanovic,³⁸ F. Marroquin,^{80b} Z. Marshall,¹⁸ M. U. F. Martensson,¹⁷² S. Marti-Garcia,¹⁷⁴ C. B. Martin,¹²⁶ T. A. Martin,¹⁷⁸ V. J. Martin,⁵⁰ B. Martin dit Latour,¹⁷ L. Martinelli,^{74a,74b} M. Martinez,^{14u} V. I. Martinez Outschoorn,¹⁰² S. Martin-Haugh,¹⁴⁴ V. S. Martoiu,^{27b} A. C. Martyniuk,⁹⁴ A. Marzin,³⁶ S. R. Maschek,¹¹⁵ L. Masetti,⁹⁹ T. Mashimo,¹⁶³ R. Mashinistov,¹¹⁰ J. Masik,¹⁰⁰ A. L. Maslennikov,^{122b,122a} L. H. Mason,¹⁰⁴ L. Massa,^{73a,73b} P. Massarotti,^{69a,69b} P. Mastrandrea,^{71a,71b} A. Mastroberardino,^{41b,41a} T. Masubuchi,¹⁶³ D. Matakias,¹⁰ A. Matic,¹¹⁴ P. Mättig,²⁴ J. Maurer,^{27b} B. Maček,⁹¹ S. J. Maxfield,⁹⁰ D. A. Maximov,^{122b,122a} R. Mazini,¹⁵⁸ I. Maznas,¹⁶² S. M. Mazza,¹⁴⁶ S. P. Mc Kee,¹⁰⁵ T. G. McCarthy,¹¹⁵ L. I. McClymont,⁹⁴ W. P. McCormack,¹⁸ E. F. McDonald,¹⁰⁴ J. A. Mcfayden,³⁶ M. A. McKay,⁴² K. D. McLean,¹⁷⁶ S. J. McMahon,¹⁴⁴ P. C. McNamara,¹⁰⁴ C. J. McNicol,¹⁷⁸ R. A. McPherson,^{176,p} J. E. Mdhluli,^{33c} Z. A. Meadows,¹⁰² S. Meehan,¹⁴⁸ T. Megy,⁵² S. Mehlhase,¹¹⁴ A. Mehta,⁹⁰ T. Meideck,⁵⁸ B. Meirose,⁴³ D. Melini,¹⁷⁴ B. R. Mellado Garcia,^{33c} J. D. Mellenthin,⁵³ M. Melo,^{28a} F. Meloni,⁴⁶ A. Melzer,²⁴ S. B. Menary,¹⁰⁰ E. D. Mendes Gouveia,^{140a,140e} L. Meng,³⁶ X. T. Meng,¹⁰⁵ S. Menke,¹¹⁵ E. Meoni,^{41b,41a} S. Mergelmeyer,¹⁹ S. A. M. Merkt,¹³⁹ C. Merlassino,²⁰ P. Mermod,⁵⁴ L. Merola,^{69a,69b} C. Meroni,^{68a} O. Meshkov,^{113,110} J. K. R. Meshreki,¹⁵¹ A. Messina,^{72a,72b} J. Metcalfe,⁶ A. S. Mete,¹⁷¹ C. Meyer,⁶⁵ J. Meyer,¹⁶⁰ J-P. Meyer,¹⁴⁵ H. Meyer Zu Theenhausen,^{61a} F. Miano,¹⁵⁶ M. Michetti,¹⁹ R. P. Middleton,¹⁴⁴ L. Mijović,⁵⁰ G. Mikenberg,¹⁸⁰ M. Mikesikova,¹⁴¹ M. Mikuž,⁹¹ H. Mildner,¹⁴⁹ M. Milesi,¹⁰⁴ A. Milic,¹⁶⁷ D. A. Millar,⁹² D. W. Miller,³⁷ A. Milov,¹⁸⁰ D. A. Milstead,^{45a,45b} R. A. Mina,^{153,dd} A. A. Minaenko,¹²³ M. Miñano Moya,¹⁷⁴ I. A. Minashvili,^{159b} A. I. Mincer,¹²⁴ B. Mindur,^{83a} M. Mineev,⁷⁹ Y. Minegishi,¹⁶³ Y. Ming,¹⁸¹ L. M. Mir,¹⁴ A. Mirto,^{67a,67b} K. P. Mistry,¹³⁷ T. Mitani,¹⁷⁹ J. Mitrevski,¹¹⁴ V. A. Mitsou,¹⁷⁴ M. Mittal,^{60c} O. Miu,¹⁶⁷ A. Miucci,²⁰ P. S. Miyagawa,¹⁴⁹ A. Mizukami,⁸¹ J. U. Mjörnmark,⁹⁶ T. Mkrtychyan,¹⁸⁴ M. Mlynarikova,¹⁴³ T. Moa,^{45a,45b} K. Mochizuki,¹⁰⁹ P. Mogg,⁵² S. Mohapatra,³⁹ R. Moles-Valls,²⁴ M. C. Mondragon,¹⁰⁶ K. Mönig,⁴⁶ J. Monk,⁴⁰ E. Monnier,¹⁰¹ A. Montalbano,¹⁵² J. Montejo Berlingen,³⁶ M. Montella,⁹⁴ F. Monticelli,⁸⁸ S. Monzani,^{68a} N. Morange,¹³² D. Moreno,²² M. Moreno Llácer,³⁶ C. Moreno Martinez,¹⁴ P. Morettini,^{55b} M. Morgenstern,¹²⁰ S. Morgenstern,⁴⁸ D. Mori,¹⁵² M. Morii,⁵⁹ M. Morinaga,¹⁷⁹ V. Morisbak,¹³⁴ A. K. Morley,³⁶ G. Mornacchi,³⁶ A. P. Morris,⁹⁴ L. Morvaj,¹⁵⁵ P. Moschovakos,³⁶ B. Moser,¹²⁰ M. Mosidze,^{159b} T. Moskalets,¹⁴⁵ H. J. Moss,¹⁴⁹ J. Moss,^{31,jj} K. Motohashi,¹⁶⁵ E. Mountricha,³⁶ E. J. W. Moyses,¹⁰² S. Muanza,¹⁰¹ J. Mueller,¹³⁹ R. S. P. Mueller,¹¹⁴ D. Muenstermann,⁸⁹ G. A. Mullier,⁹⁶ J. L. Munoz Martinez,¹⁴ F. J. Munoz Sanchez,¹⁰⁰ P. Murin,^{28b} W. J. Murray,^{178,144} A. Murrone,^{68a,68b} M. Muškinja,¹⁸ C. Mwewa,^{33a} A. G. Myagkov,^{123,kk} J. Myers,¹³¹ M. Myska,¹⁴² B. P. Nachman,¹⁸ O. Nackenhorst,⁴⁷ A. Nag Nag,⁴⁸ K. Nagai,¹³⁵ K. Nagano,⁸¹ Y. Nagasaka,⁶² M. Nagel,⁵² E. Nagy,¹⁰¹ A. M. Nairz,³⁶ Y. Nakahama,¹¹⁷ K. Nakamura,⁸¹ T. Nakamura,¹⁶³ I. Nakano,¹²⁷ H. Nanjo,¹³³ F. Napolitano,^{61a} R. F. Naranjo Garcia,⁴⁶ R. Narayan,⁴² I. Naryshkin,¹³⁸ T. Naumann,⁴⁶ G. Navarro,²² H. A. Neal,^{105,a} P. Y. Nechaeva,¹¹⁰ F. Nechansky,⁴⁶ T. J. Neep,²¹ A. Negri,^{70a,70b} M. Negrini,^{23b} C. Nellist,⁵³ M. E. Nelson,¹³⁵ S. Nemecek,¹⁴¹ P. Nemethy,¹²⁴ M. Nessi,^{36,ll} M. S. Neubauer,¹⁷³ M. Neumann,¹⁸² P. R. Newman,²¹ Y. S. Ng,¹⁹ Y. W. Y. Ng,¹⁷¹ B. Ngair,^{35e} H. D. N. Nguyen,¹⁰¹ T. Nguyen Manh,¹⁰⁹ E. Nibigira,³⁸ R. B. Nickerson,¹³⁵ R. Nicolaidou,¹⁴⁵ D. S. Nielsen,⁴⁰ J. Nielsen,¹⁴⁶ N. Nikiforou,¹¹ V. Nikolaenko,^{123,kk} I. Nikolic-Audit,¹³⁶ K. Nikolopoulos,²¹ P. Nilsson,²⁹ H. R. Nindhito,⁵⁴ Y. Ninomiya,⁸¹ A. Nisati,^{72a} N. Nishu,^{60c} R. Nisius,¹¹⁵ I. Nitsche,⁴⁷ T. Nitta,¹⁷⁹ T. Nobe,¹⁶³ Y. Noguchi,⁸⁵ I. Nomidis,¹³⁶ M. A. Nomura,²⁹ M. Nordberg,³⁶ N. Norjoharuddeen,¹³⁵ T. Novak,⁹¹ O. Novgorodova,⁴⁸ R. Novotny,¹⁴² L. Nozka,¹³⁰ K. Ntekas,¹⁷¹ E. Nurse,⁹⁴ F. G. Oakham,^{34,e} H. Oberlack,¹¹⁵ J. Ocariz,¹³⁶ A. Ochi,⁸² I. Ochoa,³⁹ J. P. Ochoa-Ricoux,^{147a} K. O'Connor,²⁶ S. Oda,⁸⁷ S. Odaka,⁸¹ S. Oerdek,⁵³ A. Ogrodnik,^{83a} A. Oh,¹⁰⁰ S. H. Oh,⁴⁹ C. C. Ohm,¹⁵⁴ H. Oide,^{55b,55a} M. L. Ojeda,¹⁶⁷ H. Okawa,¹⁶⁹ Y. Okazaki,⁸⁵ M. W. O'Keefe,⁹⁰ Y. Okumura,¹⁶³ T. Okuyama,⁸¹ A. Olariu,^{27b} L. F. Oleiro Seabra,^{140a} S. A. Olivares Pino,^{147a} D. Oliveira Damazio,²⁹ J. L. Oliver,¹ M. J. R. Olsson,¹⁷¹ A. Olszewski,⁸⁴ J. Olszowska,⁸⁴ D. C. O'Neil,¹⁵² A. Onofre,^{140a,140e} K. Onogi,¹¹⁷ P. U. E. Onyisi,¹¹ H. Oppen,¹³⁴ M. J. Oreglia,³⁷ G. E. Orellana,⁸⁸ Y. Oren,¹⁶¹ D. Orestano,^{74a,74b} N. Orlando,¹⁴ R. S. Orr,¹⁶⁷ V. O'Shea,⁵⁷ R. Ospanov,^{60a} G. Otero y Garzon,³⁰ H. Otono,⁸⁷ P. S. Ott,^{61a} M. Ouchrif,^{35d} J. Ouellette,²⁹ F. Ould-Saada,¹³⁴ A. Ouraou,¹⁴⁵ Q. Ouyang,^{15a} M. Owen,⁵⁷ R. E. Owen,²¹ V. E. Ozcan,^{12c} N. Ozturk,⁸ J. Pacalt,¹³⁰ H. A. Pacey,³² K. Pachal,⁴⁹ A. Pacheco Pages,¹⁴ C. Padilla Aranda,¹⁴ S. Pagan Griso,¹⁸ M. Paganini,¹⁸³ G. Palacino,⁶⁵ S. Palazzo,⁵⁰ S. Palestini,³⁶ M. Palka,^{83b} D. Pallin,³⁸ I. Panagoulas,¹⁰ C. E. Pandini,³⁶ J. G. Panduro Vazquez,⁹³ P. Pani,⁴⁶ G. Panizzo,^{66a,66c}

L. Paolozzi,⁵⁴ C. Papadatos,¹⁰⁹ K. Papageorgiou,^{9,s} S. Parajuli,⁴³ A. Paramonov,⁶ D. Paredes Hernandez,^{63b}
S. R. Paredes Saenz,¹³⁵ B. Parida,¹⁶⁶ T. H. Park,¹⁶⁷ A. J. Parker,⁸⁹ M. A. Parker,³² F. Parodi,^{55b,55a} E. W. P. Parrish,¹²¹
J. A. Parsons,³⁹ U. Parzefall,⁵² L. Pascual Dominguez,¹³⁶ V. R. Pascuzzi,¹⁶⁷ J. M. P. Pasner,¹⁴⁶ E. Pasqualucci,^{72a}
S. Passaggio,^{55b} F. Pastore,⁹³ P. Pasuwan,^{45a,45b} S. Patariaia,⁹⁹ J. R. Pater,¹⁰⁰ A. Pathak,¹⁸¹ T. Pauly,³⁶ B. Pearson,¹¹⁵
M. Pedersen,¹³⁴ L. Pedraza Diaz,¹¹⁹ R. Pedro,^{140a} T. Peiffer,⁵³ S. V. Peleganchuk,^{122b,122a} O. Penc,¹⁴¹ H. Peng,^{60a}
B. S. Peralva,^{80a} M. M. Perego,¹³² A. P. Pereira Peixoto,^{140a} D. V. Perepelitsa,²⁹ F. Peri,¹⁹ L. Perini,^{68a,68b} H. Pernegger,³⁶
S. Perrella,^{69a,69b} K. Peters,⁴⁶ R. F. Y. Peters,¹⁰⁰ B. A. Petersen,³⁶ T. C. Petersen,⁴⁰ E. Petit,¹⁰¹ A. Petridis,¹ C. Petridou,¹⁶²
P. Petroff,¹³² M. Petrov,¹³⁵ F. Petrucci,^{74a,74b} M. Pettee,¹⁸³ N. E. Pettersson,¹⁰² K. Petukhova,¹⁴³ A. Peyaud,¹⁴⁵ R. Pezoa,^{147b}
L. Pezzotti,^{70a,70b} T. Pham,¹⁰⁴ F. H. Phillips,¹⁰⁶ P. W. Phillips,¹⁴⁴ M. W. Phipps,¹⁷³ G. Piacquadio,¹⁵⁵ E. Pianori,¹⁸
A. Picazio,¹⁰² R. H. Pickles,¹⁰⁰ R. Piegaiia,³⁰ D. Pietreanu,^{27b} J. E. Pilcher,³⁷ A. D. Pilkington,¹⁰⁰ M. Pinamonti,^{73a,73b}
J. L. Pinfold,³ M. Pitt,¹⁸⁰ L. Pizzimento,^{73a,73b} M.-A. Pleier,²⁹ V. Pleskot,¹⁴³ E. Plotnikova,⁷⁹ P. Podberezko,^{122b,122a}
R. Poettgen,⁹⁶ R. Poggi,⁵⁴ L. Poggioli,¹³² I. Pogrebnyak,¹⁰⁶ D. Pohl,²⁴ I. Pokharel,⁵³ G. Polesello,^{70a} A. Poley,¹⁸
A. Policicchio,^{72a,72b} R. Polifka,¹⁴³ A. Polini,^{23b} C. S. Pollard,⁴⁶ V. Polychronakos,²⁹ D. Ponomarenko,¹¹² L. Pontecorvo,³⁶
S. Popa,^{27a} G. A. Popeneciu,^{27d} D. M. Portillo Quintero,⁵⁸ S. Pospisil,¹⁴² K. Potamianos,⁴⁶ I. N. Potrap,⁷⁹ C. J. Potter,³²
H. Potti,¹¹ T. Poulsen,⁹⁶ J. Poveda,³⁶ T. D. Powell,¹⁴⁹ G. Pownall,⁴⁶ M. E. Pozo Astigarraga,³⁶ P. Pralavorio,¹⁰¹ S. Prell,⁷⁸
D. Price,¹⁰⁰ M. Primavera,^{67a} S. Prince,¹⁰³ M. L. Proffitt,¹⁴⁸ N. Proklova,¹¹² K. Prokofiev,^{63c} F. Prokoshin,⁷⁹
S. Protopopescu,²⁹ J. Proudfoot,⁶ M. Przybycien,^{83a} D. Pudzha,¹³⁸ A. Puri,¹⁷³ P. Puzo,¹³² J. Qian,¹⁰⁵ Y. Qin,¹⁰⁰ A. Quadt,⁵³
M. Queitsch-Maitland,⁴⁶ A. Qureshi,¹ P. Rados,¹⁰⁴ F. Ragusa,^{68a,68b} G. Rahal,⁹⁷ J. A. Raine,⁵⁴ S. Rajagopalan,²⁹
A. Ramirez Morales,⁹² K. Ran,^{15a,15d} T. Rashid,¹³² S. Raspopov,⁵ D. M. Rauch,⁴⁶ F. Rauscher,¹¹⁴ S. Rave,⁹⁹ B. Ravina,¹⁴⁹
I. Ravinovich,¹⁸⁰ J. H. Rawling,¹⁰⁰ M. Raymond,³⁶ A. L. Read,¹³⁴ N. P. Readioff,⁵⁸ M. Reale,^{67a,67b} D. M. Rebuffi,^{70a,70b}
A. Redelbach,¹⁷⁷ G. Redlinger,²⁹ K. Reeves,⁴³ L. Rehnisch,¹⁹ J. Reichert,¹³⁷ D. Reikher,¹⁶¹ A. Reiss,⁹⁹ A. Rej,¹⁵¹
C. Rembser,³⁶ M. Renda,^{27b} M. Rescigno,^{72a} S. Resconi,^{68a} E. D. Resseguie,¹³⁷ S. Rettie,¹⁷⁵ E. Reynolds,²¹
O. L. Rezanova,^{122b,122a} P. Reznicek,¹⁴³ E. Ricci,^{75a,75b} R. Richter,¹¹⁵ S. Richter,⁴⁶ E. Richter-Was,^{83b} O. Ricken,²⁴
M. Ridel,¹³⁶ P. Rieck,¹¹⁵ C. J. Riegel,¹⁸² O. Rifki,⁴⁶ M. Rijssenbeek,¹⁵⁵ A. Rimoldi,^{70a,70b} M. Rimoldi,⁴⁶ L. Rinaldi,^{23b}
G. Ripellino,¹⁵⁴ B. Ristić,⁸⁹ I. Riu,¹⁴ J. C. Rivera Vergara,¹⁷⁶ F. Rizatdinova,¹²⁹ E. Rizvi,⁹² C. Rizzi,³⁶ R. T. Roberts,¹⁰⁰
S. H. Robertson,^{103,p} M. Robin,⁴⁶ D. Robinson,³² J. E. M. Robinson,⁴⁶ C. M. Robles Gajardo,^{147b} A. Robson,⁵⁷ E. Rocco,⁹⁹
C. Roda,^{71a,71b} S. Rodriguez Bosca,¹⁷⁴ A. Rodriguez Perez,¹⁴ D. Rodriguez Rodriguez,¹⁷⁴ A. M. Rodríguez Vera,^{168b}
S. Roe,³⁶ O. Røhne,¹³⁴ R. Røhrig,¹¹⁵ C. P. A. Roland,⁶⁵ J. Roloff,⁵⁹ A. Romaniouk,¹¹² M. Romano,^{23b,23a} N. Rompotis,⁹⁰
M. Ronzani,¹²⁴ L. Roos,¹³⁶ S. Rosati,^{72a} K. Rosbach,⁵² G. Rosin,¹⁰² B. J. Rosser,¹³⁷ E. Rossi,⁴⁶ E. Rossi,^{74a,74b} E. Rossi,^{69a,69b}
L. P. Rossi,^{55b} L. Rossini,^{68a,68b} R. Rosten,¹⁴ M. Rotaru,^{27b} J. Rothberg,¹⁴⁸ D. Rousseau,¹³² G. Rovelli,^{70a,70b} A. Roy,¹¹
D. Roy,^{33c} A. Rozanov,¹⁰¹ Y. Rozen,¹⁶⁰ X. Ruan,^{33c} F. Rubbo,¹⁵³ F. Rühr,⁵² A. Ruiz-Martinez,¹⁷⁴ A. Rummler,³⁶
Z. Rurikova,⁵² N. A. Rusakovich,⁷⁹ H. L. Russell,¹⁰³ L. Rustige,^{38,47} J. P. Rutherford,⁷ E. M. Rüttinger,^{46,mm}
Y. F. Ryabov,¹³⁸ M. Rybar,³⁹ G. Rybkin,¹³² E. B. Rye,¹³⁴ A. Ryzhov,¹²³ G. F. Rzehorz,⁵³ P. Sabatini,⁵³ G. Sabato,¹²⁰
S. Sacerdoti,¹³² H. F.-W. Sadrozinski,¹⁴⁶ R. Sadykov,⁷⁹ F. Safai Tehrani,^{72a} B. Safarzadeh Samani,¹⁵⁶ P. Saha,¹²¹ S. Saha,¹⁰³
M. Sahinsoy,^{61a} A. Sahu,¹⁸² M. Saimpert,⁴⁶ M. Saito,¹⁶³ T. Saito,¹⁶³ H. Sakamoto,¹⁶³ A. Sakharov,^{124,ee} D. Salamani,⁵⁴
G. Salamanna,^{74a,74b} J. E. Salazar Loyola,^{147b} P. H. Sales De Bruin,¹⁷² A. Salnikov,¹⁵³ J. Salt,¹⁷⁴ D. Salvatore,^{41b,41a}
F. Salvatore,¹⁵⁶ A. Salvucci,^{63a,63b,63c} A. Salzburger,³⁶ J. Samarati,³⁶ D. Sammel,⁵² D. Sampsonidis,¹⁶² D. Sampsonidou,¹⁶²
J. Sánchez,¹⁷⁴ A. Sanchez Pineda,^{66a,66c} H. Sandaker,¹³⁴ C. O. Sander,⁴⁶ I. G. Sanderswood,⁸⁹ M. Sandhoff,¹⁸²
C. Sandoval,²² D. P. C. Sankey,¹⁴⁴ M. Sannino,^{55b,55a} Y. Sano,¹¹⁷ A. Sansoni,⁵¹ C. Santoni,³⁸ H. Santos,^{140a,140b}
S. N. Santpur,¹⁸ A. Santra,¹⁷⁴ A. Saponov,⁷⁹ J. G. Saraiva,^{140a,140d} O. Sasaki,⁸¹ K. Sato,¹⁶⁹ F. Sauerburger,⁵² E. Sauvan,⁵
P. Savard,^{167,e} N. Savic,¹¹⁵ R. Sawada,¹⁶³ C. Sawyer,¹⁴⁴ L. Sawyer,^{95,nn} C. Sbarra,^{23b} A. Sbrizzi,^{23a} T. Scanlon,⁹⁴
J. Schaarschmidt,¹⁴⁸ P. Schacht,¹¹⁵ B. M. Schachtner,¹¹⁴ D. Schaefer,³⁷ L. Schaefer,¹³⁷ J. Schaeffer,⁹⁹ S. Schaepe,³⁶
U. Schäfer,⁹⁹ A. C. Schaffer,¹³² D. Schaile,¹¹⁴ R. D. Schamberger,¹⁵⁵ N. Scharmberg,¹⁰⁰ V. A. Schegelsky,¹³⁸ D. Scheirich,¹⁴³
F. Schenck,¹⁹ M. Schernau,¹⁷¹ C. Schiavi,^{55b,55a} S. Schier,¹⁴⁶ L. K. Schildgen,²⁴ Z. M. Schillaci,²⁶ E. J. Schioppa,³⁶
M. Schioppa,^{41b,41a} K. E. Schleicher,⁵² S. Schlenker,³⁶ K. R. Schmidt-Sommerfeld,¹¹⁵ K. Schmieden,³⁶ C. Schmitt,⁹⁹
S. Schmitt,⁴⁶ S. Schmitz,⁹⁹ J. C. Schmoedel,⁴⁶ U. Schnoor,⁵² L. Schoeffel,¹⁴⁵ A. Schoening,^{61b} P. G. Scholer,⁵²
E. Schopf,¹³⁵ M. Schott,⁹⁹ J. F. P. Schouwenberg,¹¹⁹ J. Schovancova,³⁶ S. Schramm,⁵⁴ F. Schroeder,¹⁸² A. Schulte,⁹⁹
H.-C. Schultz-Coulon,^{61a} M. Schumacher,⁵² B. A. Schumm,¹⁴⁶ Ph. Schune,¹⁴⁵ A. Schwartzman,¹⁵³ T. A. Schwarz,¹⁰⁵
Ph. Schwemling,¹⁴⁵ R. Schwienhorst,¹⁰⁶ A. Sciandra,¹⁴⁶ G. Sciolla,²⁶ M. Scodeggio,⁴⁶ M. Scornajenghi,^{41b,41a} F. Scuri,^{71a}

F. Scutti,¹⁰⁴ L. M. Scyboz,¹¹⁵ C. D. Sebastiani,^{72a,72b} P. Seema,¹⁹ S. C. Seidel,¹¹⁸ A. Seiden,¹⁴⁶ T. Seiss,³⁷ J. M. Seixas,^{80b}
G. Sekhniaidze,^{69a} K. Sekhon,¹⁰⁵ S. J. Sekula,⁴² N. Semprini-Cesari,^{23b,23a} S. Sen,⁴⁹ S. Senkin,³⁸ C. Serfon,⁷⁶ L. Serin,¹³²
L. Serkin,^{66a,66b} M. Sessa,^{60a} H. Severini,¹²⁸ F. Sforza,¹⁷⁰ A. Sfyrta,⁵⁴ E. Shabalina,⁵³ J. D. Shahinian,¹⁴⁶ N. W. Shaikh,^{45a,45b}
D. Shaked Renous,¹⁸⁰ L. Y. Shan,^{15a} R. Shang,¹⁷³ J. T. Shank,²⁵ M. Shapiro,¹⁸ A. Sharma,¹³⁵ A. S. Sharma,¹
P. B. Shatalov,¹¹¹ K. Shaw,¹⁵⁶ S. M. Shaw,¹⁰⁰ A. Shcherbakova,¹³⁸ M. Shehade,¹⁸⁰ Y. Shen,¹²⁸ N. Sherafati,³⁴
A. D. Sherman,²⁵ P. Sherwood,⁹⁴ L. Shi,^{158,oo} S. Shimizu,⁸¹ C. O. Shimmin,¹⁸³ Y. Shimogama,¹⁷⁹ M. Shimojima,¹¹⁶
I. P. J. Shipsey,¹³⁵ S. Shirabe,⁸⁷ M. Shiyakova,^{79,pp} J. Shlomi,¹⁸⁰ A. Shmeleva,¹¹⁰ M. J. Shochet,³⁷ S. Shojaii,¹⁰⁴
D. R. Shope,¹²⁸ S. Shrestha,¹²⁶ E. M. Shrif,^{33c} E. Shulga,¹⁸⁰ P. Sicho,¹⁴¹ A. M. Sickles,¹⁷³ P. E. Sidebo,¹⁵⁴
E. Sideras Haddad,^{33c} O. Sidiropoulou,³⁶ A. Sidoti,^{23b,23a} F. Siegert,⁴⁸ Dj. Sijacki,¹⁶ M. Silva Jr.,¹⁸¹ M. V. Silva Oliveira,^{80a}
S. B. Silverstein,^{45a} S. Simion,¹³² E. Simioni,⁹⁹ R. Simonello,⁹⁹ S. Simsek,^{12b} P. Sinervo,¹⁶⁷ V. Sinetckii,^{113,110}
N. B. Sinev,¹³¹ M. Sioli,^{23b,23a} I. Siral,¹⁰⁵ S. Yu. Sivoklov,¹¹³ J. Sjölin,^{45a,45b} E. Skorda,⁹⁶ P. Skubic,¹²⁸ M. Slawinska,⁸⁴
K. Sliwa,¹⁷⁰ R. Slovak,¹⁴³ V. Smakhtin,¹⁸⁰ B. H. Smart,¹⁴⁴ J. Smiesko,^{28a} N. Smirnov,¹¹² S. Yu. Smirnov,¹¹² Y. Smirnov,¹¹²
L. N. Smirnova,^{113,qq} O. Smirnova,⁹⁶ J. W. Smith,⁵³ M. Smizanska,⁸⁹ K. Smolek,¹⁴² A. Smykiewicz,⁸⁴ A. A. Snesev,¹¹⁰
H. L. Snoek,¹²⁰ I. M. Snyder,¹³¹ S. Snyder,²⁹ R. Sobie,^{176,p} A. Soffer,¹⁶¹ A. Søggaard,⁵⁰ F. Sohns,⁵³ C. A. Solans Sanchez,³⁶
E. Yu. Soldatov,¹¹² U. Soldevila,¹⁷⁴ A. A. Solodkov,¹²³ A. Soloshenko,⁷⁹ O. V. Solovyanov,¹²³ V. Solovyev,¹³⁸ P. Sommer,¹⁴⁹
H. Son,¹⁷⁰ W. Song,¹⁴⁴ W. Y. Song,^{168b} A. Sopczak,¹⁴² F. Sopkova,^{28b} C. L. Sotiropoulou,^{71a,71b} S. Sottocornola,^{70a,70b}
R. Soualah,^{66a,66c,rr} A. M. Soukharev,^{122b,122a} D. South,⁴⁶ S. Spagnolo,^{67a,67b} M. Spalla,¹¹⁵ M. Spangenberg,¹⁷⁸ F. Spanò,⁹³
D. Sperlich,⁵² T. M. Spieker,^{61a} R. Spighi,^{23b} G. Spigo,³⁶ M. Spina,¹⁵⁶ D. P. Spiteri,⁵⁷ M. Spusta,¹⁴³ A. Stabile,^{68a,68b}
B. L. Stamas,¹²¹ R. Stamen,^{61a} M. Stamenkovic,¹²⁰ E. Stanecka,⁸⁴ B. Stanislaus,¹³⁵ M. M. Stanitzki,⁴⁶ M. Stankaityte,¹³⁵
B. Stapf,¹²⁰ E. A. Starchenko,¹²³ G. H. Stark,¹⁴⁶ J. Stark,⁵⁸ S. H. Stark,⁴⁰ P. Staroba,¹⁴¹ P. Starovoitov,^{61a} S. Stärz,¹⁰³
R. Staszewski,⁸⁴ G. Stavropoulos,⁴⁴ M. Stegler,⁴⁶ P. Steinberg,²⁹ A. L. Steinhebel,¹³¹ B. Stelzer,¹⁵² H. J. Stelzer,¹³⁹
O. Stelzer-Chilton,^{168a} H. Stenzel,⁵⁶ T. J. Stevenson,¹⁵⁶ G. A. Stewart,³⁶ M. C. Stockton,³⁶ G. Stoicea,^{27b} M. Stolarski,^{140a}
P. Stolte,⁵³ S. Stonjek,¹¹⁵ A. Straessner,⁴⁸ J. Strandberg,¹⁵⁴ S. Strandberg,^{45a,45b} M. Strauss,¹²⁸ P. Strizenec,^{28b} R. Ströhmer,¹⁷⁷
D. M. Strom,¹³¹ R. Stroynowski,⁴² A. Strubig,⁵⁰ S. A. Stucci,²⁹ B. Stugu,¹⁷ J. Stupak,¹²⁸ N. A. Styles,⁴⁶ D. Su,¹⁵³
S. Suchek,^{61a} V. V. Sulin,¹¹⁰ M. J. Sullivan,⁹⁰ D. M. S. Sultan,⁵⁴ S. Sultansoy,^{4c} T. Sumida,⁸⁵ S. Sun,¹⁰⁵ X. Sun,³
K. Suruliz,¹⁵⁶ C. J. E. Suster,¹⁵⁷ M. R. Sutton,¹⁵⁶ S. Suzuki,⁸¹ M. Svatos,¹⁴¹ M. Swiatlowski,³⁷ S. P. Swift,² T. Swirski,¹⁷⁷
A. Sydorenko,⁹⁹ I. Sykora,^{28a} M. Sykora,¹⁴³ T. Sykora,¹⁴³ D. Ta,⁹⁹ K. Tackmann,^{46,ss} J. Taenzer,¹⁶¹ A. Taffard,¹⁷¹
R. Tafirout,^{168a} H. Takai,²⁹ R. Takashima,⁸⁶ K. Takeda,⁸² T. Takeshita,¹⁵⁰ E. P. Takeva,⁵⁰ Y. Takubo,⁸¹ M. Talby,¹⁰¹
A. A. Talyshev,^{122b,122a} N. M. Tamir,¹⁶¹ J. Tanaka,¹⁶³ M. Tanaka,¹⁶⁵ R. Tanaka,¹³² S. Tapia Araya,¹⁷³ S. Tapprogge,⁹⁹
A. Tarek Abouelfadl Mohamed,¹³⁶ S. Tarem,¹⁶⁰ G. Tarna,^{27b,tt} G. F. Tartarelli,^{68a} P. Tas,¹⁴³ M. Tasevsky,¹⁴¹ T. Tashiro,⁸⁵
E. Tassi,^{41b,41a} A. Tavares Delgado,^{140a,140b} Y. Tayalati,^{35e} A. J. Taylor,⁵⁰ G. N. Taylor,¹⁰⁴ W. Taylor,^{168b} A. S. Tee,⁸⁹
R. Teixeira De Lima,¹⁵³ P. Teixeira-Dias,⁹³ H. Ten Kate,³⁶ J. J. Teoh,¹²⁰ S. Terada,⁸¹ K. Terashi,¹⁶³ J. Terron,⁹⁸ S. Terzo,¹⁴
M. Testa,⁵¹ R. J. Teuscher,^{167,p} S. J. Thais,¹⁸³ T. Theveneaux-Pelzer,⁴⁶ F. Thiele,⁴⁰ D. W. Thomas,⁹³ J. O. Thomas,⁴²
J. P. Thomas,²¹ A. S. Thompson,⁵⁷ P. D. Thompson,²¹ L. A. Thomsen,¹⁸³ E. Thomson,¹³⁷ E. J. Thorpe,⁹² Y. Tian,³⁹
R. E. Tice Torres,⁵³ V. O. Tikhomirov,^{110,uu} Yu. A. Tikhonov,^{122b,122a} S. Timoshenko,¹¹² P. Tipton,¹⁸³ S. Tisserant,¹⁰¹
K. Todome,^{23b,23a} S. Todorova-Nova,⁵ S. Todt,⁴⁸ J. Tojo,⁸⁷ S. Tokár,^{28a} K. Tokushuku,⁸¹ E. Tolley,¹²⁶ K. G. Tomiwa,^{33c}
M. Tomoto,¹¹⁷ L. Tompkins,^{153,dd} K. Toms,¹¹⁸ B. Tong,⁵⁹ P. Tornambe,¹⁰² E. Torrence,¹³¹ H. Torres,⁴⁸ E. Torró Pastor,¹⁴⁸
C. Toscirì,¹³⁵ J. Toth,^{101,vv} D. R. Tovey,¹⁴⁹ A. Traeet,¹⁷ C. J. Treado,¹²⁴ T. Trefzger,¹⁷⁷ F. Tresoldi,¹⁵⁶ A. Tricoli,²⁹
I. M. Trigger,^{168a} S. Trincaz-Duvoid,¹³⁶ W. Trischuk,¹⁶⁷ B. Trocmé,⁵⁸ A. Trofymov,¹³² C. Troncon,^{68a} M. Trovatelli,¹⁷⁶
F. Trovato,¹⁵⁶ L. Truong,^{33b} M. Trzebinski,⁸⁴ A. Trzupek,⁸⁴ F. Tsai,⁴⁶ J. C.-L. Tseng,¹³⁵ P. V. Tsiarshka,^{107,ff} A. Tsigotis,¹⁶²
N. Tsirintanis,⁹ V. Tsiskaridze,¹⁵⁵ E. G. Tskhadadze,^{159a} M. Tsopoulou,¹⁶² I. I. Tsukerman,¹¹¹ V. Tsulaia,¹⁸ S. Tsuno,⁸¹
D. Tsybychev,¹⁵⁵ Y. Tu,^{63b} A. Tudorache,^{27b} V. Tudorache,^{27b} T. T. Tulbure,^{27a} A. N. Tuna,⁵⁹ S. Turchikhin,⁷⁹
D. Turgeman,¹⁸⁰ I. Turk Cakir,^{4b,ww} R. J. Turner,²¹ R. T. Turra,^{68a} P. M. Tuts,³⁹ S. Tzamarias,¹⁶² E. Tzovara,⁹⁹ G. Ucchielli,⁴⁷
K. Uchida,¹⁶³ I. Ueda,⁸¹ M. Ughetto,^{45a,45b} F. Ukegawa,¹⁶⁹ G. Unal,³⁶ A. Undrus,²⁹ G. Unel,¹⁷¹ F. C. Ungaro,¹⁰⁴ Y. Unno,⁸¹
K. Uno,¹⁶³ J. Urban,^{28b} P. Urquijo,¹⁰⁴ G. Usai,⁸ J. Usui,⁸¹ Z. Uysal,^{12d} L. Vacavant,¹⁰¹ V. Vacek,¹⁴² B. Vachon,¹⁰³
K. O. H. Vadla,¹³⁴ A. Vaidya,⁹⁴ C. Valderanis,¹¹⁴ E. Valdes Santurio,^{45a,45b} M. Valente,⁵⁴ S. Valentinetti,^{23b,23a} A. Valero,¹⁷⁴
L. Valéry,⁴⁶ R. A. Vallance,²¹ A. Vallier,³⁶ J. A. Valls Ferrer,¹⁷⁴ T. R. Van Daalen,¹⁴ P. Van Gemmeren,⁶ I. Van Vulpen,¹²⁰
M. Vanadia,^{73a,73b} W. Vandelli,³⁶ A. Vaniachine,¹⁶⁶ D. Vannicola,^{72a,72b} R. Vari,^{72a} E. W. Varnes,⁷ C. Varni,^{55b,55a} T. Varol,⁴²
D. Varouchas,¹³² K. E. Varvell,¹⁵⁷ M. E. Vasile,^{27b} G. A. Vasquez,¹⁷⁶ J. G. Vasquez,¹⁸³ F. Vazeille,³⁸ D. Vazquez Furelos,¹⁴

T. Vazquez Schroeder,³⁶ J. Veatch,⁵³ V. Vecchio,^{74a,74b} M. J. Veen,¹²⁰ L. M. Veloce,¹⁶⁷ F. Veloso,^{140a,140c} S. Veneziano,^{72a} A. Ventura,^{67a,67b} N. Venturi,³⁶ A. Verbytskyi,¹¹⁵ V. Vercesi,^{70a} M. Verducci,^{71a,71b} C. M. Vergel Infante,⁷⁸ C. Vergis,²⁴ W. Verkerke,¹²⁰ A. T. Vermeulen,¹²⁰ J. C. Vermeulen,¹²⁰ M. C. Vetterli,^{152,e} N. Viaux Maira,^{147b} M. Vicente Barreto Pinto,⁵⁴ T. Vickey,¹⁴⁹ O. E. Vickey Boeriu,¹⁴⁹ G. H. A. Viehhauser,¹³⁵ L. Vigani,^{61b} M. Villa,^{23b,23a} M. Villaplana Perez,^{68a,68b} E. Vilucchi,⁵¹ M. G. Vinciter,³⁴ V. B. Vinogradov,⁷⁹ G. S. Virdee,²¹ A. Vishwakarma,⁴⁶ C. Vittori,^{23b,23a} I. Vivarelli,¹⁵⁶ M. Vogel,¹⁸² P. Vokac,¹⁴² S. E. von Buddenbrock,^{33c} E. Von Toerne,²⁴ V. Vorobel,¹⁴³ K. Vorobev,¹¹² M. Vos,¹⁷⁴ J. H. Vosseveld,⁹⁰ M. Vozak,¹⁰⁰ N. Vranjes,¹⁶ M. Vranjes Milosavljevic,¹⁶ V. Vrba,¹⁴² M. Vreeswijk,¹²⁰ T. Šfiligoj,⁹¹ R. Vuillermet,³⁶ I. Vukotic,³⁷ T. Ženiš,^{28a} L. Živković,¹⁶ P. Wagner,²⁴ W. Wagner,¹⁸² J. Wagner-Kuhr,¹¹⁴ S. Wahdan,¹⁸² H. Wahlberg,⁸⁸ K. Wakamiya,⁸² V. M. Walbrecht,¹¹⁵ J. Walder,⁸⁹ R. Walker,¹¹⁴ S. D. Walker,⁹³ W. Walkowiak,¹⁵¹ V. Wallangen,^{45a,45b} A. M. Wang,⁵⁹ C. Wang,^{60c} C. Wang,^{60b} F. Wang,¹⁸¹ H. Wang,¹⁸ H. Wang,³ J. Wang,¹⁵⁷ J. Wang,^{61b} P. Wang,⁴² Q. Wang,¹²⁸ R.-J. Wang,⁹⁹ R. Wang,^{60a} R. Wang,⁶ S. M. Wang,¹⁵⁸ W. T. Wang,^{60a} W. Wang,^{15c,xx} W. X. Wang,^{60a,xx} Y. Wang,^{60a,yy} Z. Wang,^{60c} C. Wanotayaroj,⁴⁶ A. Warburton,¹⁰³ C. P. Ward,³² D. R. Wardrope,⁹⁴ N. Warrack,⁵⁷ A. Washbrook,⁵⁰ A. T. Watson,²¹ M. F. Watson,²¹ G. Watts,¹⁴⁸ B. M. Waugh,⁹⁴ A. F. Webb,¹¹ S. Webb,⁹⁹ C. Weber,¹⁸³ M. S. Weber,²⁰ S. A. Weber,³⁴ S. M. Weber,^{61a} A. R. Weidberg,¹³⁵ J. Weingarten,⁴⁷ M. Weirich,⁹⁹ C. Weiser,⁵² P. S. Wells,³⁶ T. Wenaus,²⁹ T. Wengler,³⁶ S. Wenig,³⁶ N. Wermes,²⁴ M. D. Werner,⁷⁸ M. Wessels,^{61a} T. D. Weston,²⁰ K. Whalen,¹³¹ N. L. Whallon,¹⁴⁸ A. M. Wharton,⁸⁹ A. S. White,¹⁰⁵ A. White,⁸ M. J. White,¹ D. Whiteson,¹⁷¹ B. W. Whitmore,⁸⁹ W. Wiedenmann,¹⁸¹ M. Wielers,¹⁴⁴ N. Wieseotte,⁹⁹ C. Wiglesworth,⁴⁰ L. A. M. Wiik-Fuchs,⁵² F. Wilk,¹⁰⁰ H. G. Wilkens,³⁶ L. J. Wilkins,⁹³ H. H. Williams,¹³⁷ S. Williams,³² C. Willis,¹⁰⁶ S. Willocq,¹⁰² J. A. Wilson,²¹ I. Wingerter-Seetz,⁵ E. Winkels,¹⁵⁶ F. Winklmeier,¹³¹ O. J. Winston,¹⁵⁶ B. T. Winter,⁵² M. Wittgen,¹⁵³ M. Wobisch,⁹⁵ A. Wolf,⁹⁹ T. M. H. Wolf,¹²⁰ R. Wolff,¹⁰¹ R. W. Wölker,¹³⁵ J. Wollrath,⁵² M. W. Wolter,⁸⁴ H. Wolters,^{140a,140c} V. W. S. Wong,¹⁷⁵ N. L. Woods,¹⁴⁶ S. D. Worm,²¹ B. K. Wosiek,⁸⁴ K. W. Woźniak,⁸⁴ K. Wraight,⁵⁷ S. L. Wu,¹⁸¹ X. Wu,⁵⁴ Y. Wu,^{60a} T. R. Wyatt,¹⁰⁰ B. M. Wynne,⁵⁰ S. Xella,⁴⁰ Z. Xi,¹⁰⁵ L. Xia,¹⁷⁸ X. Xiao,¹⁰⁵ D. Xu,^{15a} H. Xu,^{60a,tt} L. Xu,²⁹ T. Xu,¹⁴⁵ W. Xu,¹⁰⁵ Z. Xu,^{60b} Z. Xu,¹⁵³ B. Yabsley,¹⁵⁷ S. Yacoob,^{33a} K. Yajima,¹³³ D. P. Yallup,⁹⁴ D. Yamaguchi,¹⁶⁵ Y. Yamaguchi,¹⁶⁵ A. Yamamoto,⁸¹ F. Yamane,⁸² M. Yamatani,¹⁶³ T. Yamazaki,¹⁶³ Y. Yamazaki,⁸² Z. Yan,²⁵ H. J. Yang,^{60c,60d} H. T. Yang,¹⁸ S. Yang,⁷⁷ X. Yang,^{60b,58} Y. Yang,¹⁶³ W.-M. Yao,¹⁸ Y. C. Yap,⁴⁶ Y. Yasu,⁸¹ E. Yatsenko,^{60c,60d} J. Ye,⁴² S. Ye,²⁹ I. Yeletsikh,⁷⁹ M. R. Yexley,⁸⁹ E. Yigitbasi,²⁵ K. Yorita,¹⁷⁹ K. Yoshihara,¹³⁷ C. J. S. Young,³⁶ C. Young,¹⁵³ J. Yu,⁷⁸ R. Yuan,^{60b,zz} X. Yue,^{61a} S. P. Y. Yuen,²⁴ B. Zabinski,⁸⁴ G. Zacharis,¹⁰ E. Zaffaroni,⁵⁴ J. Zahreddine,¹³⁶ A. M. Zaitsev,^{123,kk} T. Zakareishvili,^{159b} N. Zakharchuk,³⁴ S. Zambito,⁵⁹ D. Zanzi,³⁶ D. R. Zaripovas,⁵⁷ S. V. Zeiβner,⁴⁷ C. Zeitnitz,¹⁸² G. Zemaityte,¹³⁵ J. C. Zeng,¹⁷³ O. Zenin,¹²³ D. Zerwas,¹³² M. Zgubič,¹³⁵ D. F. Zhang,^{15b} F. Zhang,¹⁸¹ G. Zhang,^{15b} H. Zhang,^{15c} J. Zhang,⁶ L. Zhang,^{15c} L. Zhang,^{60a} M. Zhang,¹⁷³ R. Zhang,²⁴ X. Zhang,^{60b} Y. Zhang,^{15a,15d} Z. Zhang,^{63a} Z. Zhang,¹³² P. Zhao,⁴⁹ Y. Zhao,^{60b} Z. Zhao,^{60a} A. Zhemchugov,⁷⁹ Z. Zheng,¹⁰⁵ D. Zhong,¹⁷³ B. Zhou,¹⁰⁵ C. Zhou,¹⁸¹ M. S. Zhou,^{15a,15d} M. Zhou,¹⁵⁵ N. Zhou,^{60c} Y. Zhou,⁷ C. G. Zhu,^{60b} H. L. Zhu,^{60a} H. Zhu,^{15a} J. Zhu,¹⁰⁵ Y. Zhu,^{60a} X. Zhuang,^{15a} K. Zhukov,¹¹⁰ V. Zhulanov,^{122b,122a} D. Ziemska,⁶⁵ N. I. Zimine,⁷⁹ S. Zimmermann,⁵² Z. Zinonos,¹¹⁵ M. Ziolkowski,¹⁵¹ G. Zobernig,¹⁸¹ A. Zoccoli,^{23b,23a} K. Zoch,⁵³ T. G. Zorbas,¹⁴⁹ R. Zou,³⁷ and L. Zwalinski³⁶

(ATLAS Collaboration)

¹Department of Physics, University of Adelaide, Adelaide, Australia²Physics Department, SUNY Albany, Albany, New York, USA³Department of Physics, University of Alberta, Edmonton, Alberta, Canada^{4a}Department of Physics, Ankara University, Ankara, Turkey^{4b}Istanbul Aydin University, Istanbul, Turkey^{4c}Division of Physics, TOBB University of Economics and Technology, Ankara, Turkey⁵LAPP, Université Grenoble Alpes, Université Savoie Mont Blanc, CNRS/IN2P3, Annecy, France⁶High Energy Physics Division, Argonne National Laboratory, Argonne, Illinois, USA⁷Department of Physics, University of Arizona, Tucson, Arizona, USA⁸Department of Physics, University of Texas at Arlington, Arlington, Texas, USA⁹Physics Department, National and Kapodistrian University of Athens, Athens, Greece¹⁰Physics Department, National Technical University of Athens, Zografou, Greece¹¹Department of Physics, University of Texas at Austin, Austin, Texas, USA^{12a}Bahcesehir University, Faculty of Engineering and Natural Sciences, Istanbul, Turkey^{12b}Istanbul Bilgi University, Faculty of Engineering and Natural Sciences, Istanbul, Turkey

- ^{12c}*Department of Physics, Bogazici University, Istanbul, Turkey*
- ^{12d}*Department of Physics Engineering, Gaziantep University, Gaziantep, Turkey*
- ¹³*Institute of Physics, Azerbaijan Academy of Sciences, Baku, Azerbaijan*
- ¹⁴*Institut de Física d'Altes Energies (IFAE), Barcelona Institute of Science and Technology, Barcelona, Spain*
- ^{15a}*Institute of High Energy Physics, Chinese Academy of Sciences, Beijing, China*
- ^{15b}*Physics Department, Tsinghua University, Beijing, China*
- ^{15c}*Department of Physics, Nanjing University, Nanjing, China*
- ^{15d}*University of Chinese Academy of Science (UCAS), Beijing, China*
- ¹⁶*Institute of Physics, University of Belgrade, Belgrade, Serbia*
- ¹⁷*Department for Physics and Technology, University of Bergen, Bergen, Norway*
- ¹⁸*Physics Division, Lawrence Berkeley National Laboratory and University of California, Berkeley, California, USA*
- ¹⁹*Institut für Physik, Humboldt Universität zu Berlin, Berlin, Germany*
- ²⁰*Albert Einstein Center for Fundamental Physics and Laboratory for High Energy Physics, University of Bern, Bern, Switzerland*
- ²¹*School of Physics and Astronomy, University of Birmingham, Birmingham, United Kingdom*
- ²²*Facultad de Ciencias y Centro de Investigaciones, Universidad Antonio Nariño, Bogota, Colombia*
- ^{23a}*INFN Bologna and Università' di Bologna, Dipartimento di Fisica, Italy*
- ^{23b}*INFN Sezione di Bologna, Italy*
- ²⁴*Physikalisches Institut, Universität Bonn, Bonn, Germany*
- ²⁵*Department of Physics, Boston University, Boston, Massachusetts, USA*
- ²⁶*Department of Physics, Brandeis University, Waltham, Massachusetts, USA*
- ^{27a}*Transilvania University of Brasov, Brasov, Romania*
- ^{27b}*Horia Hulubei National Institute of Physics and Nuclear Engineering, Bucharest, Romania*
- ^{27c}*Department of Physics, Alexandru Ioan Cuza University of Iasi, Iasi, Romania*
- ^{27d}*National Institute for Research and Development of Isotopic and Molecular Technologies, Physics Department, Cluj-Napoca, Romania*
- ^{27e}*University Politehnica Bucharest, Bucharest, Romania*
- ^{27f}*West University in Timisoara, Timisoara, Romania*
- ^{28a}*Faculty of Mathematics, Physics and Informatics, Comenius University, Bratislava, Slovak Republic*
- ^{28b}*Department of Subnuclear Physics, Institute of Experimental Physics of the Slovak Academy of Sciences, Kosice, Slovak Republic*
- ²⁹*Physics Department, Brookhaven National Laboratory, Upton, New York, USA*
- ³⁰*Departamento de Física, Universidad de Buenos Aires, Buenos Aires, Argentina*
- ³¹*California State University, California, USA*
- ³²*Cavendish Laboratory, University of Cambridge, Cambridge, United Kingdom*
- ^{33a}*Department of Physics, University of Cape Town, Cape Town, South Africa*
- ^{33b}*Department of Mechanical Engineering Science, University of Johannesburg, Johannesburg, South Africa*
- ^{33c}*School of Physics, University of the Witwatersrand, Johannesburg, South Africa*
- ³⁴*Department of Physics, Carleton University, Ottawa, Ontario, Canada*
- ^{35a}*Faculté des Sciences Ain Chock, Réseau Universitaire de Physique des Hautes Energies—Université Hassan II, Casablanca, Morocco*
- ^{35b}*Faculté des Sciences, Université Ibn-Tofail, Kénitra, Morocco*
- ^{35c}*Faculté des Sciences Semlalia, Université Cadi Ayyad, LPHEA-Marrakech, Morocco*
- ^{35d}*Faculté des Sciences, Université Mohamed Premier and LPTPM, Oujda, Morocco*
- ^{35e}*Faculté des sciences, Université Mohammed V, Rabat, Morocco*
- ³⁶*CERN, Geneva, Switzerland*
- ³⁷*Enrico Fermi Institute, University of Chicago, Chicago, Illinois, USA*
- ³⁸*LPC, Université Clermont Auvergne, CNRS/IN2P3, Clermont-Ferrand, France*
- ³⁹*Nevis Laboratory, Columbia University, Irvington, New York, USA*
- ⁴⁰*Niels Bohr Institute, University of Copenhagen, Copenhagen, Denmark*
- ^{41a}*Dipartimento di Fisica, Università della Calabria, Rende, Italy*
- ^{41b}*INFN Gruppo Collegato di Cosenza, Laboratori Nazionali di Frascati, Italy*
- ⁴²*Physics Department, Southern Methodist University, Dallas, Texas, USA*
- ⁴³*Physics Department, University of Texas at Dallas, Richardson, Texas, USA*
- ⁴⁴*National Centre for Scientific Research “Demokritos”, Agia Paraskevi, Greece*
- ^{45a}*Department of Physics, Stockholm University, Sweden*
- ^{45b}*Oskar Klein Centre, Stockholm, Sweden*

- ⁴⁶*Deutsches Elektronen-Synchrotron DESY, Hamburg and Zeuthen, Germany*
- ⁴⁷*Lehrstuhl für Experimentelle Physik IV, Technische Universität Dortmund, Dortmund, Germany*
- ⁴⁸*Institut für Kern- und Teilchenphysik, Technische Universität Dresden, Dresden, Germany*
- ⁴⁹*Department of Physics, Duke University, Durham, North Carolina, USA*
- ⁵⁰*SUPA—School of Physics and Astronomy, University of Edinburgh, Edinburgh, United Kingdom*
- ⁵¹*INFN e Laboratori Nazionali di Frascati, Frascati, Italy*
- ⁵²*Physikalisches Institut, Albert-Ludwigs-Universität Freiburg, Freiburg, Germany*
- ⁵³*II. Physikalisches Institut, Georg-August-Universität Göttingen, Göttingen, Germany*
- ⁵⁴*Département de Physique Nucléaire et Corpusculaire, Université de Genève, Genève, Switzerland*
- ^{55a}*Dipartimento di Fisica, Università di Genova, Genova, Italy*
- ^{55b}*INFN Sezione di Genova, Italy*
- ⁵⁶*II. Physikalisches Institut, Justus-Liebig-Universität Giessen, Giessen, Germany*
- ⁵⁷*SUPA—School of Physics and Astronomy, University of Glasgow, Glasgow, United Kingdom*
- ⁵⁸*LPSC, Université Grenoble Alpes, CNRS/IN2P3, Grenoble INP, Grenoble, France*
- ⁵⁹*Laboratory for Particle Physics and Cosmology, Harvard University, Cambridge, Massachusetts, USA*
- ^{60a}*Department of Modern Physics and State Key Laboratory of Particle Detection and Electronics, University of Science and Technology of China, Hefei, China*
- ^{60b}*Institute of Frontier and Interdisciplinary Science and Key Laboratory of Particle Physics and Particle Irradiation (MOE), Shandong University, Qingdao, China*
- ^{60c}*School of Physics and Astronomy, Shanghai Jiao Tong University, KLPPAC-MoE, SKLPPC, Shanghai, China*
- ^{60d}*Tsung-Dao Lee Institute, Shanghai, China*
- ^{61a}*Kirchhoff-Institut für Physik, Ruprecht-Karls-Universität Heidelberg, Heidelberg, Germany*
- ^{61b}*Physikalisches Institut, Ruprecht-Karls-Universität Heidelberg, Heidelberg, Germany*
- ⁶²*Faculty of Applied Information Science, Hiroshima Institute of Technology, Hiroshima, Japan*
- ^{63a}*Department of Physics, Chinese University of Hong Kong, Shatin, N.T., Hong Kong, China*
- ^{63b}*Department of Physics, University of Hong Kong, Hong Kong, China*
- ^{63c}*Department of Physics and Institute for Advanced Study, Hong Kong University of Science and Technology, Clear Water Bay, Kowloon, Hong Kong, China*
- ⁶⁴*Department of Physics, National Tsing Hua University, Hsinchu, Taiwan*
- ⁶⁵*Department of Physics, Indiana University, Bloomington, Indiana, USA*
- ^{66a}*INFN Gruppo Collegato di Udine, Sezione di Trieste, Udine, Italy*
- ^{66b}*ICTP, Trieste, Italy*
- ^{66c}*Dipartimento Politecnico di Ingegneria e Architettura, Università di Udine, Udine, Italy*
- ^{67a}*INFN Sezione di Lecce, Italy*
- ^{67b}*Dipartimento di Matematica e Fisica, Università del Salento, Lecce, Italy*
- ^{68a}*INFN Sezione di Milano, Italy*
- ^{68b}*Dipartimento di Fisica, Università di Milano, Milano, Italy*
- ^{69a}*INFN Sezione di Napoli, Italy*
- ^{69b}*Dipartimento di Fisica, Università di Napoli, Napoli, Italy*
- ^{70a}*INFN Sezione di Pavia, Italy*
- ^{70b}*Dipartimento di Fisica, Università di Pavia, Pavia, Italy*
- ^{71a}*INFN Sezione di Pisa, Italy*
- ^{71b}*Dipartimento di Fisica E. Fermi, Università di Pisa, Pisa, Italy*
- ^{72a}*INFN Sezione di Roma, Italy*
- ^{72b}*Dipartimento di Fisica, Sapienza Università di Roma, Roma, Italy*
- ^{73a}*INFN Sezione di Roma Tor Vergata, Italy*
- ^{73b}*Dipartimento di Fisica, Università di Roma Tor Vergata, Roma, Italy*
- ^{74a}*INFN Sezione di Roma Tre, Italy*
- ^{74b}*Dipartimento di Matematica e Fisica, Università Roma Tre, Roma, Italy*
- ^{75a}*INFN-TIFPA, Italy*
- ^{75b}*Università degli Studi di Trento, Trento, Italy*
- ⁷⁶*Institut für Astro- und Teilchenphysik, Leopold-Franzens-Universität, Innsbruck, Austria*
- ⁷⁷*University of Iowa, Iowa City, Iowa, USA*
- ⁷⁸*Department of Physics and Astronomy, Iowa State University, Ames, Iowa, USA*
- ⁷⁹*Joint Institute for Nuclear Research, Dubna, Russia*
- ^{80a}*Departamento de Engenharia Elétrica, Universidade Federal de Juiz de Fora (UFJF), Juiz de Fora, Brazil*
- ^{80b}*Universidade Federal do Rio De Janeiro COPPE/EE/IF, Rio de Janeiro, Brazil*
- ^{80c}*Universidade Federal de São João del Rei (UFSJ), São João del Rei, Brazil*

- ^{80d}*Instituto de Física, Universidade de São Paulo, São Paulo, Brazil*
- ⁸¹*KEK, High Energy Accelerator Research Organization, Tsukuba, Japan*
- ⁸²*Graduate School of Science, Kobe University, Kobe, Japan*
- ^{83a}*AGH University of Science and Technology, Faculty of Physics and Applied Computer Science, Krakow, Poland*
- ^{83b}*Marian Smoluchowski Institute of Physics, Jagiellonian University, Krakow, Poland*
- ⁸⁴*Institute of Nuclear Physics Polish Academy of Sciences, Krakow, Poland*
- ⁸⁵*Faculty of Science, Kyoto University, Kyoto, Japan*
- ⁸⁶*Kyoto University of Education, Kyoto, Japan*
- ⁸⁷*Research Center for Advanced Particle Physics and Department of Physics, Kyushu University, Fukuoka, Japan*
- ⁸⁸*Instituto de Física La Plata, Universidad Nacional de La Plata and CONICET, La Plata, Argentina*
- ⁸⁹*Physics Department, Lancaster University, Lancaster, United Kingdom*
- ⁹⁰*Oliver Lodge Laboratory, University of Liverpool, Liverpool, United Kingdom*
- ⁹¹*Department of Experimental Particle Physics, Jožef Stefan Institute and Department of Physics, University of Ljubljana, Ljubljana, Slovenia*
- ⁹²*School of Physics and Astronomy, Queen Mary University of London, London, United Kingdom*
- ⁹³*Department of Physics, Royal Holloway University of London, Egham, United Kingdom*
- ⁹⁴*Department of Physics and Astronomy, University College London, London, United Kingdom*
- ⁹⁵*Louisiana Tech University, Ruston, Louisiana, USA*
- ⁹⁶*Fysiska institutionen, Lunds universitet, Lund, Sweden*
- ⁹⁷*Centre de Calcul de l'Institut National de Physique Nucléaire et de Physique des Particules (IN2P3), Villeurbanne, France*
- ⁹⁸*Departamento de Física Teórica C-15 and CIAFF, Universidad Autónoma de Madrid, Madrid, Spain*
- ⁹⁹*Institut für Physik, Universität Mainz, Mainz, Germany*
- ¹⁰⁰*School of Physics and Astronomy, University of Manchester, Manchester, United Kingdom*
- ¹⁰¹*CPPM, Aix-Marseille Université, CNRS/IN2P3, Marseille, France*
- ¹⁰²*Department of Physics, University of Massachusetts, Amherst, Massachusetts, USA*
- ¹⁰³*Department of Physics, McGill University, Montreal, Québec, Canada*
- ¹⁰⁴*School of Physics, University of Melbourne, Victoria, Australia*
- ¹⁰⁵*Department of Physics, University of Michigan, Ann Arbor, Michigan, USA*
- ¹⁰⁶*Department of Physics and Astronomy, Michigan State University, East Lansing, Michigan, USA*
- ¹⁰⁷*B.I. Stepanov Institute of Physics, National Academy of Sciences of Belarus, Minsk, Belarus*
- ¹⁰⁸*Research Institute for Nuclear Problems of Byelorussian State University, Minsk, Belarus*
- ¹⁰⁹*Group of Particle Physics, University of Montreal, Montreal, Quebec, Canada*
- ¹¹⁰*P.N. Lebedev Physical Institute of the Russian Academy of Sciences, Moscow, Russia*
- ¹¹¹*Institute for Theoretical and Experimental Physics of the National Research Centre Kurchatov Institute, Moscow, Russia*
- ¹¹²*National Research Nuclear University MEPhI, Moscow, Russia*
- ¹¹³*D.V. Skobeltsyn Institute of Nuclear Physics, M.V. Lomonosov Moscow State University, Moscow, Russia*
- ¹¹⁴*Fakultät für Physik, Ludwig-Maximilians-Universität München, München, Germany*
- ¹¹⁵*Max-Planck-Institut für Physik (Werner-Heisenberg-Institut), München, Germany*
- ¹¹⁶*Nagasaki Institute of Applied Science, Nagasaki, Japan*
- ¹¹⁷*Graduate School of Science and Kobayashi-Maskawa Institute, Nagoya University, Nagoya, Japan*
- ¹¹⁸*Department of Physics and Astronomy, University of New Mexico, Albuquerque, New Mexico, USA*
- ¹¹⁹*Institute for Mathematics, Astrophysics and Particle Physics, Radboud University Nijmegen/Nikhef, Nijmegen, Netherlands*
- ¹²⁰*Nikhef National Institute for Subatomic Physics and University of Amsterdam, Amsterdam, Netherlands*
- ¹²¹*Department of Physics, Northern Illinois University, DeKalb, Illinois, USA*
- ^{122a}*Budker Institute of Nuclear Physics and NSU, SB RAS, Novosibirsk, Russia*
- ^{122b}*Novosibirsk State University Novosibirsk, Russia*
- ¹²³*Institute for High Energy Physics of the National Research Centre Kurchatov Institute, Protvino, Russia*
- ¹²⁴*Department of Physics, New York University, New York, New York, USA*
- ¹²⁵*Ochanomizu University, Otsuka, Bunkyo-ku, Tokyo, Japan*
- ¹²⁶*Ohio State University, Columbus, Ohio, USA*
- ¹²⁷*Faculty of Science, Okayama University, Okayama, Japan*
- ¹²⁸*Homer L. Dodge Department of Physics and Astronomy, University of Oklahoma, Norman, Oklahoma, USA*
- ¹²⁹*Department of Physics, Oklahoma State University, Stillwater, Oklahoma, USA*

- ¹³⁰Palacký University, RCPTM, Joint Laboratory of Optics, Olomouc, Czech Republic
¹³¹Center for High Energy Physics, University of Oregon, Eugene, Oregon, USA
¹³²LAL, Université Paris-Sud, CNRS/IN2P3, Université Paris-Saclay, Orsay, France
¹³³Graduate School of Science, Osaka University, Osaka, Japan
¹³⁴Department of Physics, University of Oslo, Oslo, Norway
¹³⁵Department of Physics, Oxford University, Oxford, United Kingdom
¹³⁶LPNHE, Sorbonne Université, Paris Diderot Sorbonne Paris Cité, CNRS/IN2P3, Paris, France
¹³⁷Department of Physics, University of Pennsylvania, Philadelphia, Pennsylvania, USA
¹³⁸Konstantinov Nuclear Physics Institute of National Research Centre “Kurchatov Institute”,
 PNPI, St. Petersburg, Russia
¹³⁹Department of Physics and Astronomy, University of Pittsburgh, Pittsburgh, Pennsylvania, USA
^{140a}Laboratório de Instrumentação e Física Experimental de Partículas—LIP, Portugal
^{140b}Departamento de Física, Faculdade de Ciências, Universidade de Lisboa, Lisboa, Portugal
^{140c}Departamento de Física, Universidade de Coimbra, Coimbra, Portugal
^{140d}Centro de Física Nuclear da Universidade de Lisboa, Lisboa, Portugal
^{140e}Departamento de Física, Universidade do Minho, Braga, Portugal
^{140f}Universidad de Granada, Granada, Spain
^{140g}Dep Física and CEFITEC of Faculdade de Ciências e Tecnologia,
 Universidade Nova de Lisboa, Caparica, Portugal
¹⁴¹Institute of Physics of the Czech Academy of Sciences, Prague, Czech Republic
¹⁴²Czech Technical University in Prague, Prague, Czech Republic
¹⁴³Charles University, Faculty of Mathematics and Physics, Prague, Czech Republic
¹⁴⁴Particle Physics Department, Rutherford Appleton Laboratory, Didcot, United Kingdom
¹⁴⁵IRFU, CEA, Université Paris-Saclay, Gif-sur-Yvette, France
¹⁴⁶Santa Cruz Institute for Particle Physics, University of California Santa Cruz,
 Santa Cruz, California, USA
^{147a}Departamento de Física, Pontificia Universidad Católica de Chile, Santiago, Chile
^{147b}Departamento de Física, Universidad Técnica Federico Santa María, Valparaíso, Chile
¹⁴⁸Department of Physics, University of Washington, Seattle, Washington, USA
¹⁴⁹Department of Physics and Astronomy, University of Sheffield, Sheffield, United Kingdom
¹⁵⁰Department of Physics, Shinshu University, Nagano, Japan
¹⁵¹Department Physik, Universität Siegen, Siegen, Germany
¹⁵²Department of Physics, Simon Fraser University, Burnaby British Columbia, Canada
¹⁵³SLAC National Accelerator Laboratory, Stanford, California, USA
¹⁵⁴Physics Department, Royal Institute of Technology, Stockholm, Sweden
¹⁵⁵Departments of Physics and Astronomy, Stony Brook University, Stony Brook, New York, USA
¹⁵⁶Department of Physics and Astronomy, University of Sussex, Brighton, United Kingdom
¹⁵⁷School of Physics, University of Sydney, Sydney, Australia
¹⁵⁸Institute of Physics, Academia Sinica, Taipei, Taiwan
^{159a}E. Andronikashvili Institute of Physics, Iv. Javakhishvili Tbilisi State University, Tbilisi, Georgia
^{159b}High Energy Physics Institute, Tbilisi State University, Tbilisi, Georgia
¹⁶⁰Department of Physics, Technion, Israel Institute of Technology, Haifa, Israel
¹⁶¹Raymond and Beverly Sackler School of Physics and Astronomy, Tel Aviv University, Tel Aviv, Israel
¹⁶²Department of Physics, Aristotle University of Thessaloniki, Thessaloniki, Greece
¹⁶³International Center for Elementary Particle Physics and Department of Physics,
 University of Tokyo, Tokyo, Japan
¹⁶⁴Graduate School of Science and Technology, Tokyo Metropolitan University, Tokyo, Japan
¹⁶⁵Department of Physics, Tokyo Institute of Technology, Tokyo, Japan
¹⁶⁶Tomsk State University, Tomsk, Russia
¹⁶⁷Department of Physics, University of Toronto, Toronto, Ontario, Canada
^{168a}TRIUMF, Vancouver, British Columbia, Canada
^{168b}Department of Physics and Astronomy, York University, Toronto, Ontario, Canada
¹⁶⁹Division of Physics and Tomonaga Center for the History of the Universe, Faculty of Pure and Applied
 Sciences, University of Tsukuba, Tsukuba, Japan
¹⁷⁰Department of Physics and Astronomy, Tufts University, Medford, Massachusetts, USA
¹⁷¹Department of Physics and Astronomy, University of California Irvine, Irvine, California, USA
¹⁷²Department of Physics and Astronomy, University of Uppsala, Uppsala, Sweden
¹⁷³Department of Physics, University of Illinois, Urbana, Illinois, USA
¹⁷⁴Instituto de Física Corpuscular (IFIC), Centro Mixto Universidad de Valencia—CSIC, Valencia, Spain
¹⁷⁵Department of Physics, University of British Columbia, Vancouver, British Columbia, Canada

¹⁷⁶*Department of Physics and Astronomy, University of Victoria, Victoria, British Columbia, Canada*

¹⁷⁷*Fakultät für Physik und Astronomie, Julius-Maximilians-Universität Würzburg, Würzburg, Germany*

¹⁷⁸*Department of Physics, University of Warwick, Coventry, United Kingdom*

¹⁷⁹*Waseda University, Tokyo, Japan*

¹⁸⁰*Department of Particle Physics, Weizmann Institute of Science, Rehovot, Israel*

¹⁸¹*Department of Physics, University of Wisconsin, Madison, Wisconsin, USA*

¹⁸²*Fakultät für Mathematik und Naturwissenschaften, Fachgruppe Physik,
Bergische Universität Wuppertal, Wuppertal, Germany*

¹⁸³*Department of Physics, Yale University, New Haven, Connecticut, USA*

¹⁸⁴*Yerevan Physics Institute, Yerevan, Armenia*

^aDeceased.

^bAlso at Department of Physics, King's College London, London, United Kingdom.

^cAlso at Istanbul University, Department of Physics, Istanbul, Turkey.

^dAlso at Instituto de Fisica Teorica, IFT-UAM/CSIC, Madrid, Spain.

^eAlso at TRIUMF, Vancouver, British Columbia, Canada.

^fAlso at Department of Physics and Astronomy, University of Louisville, Louisville, Kentucky, USA.

^gAlso at Physics Department, An-Najah National University, Nablus, Palestine.

^hAlso at Department of Physics, California State University, Fresno, USA.

ⁱAlso at Department of Physics, University of Fribourg, Fribourg, Switzerland.

^jAlso at Physics Dept, University of South Africa, Pretoria, South Africa.

^kAlso at Departament de Fisica de la Universitat Autònoma de Barcelona, Barcelona, Spain.

^lAlso at Tomsk State University, Tomsk, and Moscow Institute of Physics and Technology State University, Dolgoprudny, Russia.

^mAlso at The Collaborative Innovation Center of Quantum Matter (CICQM), Beijing, China.

ⁿAlso at Departamento de Física, Instituto Superior Técnico, Universidade de Lisboa, Lisboa, Portugal.

^oAlso at Università di Napoli Parthenope, Napoli, Italy.

^pAlso at Institute of Particle Physics (IPP), Canada.

^qAlso at Department of Physics, University of Adelaide, Adelaide, Australia.

^rAlso at Department of Physics, St. Petersburg State Polytechnical University, St. Petersburg, Russia.

^sAlso at Department of Financial and Management Engineering, University of the Aegean, Chios, Greece.

^tAlso at Department of Physics, California State University, East Bay, USA.

^uAlso at Institutio Catalana de Recerca i Estudis Avancats, ICREA, Barcelona, Spain.

^vAlso at Department of Physics, University of Michigan, Ann Arbor, Michigan, USA.

^wAlso at LAL, Université Paris-Sud, CNRS/IN2P3, Université Paris-Saclay, Orsay, France.

^xAlso at Graduate School of Science, Osaka University, Osaka, Japan.

^yAlso at Physikalisches Institut, Albert-Ludwigs-Universität Freiburg, Freiburg, Germany.

^zAlso at Institute of Physics, Azerbaijan Academy of Sciences, Baku, Azerbaijan.

^{aa}Also at Institute for Mathematics, Astrophysics and Particle Physics, Radboud University Nijmegen/Nikhef, Nijmegen, Netherlands.

^{bb}Also at Institute of Theoretical Physics, Ilia State University, Tbilisi, Georgia.

^{cc}Also at CERN, Geneva, Switzerland.

^{dd}Also at Department of Physics, Stanford University, Stanford, California, USA.

^{ee}Also at Manhattan College, New York, New York, USA.

^{ff}Also at Joint Institute for Nuclear Research, Dubna, Russia.

^{gg}Also at Hellenic Open University, Patras, Greece.

^{hh}Also at The City College of New York, New York, New York, USA.

ⁱⁱAlso at Institute of High Energy Physics, Chinese Academy of Sciences, Beijing, China.

^{jj}Also at Department of Physics, California State University, Sacramento, USA.

^{kk}Also at Moscow Institute of Physics and Technology State University, Dolgoprudny, Russia.

^{ll}Also at Département de Physique Nucléaire et Corpusculaire, Université de Genève, Genève, Switzerland.

^{mm}Also at Department of Physics and Astronomy, University of Sheffield, Sheffield, United Kingdom.

ⁿⁿAlso at Louisiana Tech University, Ruston, Louisiana, USA.

^{oo}Also at School of Physics, Sun Yat-sen University, Guangzhou, China.

^{pp}Also at Institute for Nuclear Research and Nuclear Energy (INRNE) of the Bulgarian Academy of Sciences, Sofia, Bulgaria.

^{qq}Also at Faculty of Physics, M.V. Lomonosov Moscow State University, Moscow, Russia.

^{rr}Also at Department of Applied Physics and Astronomy, University of Sharjah, Sharjah, United Arab Emirates.

^{ss}Also at Institut für Experimentalphysik, Universität Hamburg, Hamburg, Germany.

^{tt}Also at CPPM, Aix-Marseille Université, CNRS/IN2P3, Marseille, France.

^{uu}Also at National Research Nuclear University MEPhI, Moscow, Russia.

^{vv}Also at Institute for Particle and Nuclear Physics, Wigner Research Centre for Physics, Budapest, Hungary.

^{ww} Also at Giresun University, Faculty of Engineering, Giresun, Turkey.

^{xx} Also at Institute of Physics, Academia Sinica, Taipei, Taiwan.

^{yy} Also at LPNHE, Sorbonne Université, Paris Diderot Sorbonne Paris Cité, CNRS/IN2P3, Paris, France.

^{zz} Also at Department of Physics and Astronomy, Michigan State University, East Lansing, Michigan, USA.